رقم الترتيب: .....

رقم التسلسل: .....

People's Democratic Republic of Algeria

Ministry of Higher Education and Scientific Research

University of Echahid Hamma Lakhdar El Oued

Faculty of Exact Science

Department of Chemistry

A Thesis Submitted in Fulfillment of the Requirements for Degree of Academic Master's

Field: Materials Science

Specialization: Organic Chemistry

Presented by:

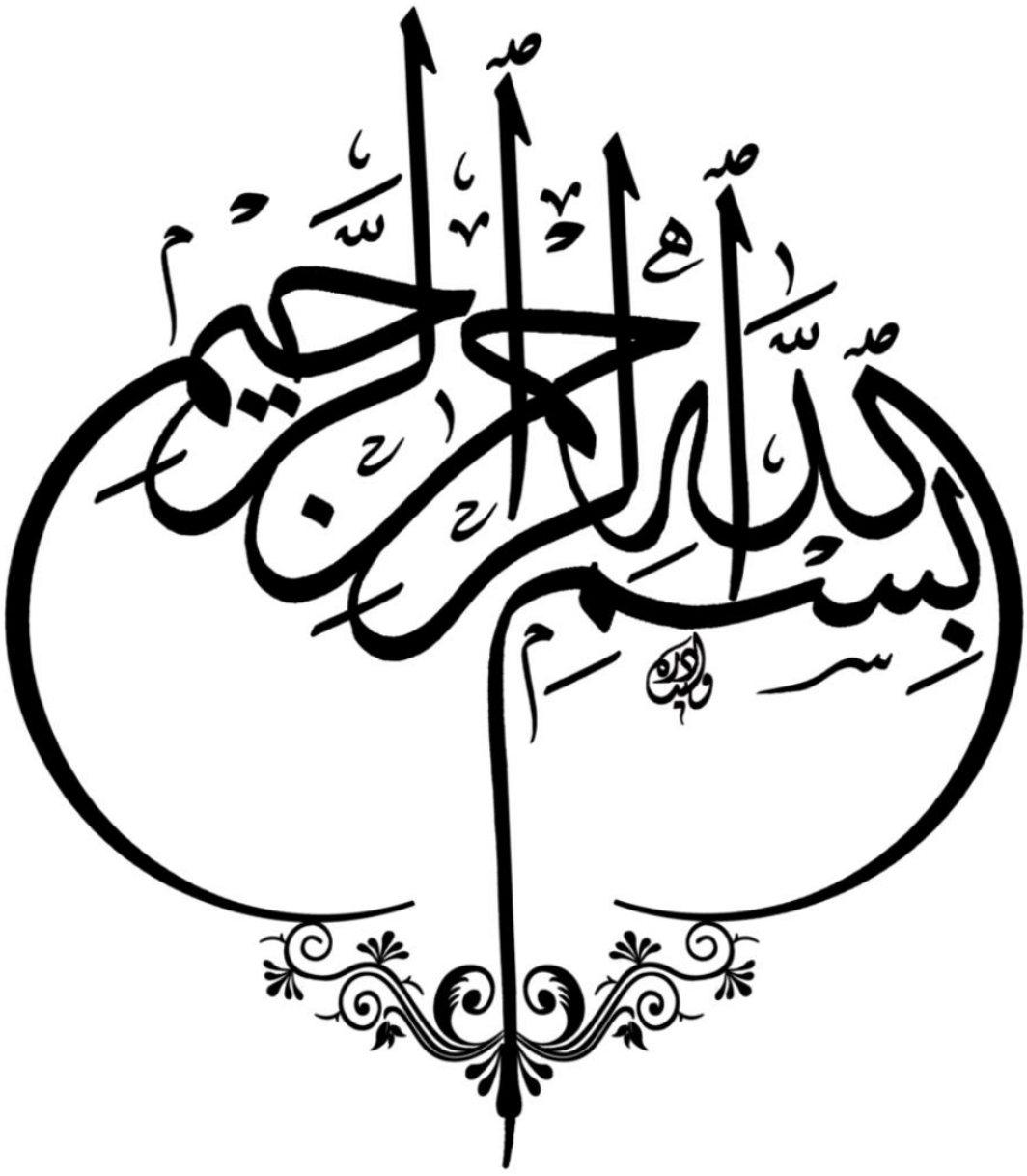
- **Bouzidi Faical**
- **Bouzidi Brahim**

The Chemical Composition, *In Vitro*, *In Vivo*, And *In Silico* Studies Of The Essential Oil Of The *Pimpinella Anisum* L Plant Found In Regions Of Algeria

Defended on 06/06/2026, in the presence of the Examination Committee:

Name	Rank	Affiliation	Role
KERASSA Aicha	PROF	University of El Oued	Chair
REBIAI Abdelkrim	PROF	University of El Oued	Examiner
ABADI Abderrezzak	MCA	University of El Oued	Supervisor

Academic Year: 2025/2026


بسم الله الرحمن الرحيم

Dedication

To those who carry in their hearts a lantern that illuminates my path, to those who, with their prayers, have forged a ladder for me to ascend toward success...

To the soul of my dear father; *the pillar of my life and the fountain of giving, who taught me that ambition knows no ceiling, and that patience is the key to every virtue.*

To my beloved mother; *my pure angel and the source of my strength, who enveloped me with her prayers in the darkness of the night, and embraced me with her tenderness whenever my steps grew weary.*

To my dear wife; *my companion on this journey, and the source of serenity and tranquility in my life. Thank you for your unwavering support, your noble patience, and your endless encouragement.*
To my dear daughter*, the flower of my life and the most beautiful gift from God, may God make her future full of success and happiness.*

To my brothers and sisters; *who have been my support and warmth at every step.*

To my friends and companions; *who shared my passion for knowledge, and with whom I shared the exhaustion of long nights and the weariness of days.*

Today, I place this Master's thesis into your hands, as a tribute of gratitude and recognition for everything you have given me. For you are, indeed, the partners in this success.

Faical

Dedication

To those whose prayers illuminated my path and whose love propelled me toward success,

To the hearts that supported me every step of the way, and to the souls that believed in my abilities even in moments of stumbling, I dedicate the fruits of this humble effort.

***To the pure soul of my father**, may God have mercy on him, who is gone in body but whose memory and prayers remain alive in my heart. May God have mercy on you as much as you wished me well and success.*

***To my dear mother**, may God protect her, the wellspring of tenderness and patience, and the one to whom, after God, I owe everything I have achieved.*

***To my esteemed wife**, my partner in life and companion in success, who has been my greatest support and help throughout my journey.*

***To my beloved daughters**, **Areej** and **Afnan**, the flowers of my life and the most beautiful gift from God. May God grant them a future filled with success and happiness.*

***To my dear brothers and sisters**, and to my dear friend **Soufiene**, who was always there with support, advice, and encouragement.*

I dedicate this humble work as a token of loyalty, love, and appreciation.

Brahim

Thanks and appreciation

All praise is due to Allah, Lord of the Worlds, by whose grace good deeds are perfected, and by whose guidance objectives are achieved. Peace and blessings be upon the one sent as a mercy to the worlds, our Master Muhammad, and upon his family and companions.

As we put the final touches on this research work, we would like to express our deepest thanks and gratitude to our honorable supervisor, Professor Abadi Abderrezak, who was most generous with his knowledge and advice, and served as our best guide and mentor throughout this research journey. We pray to Allah Almighty to bless his life and knowledge, and to reward him with the best of rewards on our behalf.

We also have the distinct honor to extend our sincere thanks and appreciation to the esteemed defense committee members, Professor Rebiai Abdelkrim and Professor Kerassa Aicha, for graciously accepting to evaluate, discuss, and guide the course of this work.

Furthermore, we would like to send a token of appreciation and recognition to our colleagues, Mammadi Mahmoud and Walid Cherif, as well as to all our eminent professors who enlightened our paths of knowledge throughout our years of study, and to everyone who helped and encouraged us, even with a kind word, to complete this modest effort.

Finally.. first and last, praise and thanks be to Allah, Lord of the Worlds.

Abstract

This study aims to comprehensively evaluate the chemical composition and biological activities of the essential oil extracted from the seeds of Algerian anise (*Pimpinella anisum* L.). The essential oil was isolated via hydrodistillation with a yield of 0.96%. Gas Chromatography-Mass Spectrometry (GC-MS) analysis revealed the presence of 31 chemical compounds, with an absolute dominance of *trans*-anethole (74.4%), followed by estragole (6.3%) and caryophyllene oxide (4.3%).

In vitro assays demonstrated outstanding antioxidant activity, with an half-maximal inhibitory concentration ($\boldsymbol{IC_{50}}$) value of 4.38 mg/mL in the DPPH (2,2-diphenyl-1-picrylhydrazyl) radical scavenging assay, and a high inhibitory capacity against the α-Amylase enzyme, reaching 85.54% at a concentration of 10 mg/mL. Furthermore, the oil exhibited notable anti-inflammatory activity by preventing bovine serum albumin (BSA) denaturation, along with potent antibacterial activity against *Escherichia coli* and *Staphylococcus aureus*, while proving its biosafety and non-toxicity toward human erythrocytes at therapeutic concentrations.

In the *in vivo* study, oral administration of the essential oil (100 mg/kg) to diabetic mice led to a significant reduction in fasting blood glucose levels (from 1.12 to 0.45 g/L) and glycated hemoglobin (HbA1c) (from 14.10 to 6.91 mmol/mol), while successfully restoring liver functions by lowering ALT and AST enzyme levels.

The *in silico* molecular docking simulation further supported these findings, revealing that caryophyllene oxide exhibited a binding energy (–5.88 kcal/mol) that outperforms the standard drug metformin in inhibiting the α-Amylase enzyme, alongside confirming ideal pharmacokinetic profiles (ADMET) for the major compounds.

In conclusion, this study demonstrates that Algerian anise represents a promising natural source for developing multi-target therapeutic agents for diabetes and associated metabolic disorders.

Keywords: Algerian anise; Essential oil; Anethole; Antidiabetic; Anti-inflammatory; In Silico; In vivo; In vitro .

الملخص:

تهدف هذه الدراسة إلى التقييم الشامل للتركيب الكيميائي والفعالية البيولوجية للزيت الأساسي المستخلص من بذور نبات اليانسون الجزائري .(*Pimpinella anisum L*) تم استخلاص الزيت عن طريق التقطير المائي بمردود قدره 0.96%، وكشف التحليل بواسطة تقنية كروماتوغرافيا الغاز المقترنة بمطيافية الكتلة عن وجود 31 مركباً كيميائياً، مع هيمنة مطلقة لمركب Anethole (74.4%)، يليه Estragole (6.3%)، Caryophyllene oxide (4.3%).

أظهرت نتائج الاختبارات المخبرية (*In vitro*) نشاطاً متميزاً لمضادات الأكسدة حيث بلغت قيمة التركيز المثبط النصفي 4.38 ملغ/مل في اختبار(2,2-diphenyl-1-picrylhydrazyl) ، وقدرة تثبيطيه عالية لإنزيم α-Amylase وصلت إلى 85.54% عند تركيز 10 ملغ/مل .كما أبدى الزيت فعالية مضادة للالتهاب من خلال منع تمسخ بروتين ألبومين المصل البقري ، ونشاطاً مضاداً لبكتيريا *E. coli* و*S. aureus*، مع إثبات أمانه الحيوي وعدم سميته تجاه كريات الدم الحمراء البشرية عند التركيزات العلاجية.

وفي الدراسة الحيوية(*In vivo*) ، أدى التجريع الفموي للزيت (100 ملغ/كغ) للفئران المصابة بالسكري إلى انخفاض جوهري في مستوى سكر الدم الصائم (من 1.12 إلى 0.45 غ/ل) والهيموغلوبين السكري (من 14.10 إلى 6.91 ممول/مول) ، مع استعادة وظائف الكبد (خفض إنزيمي *ALT* و *AST*).

وعززت دراسة المحاكاة الحاسوبية (*In silico*) هذه النتائج، حيث أظهر مركب Caryophyllene oxide طاقة ارتباط (5.88- كيلو كالوري/مول) تتفوق على دواء الميتفورمين في تثبيط إنزيم α-Amylase ، مع تأكيد الخصائص الحركية الدوائية المثالية (ADMET) للمركبات الرئيسية .

تخلص الدراسة إلى أن اليانسون الجزائري يمثل مصدراً طبيعياً واعداً لتطوير عوامل علاجية متعددة الأهداف لمرض السكري واضطرابات التمثيل الغذائي.

الكلمات المفتاحية: يانسون جزائري؛ زيت عطري؛ أنيثول؛ مضاد للسكري؛ مضاد للالتهابات؛ محاكاة حاسوبية؛ تجارب حيوية؛ تجارب مخبرية.

Index of Contents:

Index of Contents	
Dedication	**II**
Thanks and appreciation	**IV**
Abstract	**V**
Index of Contents	**VII**
List of Figures	**XII**
List of Tables	**XIV**
List of Abbreviations	**XV**
GENERAL INTRODUCTION	
General Introduction	**01**
Bibliography	**03**
THEORETICAL PART	
CHAPTER ONE(I) : General Overview of *Pimpinella anisum L*	
I.1. Introduction to Medicinal Plants	**06**
I.2. Bases for Classification of Medicinal Plants	**06**
I.3. Definition of Anise *(Pimpinella anisum L)*	**06**
I.4. Origin and Geographic Distribution	**06**
I.5. Scientific Classification of *Pimpinella anisum L*	**07**
I.6. Importance of *Pimpinella anisum L*	**07**
I.7. Plant Description	**08**
I.7.1. Roots	**08**
I.7.2. Stem	**09**
I.7.3. Flowers	**09**
I.7.4. Leaves	**10**
I.7.5. Fruit	**10**
I.7.6. Seeds	**11**
I.8. Cultivation Requirements of *Pimpinella anisum L*	**11**
I.9. Chemical Composition of *Pimpinella anisum L*	**11**
I.9.1. Phenylpropanoids	**12**
I.9.2. Monoterpenes (C10)	**12**
I.9.3. Sesquiterpene Family (C15)	**13**

Index of Contents

Bibliography	**14**
CHAPTER TWO (II): biological activities	
Introduction	**17**
II.1. Antioxidants	**17**
II.1.1. Definition of Antioxidants	**17**
II.1.2. Classification of Antioxidants	**18**
II.1.3. Comparison of types of antioxidants	**19**
II.1.4. The Mechanisms of the Antioxidant Defense System	**20**
II.1.5. Free Radicals	**21**
II.1.5.1. Definition of Free Radicals	**21**
II.1.5.2. Types of free radicals	**22**
II.1.5.3. Classification of Free Radicals by Lifespan	**22**
II.1.5.4. Sources of Free Radicals	**23**
II.2. Anti-inflammatory Activity	**24**
II.2.1. Protein Denaturation	**24**
II.2.2. Mechanism of Protein Stabilization	**24**
II.3. Antimicrobial Activity	**24**
II.3.1. Definition of Bacteria	**24**
II.3.2. General Structure of Bacteria	**25**
II.3.3. Bacterial Cell Wall Structure	**25**
II.3.4. Mechanism of Action (Killing Mechanism)	**26**
II.3.5. Synergistic Effect of Compounds	**26**
II.3.6. Classification of Bacteria	**26**
II.3.7. Antibiotics and Resistance	**27**
II.4.Cytotoxicity and Hemotoxicity as Biosafety Standards	**27**
II.4.1. Hemolysis Assay	**27**
II.4.2. Safety Criteria	**27**
II.4.3. Selectivity Index (SI)	**28**
II.5.Anti-Diabetes Action	**28**
II.5.1. Definition of Diabetes	**28**
II.5:2. classifications of Diabetes	**28**
II.5.3. Antidiabetic activity	**29**

Index of Contents

II.5.4. Oral treatments for type 2 diabetes	**29**
II.5.5. Alpha-amylase enzyme	**29**
II.5.6. The Enzyme's Relationship to Diabetes (Biological Link)	**29**
Bibliography	**30**
CHAPTER THREE(III): In Silico Studies	
Introduction	**34**
III.1. Definition of Computer Simulation	**34**
III.2. The Concept of Molecular Docking	**34**
III.2.1. Definition and Basic Principles	**34**
III.2.2. Steps of Molecular Docking	**34**
III.3. AutoDock 4.2	**35**
III.3.1. Software Overview	**35**
III.3.2. Algorithms Used	**35**
III.3.3. Energy Evaluation Function in AutoDock	**35**
III.4.Detailed Work Procedures	**36**
III.4.1.File Preparation	**36**
III.4.2. Basic setup files	**36**
III.4.1.Key Parameters in LGA	**37**
III.5.Free Binding Energy and Inhibition Constant	**37**
III.6.Cluster Analysis	**38**
III.7.In Silico ADMET and Toxicity Profiling	**38**
III.7.1.The SwissADME Platform	**38**
III.7.2.The ProTox-II Server	**38**
III.8.Detailed Energy Components	**39**
Bibliography	**40**
PRACTICAL PART	
CHAPTER FOUR(IV): Methods And Materials	
Introduction	**44**
IV.1. 1.Materials and Methods	**45**
IV.1.1.Used equipment	**45**
IV.1.2.Used materials	**45**
IV.2.Essential oil extraction	**46**

Index of Contents

IV.2.1.Hydrodistillation Method	**46**
IV.2.2.Calculation of Extraction Yield	**46**
IV.3.Gas Chromatography-Mass Spectrometry (GC-MS) Analysis	**46**
IV.I. In Vitro Study	
IV.I.1.Evaluation of Antioxidant Activity	**47**
IV.I.1.1.DPPH Radical Scavenging Assay	**47**
IV.I.1.2.Experimental Procedure	**48**
IV.I.1.3.Calculation of Antioxidant Capacity	**48**
IV.I.2.Evaluation of Anti-diabetic activity	**49**
IV.I.3.Evaluation Anti-inflammatory Activity	**50**
IV.I.4.Evaluation Antimicrobial Activity	**51**
IV.I.5.Evaluation Cytotoxicity and Hemotoxicity as Biosafety Standards	**51**
IV.II. In Silico Study	
IV.II.1.In Silico ADMET Study	**52**
IV.II.1.1.Physicochemical Properties	**52**
IV.II.1.2.Pharmacokinetic Profile (ADME)	**52**
IV.II.1.3.Toxicological Assessment	**53**
IV.II.2.Molecular Docking Protocol	**53**
IV.II.2.1.Preparation Phase	**53**
A. Receptor Preparation (Protein)	**53**
B. Ligand Preparation	**53**
IV.II.2.2.Method Validation (Re-docking)	**54**
IV.II.2.3.Grid Box Configuration	**54**
IV.II.2.4.Docking Simulation	**54**
IV.II.2.5.Post-Docking Analysis	**54**
IV.III. In vivo Study	
IV.III.1.Experimental Animals	**55**
IV.III.2.Induction of Diabetes	**55**
IV.III.3.Acute toxicity test	**55**
IV.III.4.Experimental Design and Treatment	**56**
IV.III.5.Biochemical analysis	**56**
IV.III.6.Histological preparation of liver, pancreas, and kidney	**56**

Index of Contents

Bibliography	**58**
CHAPTER FIVE(V): Results And Discussion	
V.1.Results of Essential Oil Extraction	**61**
V.1.1.Physical Properties of the Essential Oil	**61**
V.1.2.Essential Oil Yield	**61**
V.1.3.Discussion of Extraction Yield	**61**
V.2.Gas Chromatography-Mass Spectrometry (GC-MS) Analysis	**61**
V.3.Antioxidant Activity	**63**
V.3.1.Assessment of Antioxidant Activity	**63**
V.3.2.Results and Discussion	**64**
V.4.Anti-diabetic activity	**64**
V.4.1.Assessment of anti-diabetic activity	**64**
V.4-2. Results and Discussion	**65**
V.5.Anti-inflammatory Activity	**66**
V.5.1.Assessment of Anti-inflammatory Activity	**66**
V.5.2.Results and Discussion	**66**
V.6.Antimicrobial Activity	**67**
V.6.1.Assessment of Antimicrobial Activity	**67**
V.6.2.Results and Discussion	**67**
V.7.Cytotoxicity and Hemotoxicity as Biosafety Standards	**67**
V.7.1.Assessment of Antimicrobial Activity	**68**
V.7.2.Results and Discussion	**69**
V.8. In Silico ADMET Study	**69**
V.8.1. Results In Silico ADMET and Toxicity Profiling	**69**
V.8.2.Discussion In Silico ADMET and Toxicity Profiling	**70**
V.8.2.1.Physicochemical Properties and Lipinski's Rule of Five	**70**
V.8.2.2.Pharmacokinetic Profile (BOILED-Egg Model)	**70**
V.8.2.3.Toxicological Assessment and Safety Margins	**71**
V.8.2.4.Structural Alerts (Brenk Alerts)	**71**
V.9.Molecular Docking	**71**
V.9.1.Results of Validation (Re-docking)	**71**
V.9.2.Discussion And Analysis Results Of Validation (Re-docking)	**72**

Index of Contents

V.9.3.Results of Molecular Docking Simulation	**72**
V.9.4.Discussion and analysis of Docking results	**73**
V.9.4.1.Inhibitory Efficacy Against α-Amylase (PDB ID: 4GQR)	**73**
V.9.4.2.Inhibitory Efficacy Against α-Glucosidase (PDB ID:3W37)	**74**
V.9.4.3.Structural Interpretation of Complex Stability	**76**
V.10.In vivo antidiabetic activities	**76**
V.10.1.Antihyperglycemic effect and glycemic control	**76**
V.10.2.Hepatoprotective activity	**77**
V.10.3.Mechanistic basis	**79**
V.10.4.Histopathological Analysis	**81**
V.10.4.1.Liver Histology	**81**
A). Histological Interpretation of Liver Sections	**81**
B).Histological Conclusion	**82**
V.10.4.1.Kidney Histology	**82**
A). Histological Interpretation of Kidney Sections	**82**
B). Histological Conclusion	**84**
V.10.4.1.Pancreas Histology	**84**
A).Histological Interpretation of Pancreas Sections	**84**
B). Histological Conclusion	**85**
GENERAL SUMMARY	**87**

List of Figures:

figure (I-1) The importance of the Pimpinella anisum L 8
figure (I-2) Image of a Pimpinella anisum L stem 9
figure(I-3) Image of Pimpinella anisum L flowers 9
figure(I-4) Image of Pimpinella anisum L leaves 10
figure(I-5) Image of Pimpinella anisum L fruit 10
figure (I-6) Image of Pimpinella anisum L seeds 11
figure (II-1) Chemical structures of (PG, TBHQ, BHA, BHT) *19*
Figure(II-2) integrated Network Antioxidant Defense Mechanisms *21*
figure (II-3) The mechanism of action of antioxidants in neutralizing free radicals *21*
figure (II-4) Bacterial cell structure and its components *25*
Figure(II-5) Classification of Bacteria *26*
figure(IV-1) Diagram illustrating the work plan of this study 44
figure (IV-2) Clevenger device 45
figure (IV-3) sensitive electronic scale 45
figure(IV-4) UV-Visible device 45
figure (IV-5) DPPH free radical reacts with an antioxidant compound 48
figure (IV-6) An illustration of how the DPPH test works. 49
figure(IV-7) Steps for performing a protein mutagenesis (BSA) inhibition test. 50
figure (IV-8) practical steps for the burrowing diffusion method 51
figure (IV-9) Hemolysis test using (96-well microplate) technology and a centrifuge. 52
figure (V-1) The curve of change in free radical inhibition (DPPH) as a function of oil concentrations 63
figure (V-2) Curve showing the change in the inhibition ratio of α-Amylase as a function of oil concentration. 65
figure (V-3) A curve showing the percentage of protein denaturation inhibition as a function of anise oil concentrations. 66
figure (V-4) Antibacterial activity of the essential oil on Mueller-Hinton agar plates 67
figure (V-5) BOILED-Egg model for predicting gastrointestinal absorption (HIA) and brain penetration (BBB) of the studied compounds 69
figure (V-6) Predicted acute toxicity (LD50) and toxicity classes and Bioavailability radars illustrating the physicochemical properties and drug-likeness of the major compounds in

List of Figures

Pimpinella anisum L essential oil, obtained via the SwissADME platform and using the ProTox-II server. 70
figure (V-7) 2D interaction map of Caryophyllene oxide in 4GQR 73
figure (V-8) 2D interaction map of Anethole in 4GQR 73
figure (V-9) 2D interaction map of Anethole in 3W37 74
figure (V-10) 2D interaction map of Estragole in 3W37 75
figure(V-11) Effect of Pimpinella anisum L essential oil (100 mg/kg) on fasting blood glucose (A) and HbA1c levels (B) in alloxan-induced diabetic rats. 77
figure (V-12) Effect of Pimpinella anisum L essential oil on serum liver enzymes (ALT and AST) in diabetic rats compared with control and metformin groups. 79
figure (V-13) Graphical abstract of the multi-target antidiabetic and hepatoprotective mechanisms of Pimpinella anisum L essential oil. 80
figure (V-14) Comparative histological analysis of liver sections from Normal Control (Nc), Diabetic Control (D), Treatment (Pimpinella anisum L, T), and Positive Control (Metformin, Pc) groups, X400. 81
figure (V-15) Comparative histological analysis of Kidney sections from Normal Control (Nc), Diabetic Control (D), Treatment (Pimpinella anisum L, T), and Positive Control (Metformin, Pc) groups, X400. 82
figure (V-16) Comparative histological analysis of Pancreas sections from Normal Control (Nc), Diabetic Control (D), Treatment (Pimpinella anisum L, T), and Positive Control (Metformin, Pc) groups, X400. 84

List of Tables:

table(II-1) Comparison of types of antioxidants 19
table (II-2) The Mechanisms of the Antioxidant Defense System 20
table (II-3) External sources of free radicals and their biological mechanisms 23
table(III- 1) Comparison of search algorithms in molecular docking programs 35
table(III-2) File types and their functions in the Docking process 36
table (III-3) Parameters and settings used for the Genetic Algorithm (GA) 37
table (III-4) Classification of ligand binding affinity based on ΔG and Ki values 37
table (IV-1)GC-MS operating parameters and conditions 47
table (V-1) Results of oil extraction yield 61
table (V-2) Results of GC MS analysis of the essential oil of the (Pimpinella anisum L) ... 62
table (V-3) Percentage (I%) at different concentrations using the DPPH test. 63
table (V-4) Percentage inhibition of α-amylase of oil as a function of concentrations 65
table (V-5) Anti-inflammatory activity of essential oil using protein denaturation inhibition assay. 66
table (V-6) Antimicrobial activity of the essential oil against tested bacterial strains 67
table (V-7) Hemolysis percentage of Pimpinella anisum L essential oil (Mean ± SD). 68
table (V-8) Prediction of physicochemical properties, pharmacokinetics (ADME), and acute toxicity of the major compounds of Pimpinella anisum L essential oil. 70
table (V-9) Molecular Redocking Validation Results 71
table (V-10) Molecular docking results of selected ligands with target proteins 72
table (V-11) Effect of Pimpinella anisum L essential oil (100 mg/kg) on fasting blood glucose and HbA1c in diabetic rats 77
table (V-12) Effect of Pimpinella anisum L essential oil (100 mg/kg) on serum liver enzymes in diabetic rats 78

List of Abbreviations:

Abbreviations	The full term	Meaning/Connotation in Arabic
GC-MS	Gas Chromatography-Mass Spectrometry	كروماتوغرافيا الغاز - مطيافية الكتلة (تقنية لتحليل وفصل مكونات الزيت العطري)
DPPH	2,2-diphenyl-1-picrylhydrazyl	اختبار تقييم النشاط المضاد للأكسدة (جذر حر كيميائي مستقر يُستخدم في المختبر)
IC_{50}	Half Maximal Inhibitory Concentration	التركيز المثبط النصفي (تركيز الزيت المطلوب لتثبيط 50% من النشاط الحيوي أو الجذور الحرة)
HbA1c	Glycated Hemoglobin	الهيموغلوبين السكري (السكري التراكمي)
ALT	Alanine Aminotransferase	إنزيم ناقلة أمين الألانين (أحد إنزيمات الكبد الرئيسية)
AST	Aspartate Aminotransferase	إنزيم ناقلة أمين الأسبرتات (أحد إنزيمات الكبد الرئيسية)
COX-2	Cyclooxygenase-2	إنزيم سيكلوأكسيجينيز-2 (المسؤول عن الالتهابات والألم)
ADMET	Absorption, Distribution, Metabolism, Excretion, and Toxicity	الامتصاص، التوزيع، الاستقلاب، الإخراج، والسمية (خصائص حركية الدواء في الجسم)
BSA	Bovine Serum Albumin	ألبومين المصل البقري (بروتين مستخدم في اختبارات تثبيط تمسخ البروتين للالتهابات)
LD_{50}	Median Lethal Dose	الجرعة القاتلة النصفية (مقياس لسمية المواد الكيميائية حاسوبياً أو حيوياً)
ANOVA	Analysis of Variance	تحليل التباين (اختبار إحصائي رياضي لتحليل النتائج)
PDB	Protein Data Bank	بنك بيانات البروتينات (قاعدة البيانات العالمية التي تُستخرج منها هياكل البروتين ثلاثية الأبعاد)
PDBQT	Protein Data Bank, Partial Charge (Q), & Atom Type (T)	صيغة ملفات مخصصة لبرنامج محاكاة الالتحام الجزيئي AutoDock
RMSD	Root-Mean-Square Deviation	جذر متوسط مربع الانحراف (مقياس يُستخدم لتقييم دقة المحاكاة الحاسوبية والالتحام)
GI	Gastrointestinal	الجهاز الهضمي (يُستخدم لوصف الامتصاص المعوي)
BBB	Blood-Brain Barrier	الحاجز الدموي الدماغي (مقياس نفاذية المركبات إلى الدماغ)
CYP450	Cytochrome P450	سيتوكروم بي450 (عائلة إنزيمات مسؤولة عن استقلاب الأدوية في الكبد)

List of Abbreviations

P-gp	P-glycoprotein	P-البروتين السكري ناقل خلوي يؤثر على امتصاص الأدوية (وتوزيعها)
PBS	Phosphate-Buffered Saline	المحلول الملحي المنظم بالفوسفات (محلول منظم يُستخدم في تجارب خلايا الدم)
UV-Vis	Ultraviolet-Visible Spectroscopy	مطيافية الأشعة فوق البنفسجية والمرئية (جهاز قياس الامتصاص الضوئي)
GA / LGA	Lamarckian Genetic Algorithm	الخوارزمية الجينية اللاماركية (خوارزمية البحث المستخدمة في برنامج AutoDock)
RI	Retention Index	مؤشر الاحتفاظ (يُستخدم لتأكيد هوية المركبات الكيميائية في تحليل GC-MS)
SOD	Superoxide Dismutase	مضاد (إنزيم ديسموتاز سوبراوكسيد إنزيم الفائق الأكسيد) أيون يحوّل للأكسدة
CAT	Catalase	إنزيم الكتالاز (إنزيم يحتوي على مجموعة هيم يحلل بيروكسيد الهيدروجين)
GPx	Glutathione Peroxidase	إنزيم غلوتاثيون بيروكسيداز (يحتوي على السيلينيوم، يُحلّل H_2O_2 والبيروكسيدات)
GSH	Reduced Glutathione	الغلوتاثيون المختزل(مضاد أكسدة يُستخدم من قِبَل إنزيمGPx)
ROS	Reactive Oxygen Species	أنواع الأكسجين التفاعلية(جذور حرة تسبب تلفاً خلوياً)
SI	Selectivity Index	مؤشر الانتقائية (يُميّز بين التأثير العلاجي والسام للمادة)
FBG	Fasting Blood Glucose	سكر الدم الصائم(قياس مستوى السكر بعد الصيام)
MIC	Minimum Inhibitory Concentration	الحد الأدنى للتركيز المثبط (أدنى تركيز يمنع نمو البكتيريا)
SD	Standard Deviation	الانحراف المعياري(مقياس إحصائي لتشتت البيانات)
RBC	Red Blood Cells	خلايا الدم الحمراء(كريات الدم الحمراء)
DNA	Deoxyribonucleic Acid	الحمض النووي الديوكسيريبوزي
WHO	World Health Organization	منظمة الصحة العالمية
ATCC	American Type Culture Collection	مجموعة المزارع الأمريكية القياسية (مرجع للسلالات البكتيرية)
BHA	Butylhydroxyanisole	بيوتيل هيدروكسي أنيزول (مضاد أكسدة اصطناعي)
BHT	Butylhydroxytoluene	بيوتيل هيدروكسي تولوين (مضاد أكسدة اصطناعي)
TBHQ	Tert-Butylhydroquinone	تيرت-بيوتيل هيدروكينون (مضاد أكسدة اصطناعي)
PG	Propyl Gallate	غاليت البروبيل (مضاد أكسدة اصطناعي)

GENERAL INTRODUCTION

General Introduction

Modern pharmaceutical and medical sciences are witnessing a rapid trend toward exploring medicinal and aromatic plants as natural and safe alternatives to manufactured chemical compounds. Plant extracts and essential oils are considered a rich source of bioactive molecules that contribute to the prevention and treatment of many diseases and physiological disorders [1]. Among these promising plant treasures, anise *(Pimpinella anisum L)* stands out. This herbaceous plant, belonging to the Apiaceae family, is highly valued in traditional medicine and the food and pharmaceutical industries thanks to its diverse therapeutic properties [2].

The biological value of anise lies in the unique diversity of its chemical composition. Its essential oil contains key phenolic and aromatic compounds [3]. This natural combination gives the plant a remarkable ability to exhibit multiple biological activities, primarily its anti-inflammatory activity, its ability to inhibit protein denaturation, and its potent antimicrobial activity through the penetration and destruction of bacterial and fungal cell membranes [4], while maintaining excellent biosafety levels against hematotoxicity and cytotoxicity [5]. This study is of exceptional importance as it focuses on anise growing in Algerian regions. The diverse climatic and environmental conditions in Algeria play a crucial role in influencing the plant's secondary metabolism, which in turn affects its chemical composition and biological activity [6].

What distinguishes this research and lends it innovative depth is its adoption of a comprehensive, multidimensional scientific methodology that integrates three complementary research approaches [7]:

In vitro studies: to directly and rigorously evaluate the anti-inflammatory, antimicrobial, and hemolytic activity.

in vivo studies: to assess the efficacy and safety of the extract within living systems and determine safe dosages.

in Silico computational studies: to predict the mechanisms of interaction and molecular binding between the plant's active compounds and biological targets with high accuracy, thus saving time and effort in uncovering the precise mechanisms of pharmacological action [8].

The central problem of this research revolves around identifying and characterizing the chemical composition of Algerian anise extract and evaluating its biological activity and biosafety through the systematic integration of three pathways (in vitro, in vivo, and in

Silico). This aims to provide a comprehensive scientific perspective that supports the exploitation of this plant as a promising medicinal resource.

To present the details of this research, the work is divided into two main parts:

First: Theoretical Part, comprising three chapters:

Chapter 1: (General Overview of *Pimpinella anisum L*): This chapter provides a comprehensive botanical and taxonomic description of the Pimpinella anisum L. plant. It reviews its geographical distribution, traditional medicinal uses, and details the chemical profile of its essential oil, with a specific focus on its major phytoconstituents.

Chapter 2: (Biological Activities): This chapter explores the therapeutic potential of anise essential oil by reviewing previous scientific literature. It covers the theoretical principles underlying its antioxidant, anti-diabetic, anti-inflammatory, and antimicrobial properties, as well as its toxicological safety profiles.

Chapter 3: (In Silico Studies): This chapter introduces the fundamental concepts of computational chemistry and molecular modeling. It focuses on the principles of molecular docking, virtual screening, and pharmacokinetic evaluations (ADMET), highlighting how computer-aided drug design bridges theoretical chemistry and biological efficacy.

Second: Applied Part, comprising two chapters:

Chapter 4: (Methods And Materials): This chapter reviews the experimental protocols used in the extraction processes, chemical analysis, and biological and computational evaluations.

Chapter 5: (Results and Discussion): This chapter presents the experimental results and computer modeling, scientifically analyzing and comparing them with reference studies to demonstrate the efficacy and safety of Algerian anise.

In conclusion, this study culminates in a general summary outlining the most significant scientific findings and presenting future prospects for utilizing these results in the pharmaceutical and therapeutic industries.

Bibliography

[1] Newman, D. J., & Cragg, G. M. (2020). Natural products as sources of new drugs over the nearly four decades from 01/1981 to 09/2019. Journal of Natural Products, 83(3), 770-803

[2] Shojaii, A., & Fard, M. A. (2012). Review of pharmacological properties and chemical constituents of *Pimpinella anisum L*. ISRN Pharmaceutics, 2012, 1-8.

[3] Acimovic, M., Tešević, V., Smiljanić, K., Cvetković, M., Stanković, J., & Todosijević, M. (2015). Chemical composition of *Pimpinella anisum L* essential oil from Serbia. Natural Product Communications, 10(3), 1934578X1501000338.

[4] Sun, W., Shahrajabian, M. H., & Cheng, Q. (2019). Anise (*Pimpinella anisum L* L.), a dominant spice and traditional medicinal herb for both humans and livestock. Bioscience Journal, 35(6), 1912-1926.

[5] Krishnaiah, D., Sarbatly, R., & Nithyanandam, R. (2011). A review of the antioxidant potential of medicinal plant extracts. Scientific Research and Essays, 6(1), 24-33.

[6] Bendiabdellah, A., El Amine Dib, M., Meliani, N., Muselli, A., Nassim, D., Tabti, B., & Costa, J. (2012). Antibacterial activity and chemical composition of the essential oil of *Pimpinella anisum L* from Algeria. Journal of Essential Oil Bearing Plants, 15(3), 414-421.

[7] Sliwoski, G., Kothiwale, S., Meiler, J., & Lowe, E. W. (2014). Computational methods in drug discovery. Pharmacological Reviews, 66(1), 334-395.

[8] Mavromoustakos, T., et al. (Eds.). (2018). Computations in Drug Discovery: Integration of In Silico, In Vitro, and In Vivo Approaches. Methods in Molecular Biology (Vol. 1762). Springer, New York.

THEORETICAL PART

CHAPTER ONE:

GENERAL OVERVIEW OF PIMPINELLA ANISUM

1. The Concept of Medicinal Plants:

Medicinal plants are defined as living plant organisms that store in their tissues (whether in a specific part of them or in their entire structure) active chemical compounds that possess healing properties. These plants are utilized in two main ways: either through the direct use of their various parts, such as roots, leaves, flowers, and seeds, in traditional medicine, or through the extraction and isolation of their active ingredients in the laboratory for use in the manufacture of modern medicines and drugs [1].

2. Principles of Classifying Medicinal Plants:

The criteria used in classifying medicinal plants vary depending on the purpose of the study; some are classified according to commercial importance or therapeutic effect. However, morphological (formal) classification stands out as a fundamental approach in botany, as this classification focuses mainly on identifying the plant organ used and the location of concentration of the active ingredient within it [2,3].

3. An Introduction to Anise *(Pimpinella anisum L)* :

Anise is scientifically known as *Pimpinella anisum L*, an annual herb belonging to the Apiaceae family [4]. This plant has various names depending on the culture and geographical region; in North Africa, it is known as "Habba Halawa" (sweet seed), in ancient Egypt it was called "Anit," in Greece it is called "Anisoon," while in English it is known as "Anise" and in French as "Anis vert" [5]. Linguistically, the genus name Pimpinella is believed by some to be derived from the Latin word "Dipinella," which refers to the shape of its double, feathery leaves [6].

4. Origin and Geographic Distribution:

The eastern Mediterranean region and Egypt are considered the original habitat of anise, where its medicinal and aromatic properties have been used since Pharaonic times [7].
Over time, its cultivation spread to most warm and temperate regions of the world.
Today, anise is cultivated in extensive areas, including:

- **Europe**: specifically in Spain, Italy, and Greece.
- **Asia**: particularly in Turkey, India, China, and Iran.
- **The Americas**: where it is grown in Mexico and Chile [8].

It is estimated that Mediterranean countries remain the primary producers of the finest essential oils extracted from anise seeds, due to the climate's suitability for the growth of the active ingredient, anethole, in high concentrations [9].

5. Scientific Classification of *Pimpinella anisum L* :

The anise plant was classified within the Kingdom Plantae and belongs to the Apiaceous family. The following hierarchy represents its botanical lineage [10]:

Table (I- 1): Taxonomic Classification of Pimpinella anisum L

Rank	**Scientific Name**
Kingdom	Plantae
Order	Apiales
Family	Apiaceae (Umbelliferae)
Subfamily	Apioideae
Tribe	Pimpinelleae
Genus	*Pimpinella*
Species	*Pimpinella anisum L.*

6. The Importance of Anise *Pimpinella anisum L* :

Anise is one of the oldest known medicinal and aromatic plants in the Mediterranean and Far Eastern civilizations, where it has been used for thousands of years in traditional medicine for its diverse healing properties [11]. Modern research has focused on extracting its active ingredients, especially the essential oil, to determine their direct effects on human health [12]. Different parts of the plant, specifically the fruits (seeds) and the oil extracted from them, are used to treat digestive disorders such as bloating and colic, and to alleviate symptoms of respiratory problems such as asthma and coughs [7].

Anise also possesses a wide range of medicinal properties, including antimicrobial, antifungal, and anti-inflammatory effects, in addition to its calming and mood-regulating effects [13]. It is used as an expectorant, antispasmodic, and milk-stimulating agent in nursing mothers. Studies have also demonstrated its role as an antioxidant and liver protectant [9]. Some research indicates the effectiveness of its extracts in regulating blood sugar levels and alleviating menopausal symptoms, in addition to its use in treating loss of appetite and intestinal problems [14].

Besides its medicinal importance, anise is widely used in the food industry as a flavoring agent, and in the manufacture of perfumes and cosmetics (soaps and toothpastes). The seed residue after oil extraction is used as a protein-rich animal feed, and its oil acts as a natural pesticide against some types of parasitic insects [15].

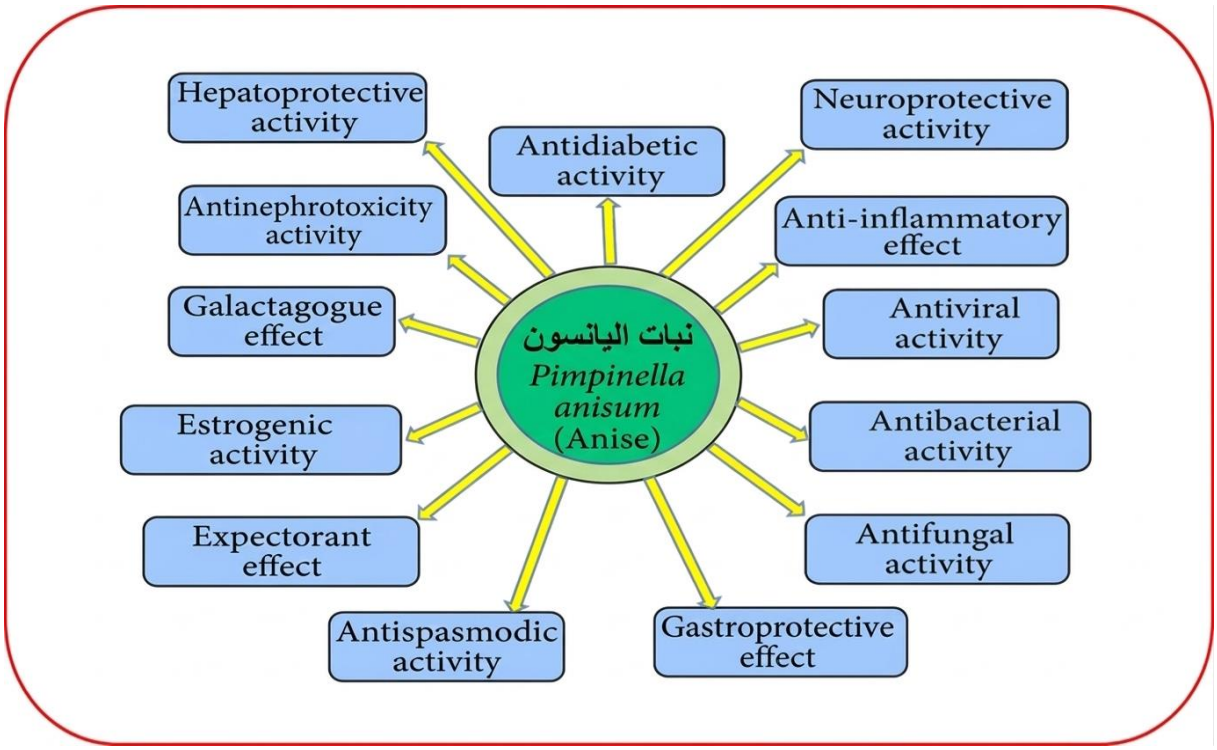


Figure (I-1) The importance of the Pimpinella anisum L

7. Plant Description of *Pimpinella anisum L* :

Anise is a fast-growing annual herb characterized by an upright, branching stem covered with fine, soft hairs [11]. It is a medium-sized plant, reaching a height of 30 to 60 cm, with a large, rounded crown of compound flower umbels up to 5 cm in diameter [16]. The plant begins to flower approximately three months after planting and reaches full fruit production within 120 to 150 days, producing abundant quantities of aromatic seeds annually before completing its life cycle, which does not exceed one year [17].

7-1. Roots:

The anise root system consists of a slender main taproot and a network of fine, well-developed lateral roots that spread throughout the surface layers of the soil [18].

7-2. Stem:

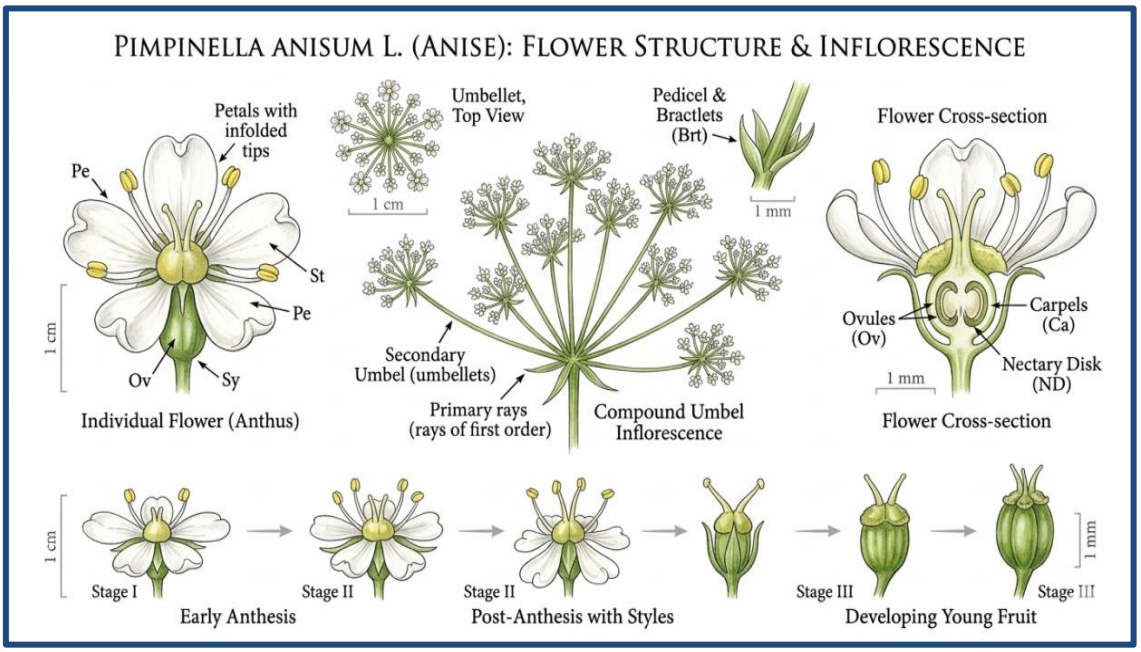
The stem is straight and cylindrical, with a diameter ranging from 2 to 5 mm. Its bark is light green, and it is hollow inside with distinct longitudinal striations [19]. It is often branched at the apex and resistant to natural pests due to its essential oil content [20].



Figure (I-2) Image of a Pimpinella anisum L stem

7-3. Flowers:

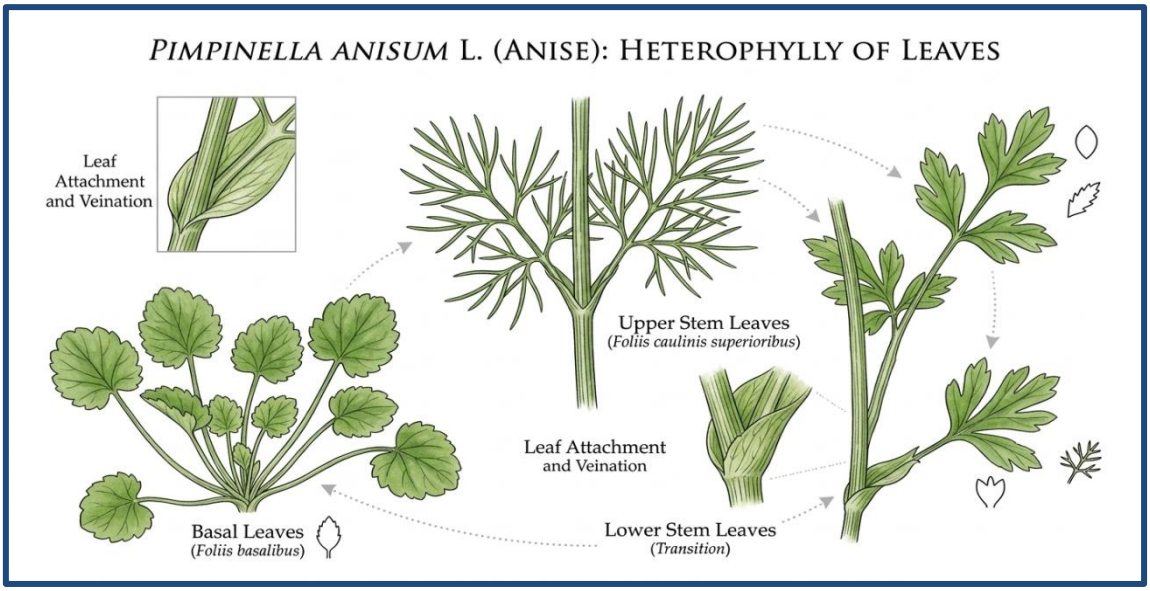
The flowers are small, white, bisexual, and borne in compound, drooping umbel-like clusters [21]. Each flower is approximately 1-2 mm long and has a strong, aromatic scent that attracts many bees and pollinating insects [22].



Figure(I-3) Image of Pimpinella anisum L flowers

7-4. Leaves:

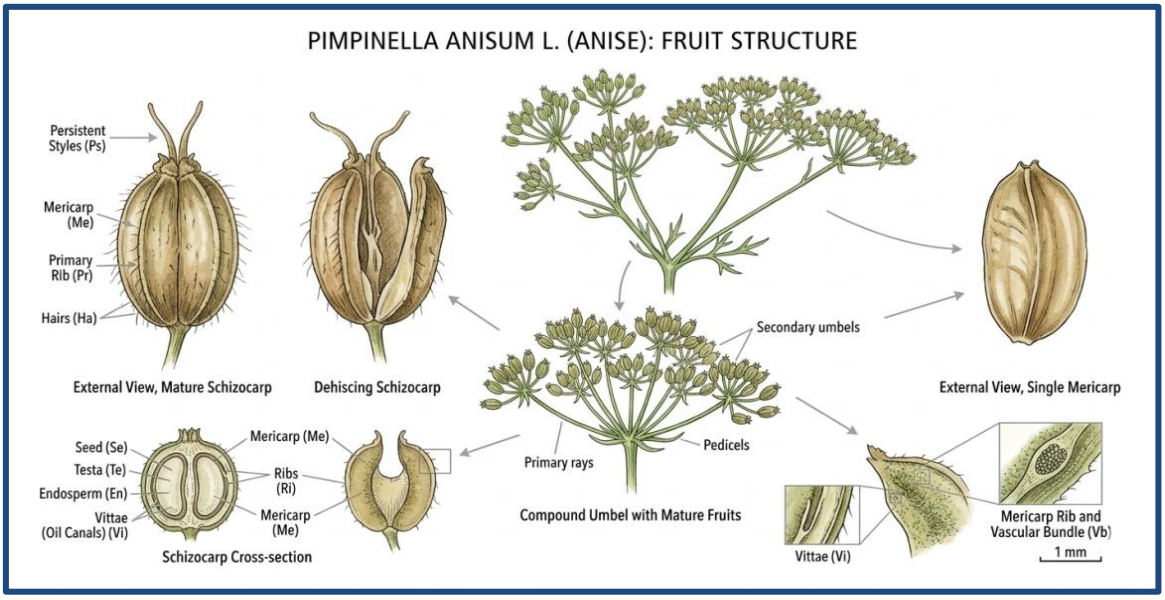
The leaves are characterized by a varied arrangement. The basal leaves have long petioles and a heart-shaped, toothed appearance, while the upper leaves are denser at the margins, pinnate, and divided into fine, thread-like lobes [23]. The leaves range in length from 2 to 5 cm. Young leaves are bright green, and when mature, they retain their asymmetrical, toothed shape at the margins [24].



Figure(I-4) Image of Pimpinella anisum L leaves .

7-5. Fruit:

The fruit is a dry, smooth, oval or pear-shaped drupe, approximately 3-5 mm long. When ripe, it is grayish-green and consists of a pulp containing the active ingredient [25].



Figure(I-5) Image of Pimpinella anisum L fruit

7-6. Seeds:

The seed consists of fine oil channels (vittae) found in the fruit's outer layer. It is the most commonly used part in the pharmaceutical, food, and pest control industries [26].

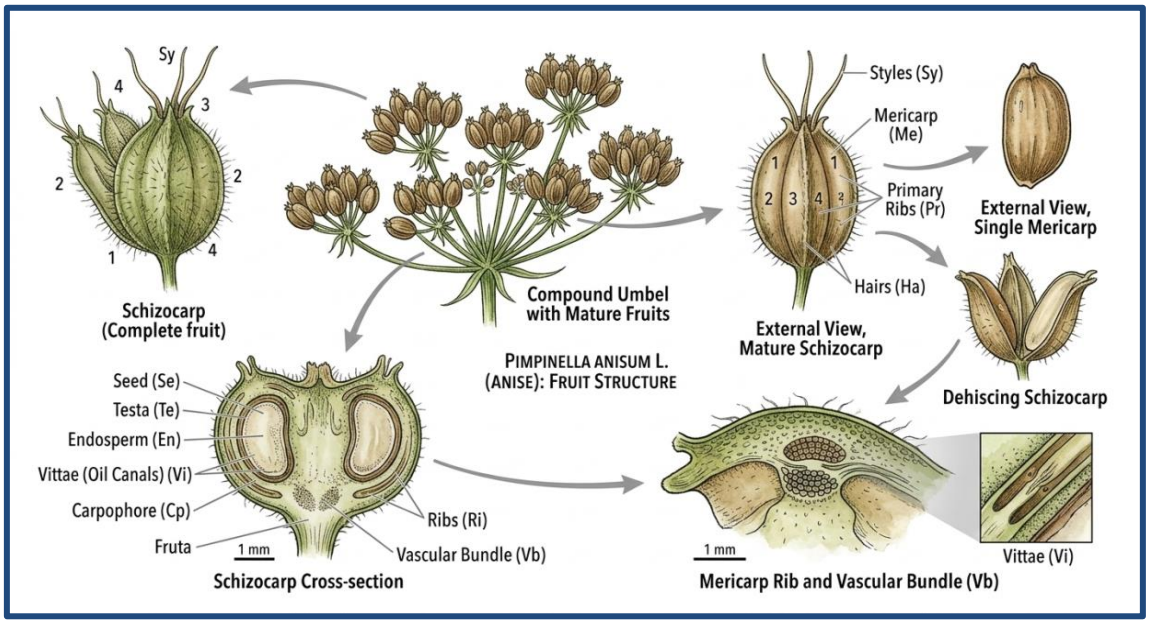


Figure (I-6) Image of Pimpinella anisum L seeds

8. Cultivation Requirements of *Pimpinella anisum L*:

The tree's morphology is adapted to temperate and warm climates [23].It grows well in fertile, well-drained (sandy loam) soils and requires little water and plenty of direct sunlight [17]. It grows naturally in areas with rainfall ranging from 400 to 600 mm [24]. It thrives in temperatures between 18 and 25°C and cannot tolerate waterlogged soil [25]. The optimal pH range for its growth is 6.0 to 7.5. When planting, row spacing of at least 30 to 40 cm should be maintained to ensure proper growth [26].

9. Chemical Composition of *Pimpinella anisum L* :

Anise is a unique aromatic and medicinal plant containing a complex mixture of bioactive compounds, primarily concentrated in its seeds (fruits). Anise contains between 2% and 7% volatile oils, which are responsible for its therapeutic properties and distinctive aroma [27].

The chemical constituents of anise can be classified into phenolic compounds, terpenes, and flavonoids, in addition to fixed oils and proteins [28].

9-1. Phenylpropanoids:

Phenylpropanoids constitute the most prevalent chemical family in anise essential oil (85–97%). All its compounds share a single basic structure: a benzene ring attached to a three-carbon chain (C_6–C_3).

- **Anethole** ($C_{10}H_{12}O$, 148.20 g/mol, 80–95%) is the undisputed dominant compound in the oil. Its full chemical name is (E)-1-methoxy-4-(prop-1-en-1-yl)benzene. Its structure consists of a benzene ring containing a methoxy group (-OCH_3) in the Para position and a propenyl group in the E (trans) position. This structure gives it high thermal stability and strong biological activity (antimicrobial, phytoestrogenic, anti-inflammatory). It is primarily responsible for the oil's characteristic anethole odor [29].
- **Estragon-methyl chavicol** ($C_{10}H_{12}O$, 148.20 g/mol, 1–5%): It differs from anethole in the position of the double bond (at the end of the side chain, not in the middle). It has antibacterial and antifungal activity, but there are concerns about its potential genotoxicity when ingested in concentrated doses[30].
- **Anisaldehyde/para-anisaldehyde** ($C_8H_8O_2$, molecular weight 136.15 g/mol, traces - 0.3%): a partial oxidation product of trans-anethole. It imparts a delicate, sweet, and floral note to the oil and is used in perfumery [30].

9-2. Monoterpenes (C_{10}) :

Monoterpenes are compounds containing ten carbon atoms (C_{10}) and constitute 1-4% of essential oil. They are classified as hydrocarbons (without oxygen) and oxidized (containing an oxygen group):

- **α-Pinene and β-Pinene** ($C_{10}H_{16}$, molecular weight 136.23 g/mol): bicyclic compounds of the Pinene family. It imparts a woody, resinous aroma. Its concentration is less than 0.5%, but it contributes to a synergistic antimicrobial effect[35].
- **Limonene** ($C_{10}H_{16}$, 136.23 g/mol, traces -1%): A monocyclic terpene with a lemony aroma. Extensive studies have demonstrated its antioxidant and anticancer properties[31].
- **Linalool** ($C_{10}H_{18}O$, 154.25 g/mol): A monoterpene alcohol with a floral aroma. It is known for its calming effect on the central nervous system and its anxiolytic properties. [31]
- **1,8Cineole-eucalyptol** ($C_{10}H_{18}O$, 154.25 g/mol): A monoterpene oxide with a camphor-like odor. It stimulates the cilia of the respiratory tract and is used to treat congestion and coughs[31].

9-3. Sesquiterpene Family (C_{15})

Sesquiterpene are compounds containing fifteen carbon atoms (C_{15}) and constitute between 0.5 and 4% of the essential oil, giving it aromatic richness and additional biological depth:

- **Alpha-Hemachaline** ($C_{15}H_{24}$, 204.35 g/mol, 0.5–3%): A tricyclic Sesquiterpene from the hemachaline family, rare and characteristic of this plant species. It has documented insecticidal activity and is a key chemical indicator for Algerian anise[32].
- **Caryophyllene oxide** ($C_{15}H_{24}O$, 220.35 g/mol): This is the oxidation product of beta-Caryophyllene and contributes to the antifungal and insecticidal activity[32].

In addition to volatile oils, anise contains non-volatile compounds that contribute to its efficacy, such as caffeic acid and chlorogenic acid, both potent antioxidants[33].

Non-isoprenoid components also include lipids (approximately 10–25%), proteins (approximately 18%), and essential minerals[34].

These active compounds are highly soluble in organic solvents such as ethanol and methanol, making anise extracts extremely effective against fungi and plant pathogens[35].

Bibliography

[1] Ba-Deeb, A. S. (2018). Medicinal Plants in Yemen. Sana'a: Al-Irshad Library.

[2] Abdo Omran, M., & Fikri Kamal, K. (2019). Medicinal and Aromatic Plants and Their Medical Uses: Herbs, Oils, and Plants. Herbs, Oils and Plants Publishing.

[3] E. J. Allan, T. Stuchbury, and A. J. Mordue, Eds., Biotechnology in Agriculture and Forestry. Medicinal and Aromatic Plants XI, Y. P. S. Bajaj., vol. Azadirachta indica n. India, 1999.

[4] USDA, Agricultural Research Service. (2024). *Pimpinella anisum L*. Germplasm Resources Information Network (GRIN).

[5] Quattrocchi, U. (2016). CRC World Dictionary of Medicinal and Poisonous Plants. CRC Press.

[6] Gledhill, D. (2008). The Names of Plants (4th ed.). Cambridge University Press.

[7] World Health Organization. (1999). WHO monographs on selected medicinal plants (Vol. 1). Geneva: WHO.

[8] Ross, I. A. (2001). Medicinal Plants of the World: Chemical Constituents, Traditional and Modern Medicinal Uses. Humana Press.

[9] Evans, W. C. (2009). Trease and Evans' Pharmacognosy (16th ed.). Saunders Elsevier.

[10] Simpson, M. G. (2019). *Plant Systematics* (3rd ed.). Academic Press.

[11] Ross, I. A. (2001). Medicinal Plants of the World. Humana Press.

[12] Shojaii, A., & Abdollahi Fard, M. (2012). Review of Pharmacological Properties and Chemical Constituents of *Pimpinella anisum L*. ISRN Pharmaceutics.

[13]Sun, W., et al. (2019). Bioactive compounds for management of inflammation and oxidative stress in Anise. Journal of Functional Foods.

[14]European Medicines Agency. (2014). Assessment report on *Pimpinella anisum L*., fructus.

[15] Heuzé, V., et al. (2017). Anise *(Pimpinella anisum L)* seeds and oil meal. Feedipedia.

[16] World Health Organization. (1999). WHO monographs.

[17] Simpson, M. G. (2019). Plant Systematics.

[18] Evans, W. C. (2009). Trease and Evans' Pharmacognosy.

[19] Gledhill, D. (2008). The Names of Plants.

[20] Flora of China. Vol. 14 (Apiaceae).

[21] Weiss, E. A. (2002). Spice Crops.

[22] Gupta, V. K., et al. (2014). Agronomic Requirements of Anise.

[23] European Medicines Agency. (2014). Assessment report on P. anisum.

[24] Heuzé, V., et al. (2017). Anise seeds. Feedipedia.

[25] USDA. (2024). GRIN Database.

[26] IPNI. (2024). *Pimpinella anisum L*.

[27] Orav, A., et al. (2008). Composition of the essential oil of *Pimpinella anisum L*. from different countries.

[28] Shahamat, M., et al. (2020). Chemical composition and pharmacological properties of Anise.

[29] Khalil, A. A., et al. (2016). Essential oil of Anise: Current applications and future prospects.

[30] Rodrigues, V. M., et al. (2003). Isolation of anise essential oil by supercritical extraction.

[31] Ullah, H., et al. (2021). Phytochemical and therapeutic potential of *Pimpinella anisum L*.

[32] Hammoudi, S. M., et al. (2011). Chemical composition and antioxidant activity of the essential oil of *Pimpinella anisum L*. from Algeria. Journal of Essential Oil Bearing Plants, 14(3), 320-327.

[33] Sun, W., et al. (2019). Phenolic compounds and antioxidant activities of edible seeds.

[34] Singh, G., et al. (2002). Chemical constituents of the essential oil and oleoresin of Anise.

[35] Akhtar, M. S., et al. (2014). Antifungal activity of Anise essential oil against plant pathogens.

CHAPTER TWO

BIOLOGICAL ACTIVITIES

Introduction:

The biological activity of phenolic compounds refers to their ability to influence vital processes within living organisms, whether these effects are beneficial or harmful. Phenolic compounds are among the most prominent secondary metabolites found in the plant kingdom, characterized by their common chemical structure based on an aromatic ring linked to one or more hydroxyl groups (-OH) [1].

In the biological and medical fields, pharmaceutical and experimental studies have demonstrated that phenolic compounds possess a wide range of biological activities, foremost among them antioxidant activity, which is based on their ability to neutralize free radicals and reduce the production of reactive oxygen species (ROS) [2].

In addition, they exhibit anti-inflammatory activity by inhibiting enzyme pathways such as COX-2 and LOX [3], and antimicrobial activity by targeting the biological membranes of pathogenic organisms [4].

This multifaceted biological activity stems from three overlapping mechanistic levels: firstly, at the direct molecular level, through their interaction with and removal of free radicals; Secondly, at the level of enzyme regulation, they inhibit or activate defensive enzyme chains such as SOD, CAT, and GPx; and thirdly, at the level of gene expression [5].

Based on this, assessments of the biological efficacy of phenolic compounds have become a fundamental methodological pillar in multiple fields, including medicine and pharmaceuticals (within the framework of novel drug discovery), functional nutrition, sustainable agriculture (as biopesticides), and the food industry (as natural preservatives) [6].

This assessment essentially aims to determine the efficacy and biosafety of these compounds before their use in therapeutic or preventative applications.

1. Antioxidants:

1-1. Definition of Antioxidants:

Antioxidants are molecules or chemical compounds capable of inhibiting or delaying oxidation processes occurring in other substances, even when present in very low concentrations compared to the oxidizable substance [7]. In 1999, Halliwell defined antioxidants as: "Any substance that significantly inhibits or reduces the oxidative oxidation of a substrate when present in concentrations low compared to that substrate" [8].

Chemically, antioxidants act as electron donors or hydrogen donors, enabling them to neutralize free radicals and halt oxidative chain reactions [9].

Basic Chemical Equation: The mechanism of action is illustrated by the following reaction:

$$AH + R\bullet \longrightarrow A\bullet + RH$$

Where: **AH**: Antioxidant (reduced form).

R•: Free radical (unstable).

A•: Antioxidant radical (chemically stable form due to resonance).

RH: The neutral (safe) compound.

1-2. Classification of Antioxidants:

Antioxidants are classified according to source and chemical nature criteria into:

☒ Natural Antioxidants:

- **Antioxidant Enzymes**: These represent the first line of defense within cells. They are specialized enzymes that break down free radicals and convert them into less harmful compounds. They work cooperatively:

a) Superoxide dismutase (SOD): Converts the superoxide ion $O_2^{\bullet -}$ to hydrogen peroxideH_2O_2.

$$2O_2^{\bullet -} + 2H^+ \overset{\text{SOD}}{\Longrightarrow} H_2O_2 + O_2$$

b) Catalase (CAT): An enzyme containing a heme group, it breaks down H_2O_2 into water and oxygen at tremendous speed.

$$2H_2O_2 \overset{\text{CAT}}{\Longrightarrow} 2H_2O + O_2$$

c) Glutathione peroxidase (GPx) : An enzyme containing selenium, it hydrolyzes H_2O_2 and organic peroxides using reduced glutathione (GSH)

$$H_2O_2 + 2\ \text{GSH} \overset{\text{GPx}}{\Longrightarrow} 2H_2O + GSSG$$

d) Peroxyridoxine (Prx): A thiol-group-dependent enzyme family that processes locally produced hydrogen peroxide.

- **Non-enzymatic antioxidants:** Water-soluble: such as vitamin C (ascorbic acid), glutathione (GSH), and uric acid. Fat-soluble: such as vitamin E (tocopherol) and carotenoids (such as beta-carotene).
- **Synthetic antioxidants**: These are chemical compounds added industrially to food products and oils to prevent their oxidation and spoilage. The most important are:

BHA: butylhydroxyanisole.

BHT: butylhydroxytoluene.

TBHQ: tert-butylhydroquinone.

PG: propyl gallate.

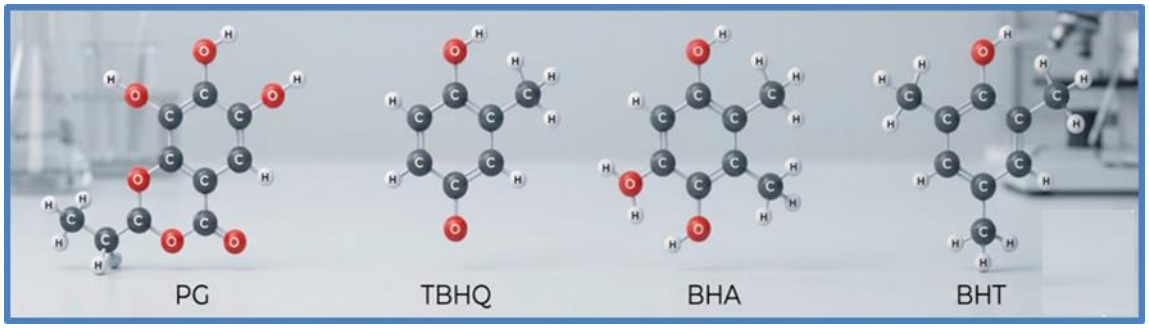


figure (II 1) Chemical structures of (PG, TBHQ, BHA, BHT).

1-3. Comparison of types of antioxidants:

Table(II-1) Comparison of types of antioxidants

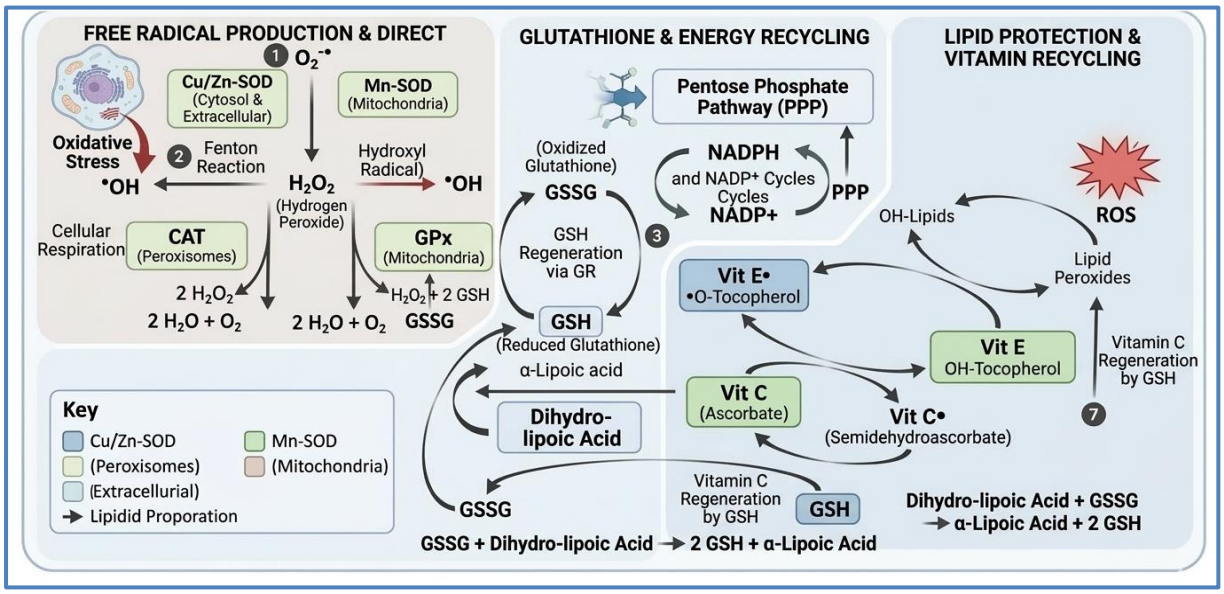
Type	Site	Substrate	Example
Enzymatic	Intracellular	O_2•$^-$, H_2O_2	SOD, CAT, GPx
Vitamins	All Tissues	R•, ROO•	Vit C, Vit E
Polyphenols	Nutritional / Plasma	Multiple	Quercétine, Resveratrol
Auxiliary metals	As a catalyst	Indirectly	Se, Zn, Mn, Cu

1-4. The Mechanisms of the Antioxidant Defense System:

Exposure of cells, tissues, and extracellular matrix to oxidative stress triggers a complex internal defense response. Antioxidants, operating through multiple molecular mechanisms, neutralize free radicals and their derivatives.The roles of the molecules comprising the antioxidant defense network in living systems are distributed across two levels: protective and therapeutic. Based on their sequence of functions in the face of oxidative stress, this system can be classified into four main lines of defense, as shown in the table.

table (II-2) The Mechanisms of the Antioxidant Defense System

defense lines	**Mechanism of action and Participants**
First line of defense (protective defense)	***Mechanism of action:*** Prevents the formation of free radicals in the cell in the first place. ***Participants:*** Enzymatic antioxidants (such as SOD) with metal-binding proteins and non-enzymatic protective antioxidants.
Second line of defense (capture and neutralization)	***Mechanism of action***: Rapidly inactivates free radicals and reactive oxidants to prevent the spread of the chain reaction. ***Participants:*** Non-enzymatic antioxidants (such as vitamins C and E) that capture and neutralize the radicals.
Third line of defense (repair and restoration)	***Mechanism of action:*** Repairs biological damage that has already occurred in DNA, proteins, and lipids. ***Participants:*** Specific repair enzymes that target molecules damaged by reactive oxygen species (ROS).
Fourth line of defense (adaptation and signal transduction):	***Mechanism of action:*** Activates the cellular response and signaling system to precisely transport appropriate antioxidants to damaged sites. ***Participants:*** Cellular signaling pathways and sensory receptors that regulate oxidative balance.



Figure(II-2) integrated Network Antioxidant Defense Mechanisms

1-5. Free radicals:

1-5.1. Definition of free radicals:

Free radicals are defined as chemical particles atoms, molecules, or ions Its electronic structure contains one or more unpaired electrons in its outer orbits, which gives it a highly active chemical character [10]. As a result of this pursuit of electronic stability, these particles interact very rapidly with neighboring molecules, attempting to snatch the missing electron or get rid of the excess, During these reactions, highly active intermediate compounds are generated, which follow successive chains of reactions that may lead to cumulative damage at the cellular level.

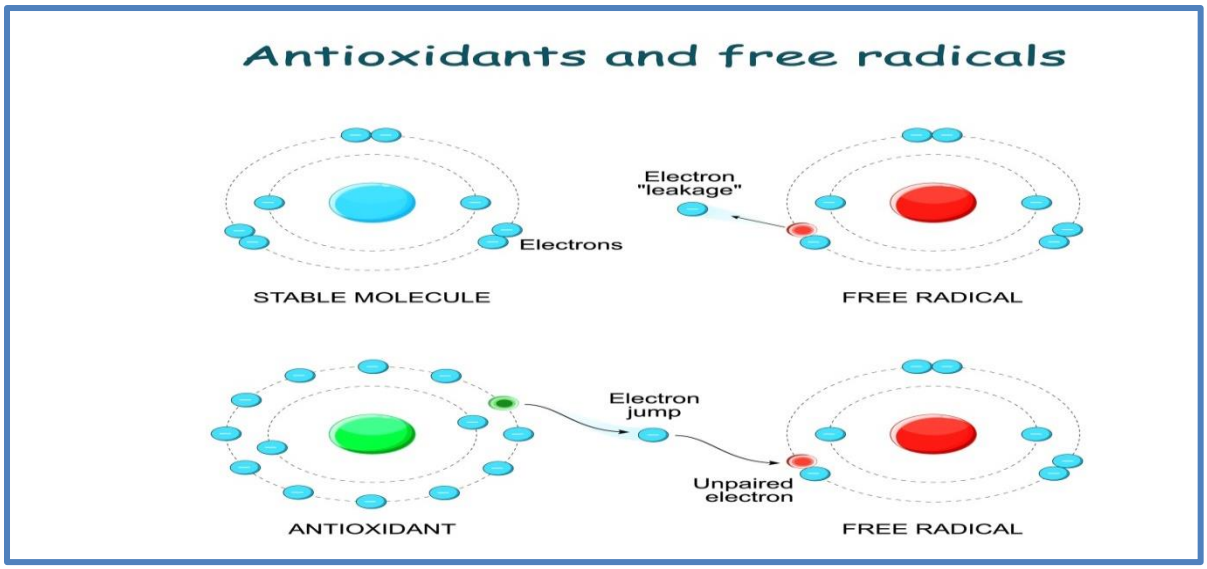


figure (II-3) The mechanism of action of antioxidants in neutralizing free radicals

1-5.2. Types of free radicals:

Free radicals originate primarily from normal metabolic processes within living cells , and are mostly derived from oxygen and nitrogen molecules, classifying them into two main categories :

- **Reactive Oxygen Species (ROS):**

This group includes a number of active compounds, most notably : monooxygen (O_2^1) , superoxide anion ($O_2•^-$), and hydroxyl radical. (•OH) Which is one of the most reactive free radicals and the most damaging to cellular components ,In addition to hydrogen peroxide (H_2O_2), which is classified as an oxidizing agent capable of releasing hydroxyl radicals by reacting with transition metal ions[11].

- **Reactive Nitrogen Species (RNS):**

These species primarily include the nitric oxide radical (•NO) , a molecule with a dual physiological role , at normal concentrations, it acts as a mediator of nerve and vascular signaling , while its overproduction leads to other problems. Toxic effects are particularly evident through its reaction with the superoxide anion to form peroxynitrite. ($ONOO^-$) , which is a highly effective oxidizing and nitrating agent [12] .

1-5.3. Classification of Free Radicals by Lifespan:

- **Very Short-Life Radicals:**

This class consists of highly reactive radicals that have a very short half-life under normal conditions, These radicals include hydrogen and nitrogen atoms, halogens, and small molecular radicals with low molecular weights such as the methyl radical ($• CH_3$), the ethyl radical ($• C_2H_5$), the phenyl radical ($• C_6H_5$), and the hydroxyl radical (•OH). The half-life of these radicals ranges from fractions of a second to microseconds, and therefore they cause immediate and localized damage at their point of origin [13].

- **Relatively Long-Life Radicals:**

This category includes radicals whose lifetimes are measured in seconds, minutes, hours, and possibly days. A prime example is the diphenylpicrylate radical. The highly stable synthetic organic compound hydrazyl (DPPH•) is a purple solid powder that is stable at room temperature. This exceptional stability is due to the fact that most aromatic radicals possess multiple resonant structures that distribute the density of unpaired electrons over a wide molecular area, preventing them from concentrating in one place and slowing their reactivity [14].

1-5.4. Sources of Free Radicals :

❖ **Internal (Endogenous) Sources:**

Living cells produce free radicals as inevitable byproducts of many basic biological processes. Among the most prominent of these processes are oxidation reactions in the electron transport chains within mitochondria. Phagocytic cells and immune cells also produce large quantities of free radicals to fight foreign substances in cases of inflammatory and immune responses. Chronic psychological and physical stress, low blood oxygen levels (ischemia), and decreased oxidative efficiency associated with aging also contribute to this [15].

❖ **External (Environmental) Sources:**

The body is exposed to a wide range of environmental factors that induce the generation of free radicals, the most prominent of which are shown in the following table.

table (II-3) External sources of free radicals and their biological mechanisms

Source	Mechanism / Mécanisme
Smoking (Tabac)	Smoking tobacco contains more than 4,000 substances, including more than 40 carcinogenic substances; and produces 10^{15} gluten-free roots per grain.
radiation Ionizing (UV, X, γ)	Dismantle molecules Water : $H_2O \rightarrow$ OH• + H• ; It causes Fractures double In DNA
pollution Environmental ($PM2.5, O_2$)	particles minute to bear minerals transitional Stimulates interaction Fenton in lung
Medicines	Paracetamol In doses High, The chemical compound doxorubicin , Nitrofurantoin
pesticides Insecticides	Parquet , Rotenone disables Complex I in mitochondria Generating O2 • ⁻
alcohol ethyl	Oxidized to acetaldehyde then to root Hydroxyethyl CH_3CH • OH causing fibrosis liver
X-rays above Violet (UVA/UVB)	Single oxygen (O_2) is produced by the visual sensory process. It causes the oxidation of guanine in DNA.

2. Anti-inflammatory Activity:

Inflammation is defined as a physiological defensive response of living tissues to harmful stimuli, such as microbial agents, physical injuries, and irritating chemical substances [16]. However, its progression into a chronic state paves the way for serious diseases such as diabetes, cancer, cardiovascular diseases, and arthritis [17]. The acute inflammatory response occurs through four sequential and interconnected stages:

- Recognition and Detection.
- Release of Inflammatory Mediators.
- Vasodilation and Increased Permeability.
- Leukocyte Migration.

2-1. Protein Denaturation:

Exposure of proteins to factors such as heat or oxidation leads to the loss of their functional structure. The immune system recognizes these denatured proteins as Damage-Associated Molecular Patterns (DAMPs), triggering an extensive cascade of inflammatory signals. In the context of immune and inflammatory responses, protein denaturation represents a critical axis [18].

2-2. Mechanism of Protein Stabilization:

Phenolic compounds inhibit the denaturation of albumin through two primary mechanisms:

1) Formation of hydrophobic bonds with the non-polar regions of the protein, thereby enhancing its structural stability.

2) Inhibition of the oxidation of free sulfhydryl (–SH) groups in the protein, which are considered among the most vulnerable sites to oxidative denaturation [19].

Anti-inflammatory activity is evaluated in vitro via the Bovine Serum Albumin (BSA) denaturation inhibition assay [20].

3. Antimicrobial Activity:

This activity relies on the substance's ability to inhibit the growth of microorganisms (bacteriostatic) or kill them (bactericidal/fungicidal).

3-1. Definition of Bacteria:

Bacteria are microscopic, single-celled organisms invisible to the naked eye. They lack a nuclear envelope and are surrounded by membranes. They occur naturally in various shapes (rod-shaped, spherical, spiral) and typically range in size from 0.5 to 5 micrometers. They have the ability to survive for extended periods without being affected by unfavorable environments and harsh conditions [21].

3-2. General Structure of Bacteria:

Bacteria consist of basic components found in all types of bacteria, including:

- **Cell Wall**: Characterized by its rigidity, it protects the bacteria from external attack due to its distinctive shape. It is composed of two substances: carbohydrates and peptides.
- **Plasma**: A thin membrane composed of lipids and proteins, approximately 7.5 nm thick, responsible for regulating the passage of substances.
- **Cytoplasm**: A gel-like substance in which the genetic material (DNA) and ribosomes, the site of protein synthesis, are suspended [22].
- **Nucleus**: A chromosome coiled upon itself, not enclosed by a nuclear envelope, located in the center of the cell. It is responsible for controlling the cell's functions and characteristics.

Bacteria also possess appendages found in certain types, such as flagella for movement, cilia for attachment, and spores to prevent bacterial adhesion to phagocytic cells. The spores, present in some types of bacteria, serve as a form of resistance against harsh environmental conditions, allowing them to survive for longer periods [23].

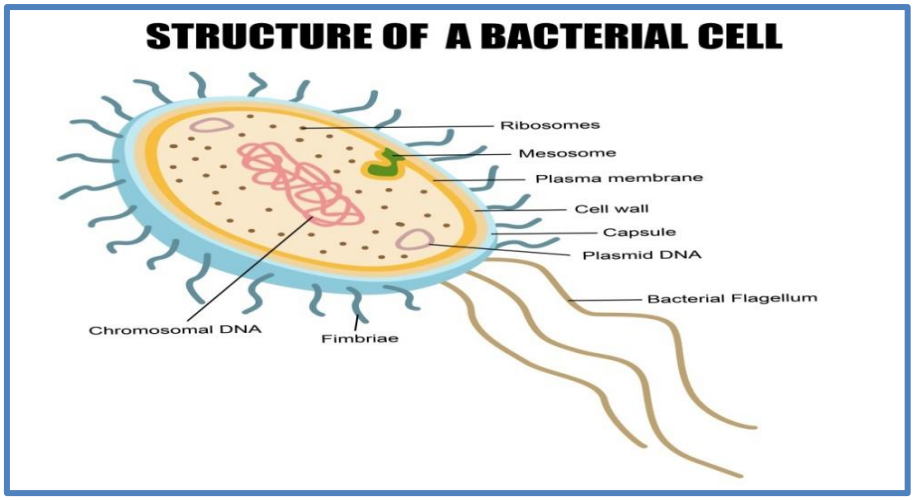


figure (II-4) Bacterial cell structure and its components

3-3. Bacterial Cell Wall Structure:

Sensitivity to essential oils varies based on the type of bacteria:

- **Gram-positive bacteria (G+):** More sensitive due to the ease of oil penetration through the thick, porous peptidoglycan layer.
- **Gram-negative bacteria (G-):** Exhibit higher resistance due to the presence of an outer membrane (LPS) that acts as a selective barrier [24].

3-4. Mechanism of Action (Killing Mechanism):

Essential oils utilize their Lipophilicity to integrate into the cytoplasmic membrane. This integration causes:

- Increased membrane fluidity and disruption of its molecular organization.
- Leakage of vital cellular contents (e.g., potassium ions and ATP), ultimately leading to cell death. [25]

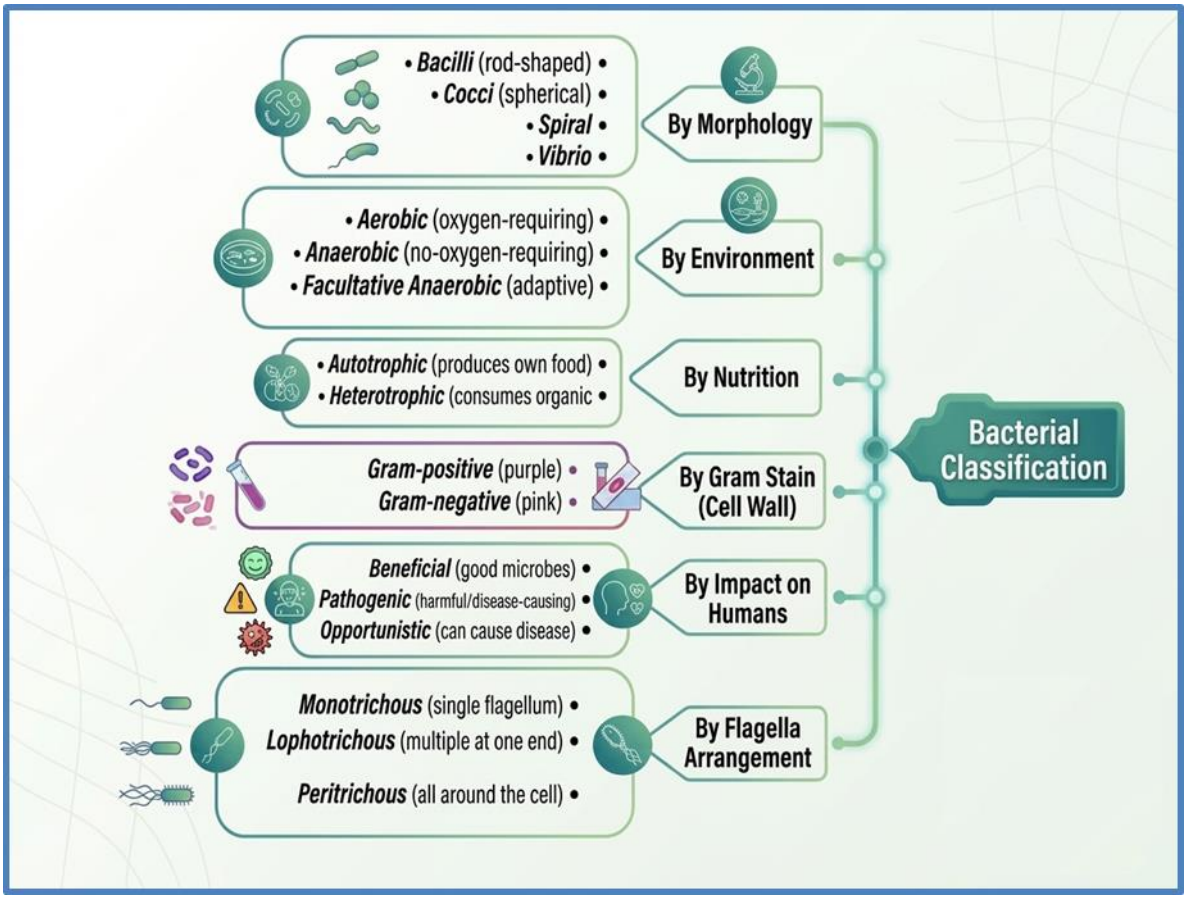
3-5. Synergistic Effect of Compounds:

Volatile oil compounds do not act in isolation; rather, their mixture exerts a synergism that multiplies the antimicrobial efficacy. This explains why the whole essential oil achieves higher effectiveness than a single isolated compound, due to:

- Diversity of attack sites on the bacterial cell simultaneously.
- Reduction in the chances of bacterial resistance compared to single-target antibiotics.
- The role of some secondary compounds in enhancing membrane permeability, facilitating the entry of other compounds[26].

3-6. Classification of Bacteria:

Bacteria are classified as follows: [22]



Figure(II-5) Classification of Bacteria

3-7. Antibiotics and Resistance:

❖ **Types of Antibiotics:**

They are classified according to their effect into:

- Bactericidal antibiotics: These kill bacteria directly (such as penicillin).
- Bacteriostatic antibiotics: These prevent bacterial growth (such as sulfonamide) [27].

❖ **Actions of Antibiotics:**

They work by targeting specific weaknesses in the bacterial cell:

1. Inhibiting cell wall synthesis.
2. Inhibiting protein synthesis (via ribosomes).
3. Inhibiting nucleic acid synthesis (DNA/RNA).

❖ **Bacterial Resistance:**

This refers to the ability of bacteria to withstand the effects of antibiotics that previously killed them. This occurs naturally as a result of genetic mutations or is acquired through the acquisition of resistance genes, leading to modification of the target or the secretion of enzymes that break down the antibiotic (such as β-lactamase) [28].

4. Cytotoxicity and Hemotoxicity as Biosafety Standards:

Toxicological studies are essential to determine the safety of plant extracts before medical use. Cytotoxicity is the ability to cause damage or death to living cells independently of immune effects. It is evaluated by the CC_{50} (Cytotoxic Concentration 50), which is the concentration required to damage or kill 50% of in vitro cultured cells over a specific period. Standardized cell lines are used, such as Vero, HeLa, MCF-7, HepG2, and human red blood cells (RBCs) [29].

4-1. Hemolysis Assay:

Hemolysis is the rupture of red blood cell membranes and the leakage of their hemoglobin content into the surrounding medium. The effect is estimated by measuring the released hemoglobin at 540 nm relative to a positive control (distilled water = 100% hemolysis) [30].

- This assay measures the substance's impact on RBC membranes.
- It serves as an ideal model for studying effects on the phospholipid bilayer.

4-2. Safety Criteria:

A substance is classified according to ASTM F756 standards as:

- Safe (Non-hemolytic): If the hemolysis percentage is less than 5%.

- Rejected for biological use: If the percentage exceeds 25%[31].

4-3. Selectivity Index (SI):

The Selectivity Index (SI) is used to distinguish between the effective therapeutic concentration and the toxic concentration. A substance is medically accepted if its SI value exceeds 10[32].

5. Anti-Diabetes Action:

5-1. Definition of Diabetes:

Diabetes is defined as a chronic metabolic disorder characterized by persistent hyperglycemia. This dysfunction stems from insufficient insulin secretion by the beta cells (β-cells) in the pancreas, or from a decreased response of surrounding tissues to this hormone (insulin resistance), or a combination of both factors, leading to a profound imbalance in the body's carbohydrate, lipid, and protein metabolism [33].

5-2. classifications of Diabetes:

Diabetes is classified according to its pathogenesis into three main types:

A). Type 1 Diabetes (Type 1 DM): Also known as insulin-dependent diabetes mellitus (IDDM), it is an autoimmune disease resulting from the selective destruction of pancreatic beta cells by antibodies, leading to a severe and absolute insulin deficiency. It usually appears in childhood or adolescence and is divided into two subtypes:

- **Type 1a**: Represents about 90% of cases and has a clear autoimmune origin.
- **Type 1b**: Represents about 9% and is idiopathic (of unknown cause).

There is also another type of diabetes that affects children, type **MODY**: a rare form resulting from specific gene mutations that affect the function of beta cells without immune intervention.

B). Type 2 Diabetes (Type 2 DM): This is the most common type worldwide (up to 95%), and is known as non-insulin-dependent diabetes mellitus (NIDDM) [34].

It is characterized by tissue resistance to insulin with a relative deficiency in its secretion. It is often associated with lifestyle factors such as obesity, advancing age, and genetic predisposition. It may remain undiagnosed for extended periods due to its mild clinical symptoms in its early stages.

C). Gestational Diabetes: A condition of glucose intolerance that first appears during the second or third trimester of pregnancy. Although blood sugar levels often return to normal after delivery, it is a strong indicator of an increased risk of the mother developing type 2 diabetes later in life [33].

5-3. Antidiabetic activity:

Antidiabetic activity refers to the ability of chemical compounds (whether plant extracts or synthetic molecules) to restore blood glucose homeostasis through multiple biochemical pathways, the most important of which are:

- Stimulation of the pancreatic axis: by promoting insulin secretion from the remaining beta cells.
- Modulation of the cellular response: by reducing insulin resistance and increasing glucose permeability across the cell membrane.
- Inhibition of enzymes: Some compounds act as inhibitors of digestive enzymes such as α-amylase, slowing the breakdown of complex carbohydrates and reducing glucose absorption in the intestine [35].
- Control of hepatic glucose levels: by inhibiting gluconeogenesis.

5-4. Oral treatments for type 2 diabetes:

The treatment strategy for type 2 diabetes relies on the use of oral hypoglycemic agents, through multiple mechanisms, when diet and physical activity are insufficient. These drugs (such as biguanides and sulfonylureas) improve insulin sensitivity or reduce glucose production in the liver.

5-5. Alpha-amylase enzyme:

This enzyme is secreted by saliva and the pancreas. It breaks down the chemical bonds in complex starches, converting them into simple sugars (glucose). Alpha-amylase is classified as one of the most important digestive enzymes and belongs to the hydrolase family. It plays a pivotal role in carbohydrate metabolism in mammals and is primarily secreted by the salivary glands and pancreas.

Mechanism of Action:

The enzyme attacks the α1,4-glycosidic bonds found in the inner chains of starch and glycogen. As an endosymbiotic enzyme, it randomly breaks down these long chains into smaller molecules.

5-6. The Enzyme's Relationship to Diabetes (Biological Link):

Under normal conditions, the activity of this enzyme leads to a rapid release of glucose in the small intestine, raising blood sugar levels after meals. In diabetic patients, the activity of this enzyme becomes a therapeutic target. Researchers are seeking to find natural inhibitors capable of partially suppressing enzyme activity, thereby slowing down starch digestion and preventing sudden and sharp spikes in blood sugar levels [36].

Bibliography:

[1] Minatel, I. O., et al. (2017). "Phenolic Compounds: Physicochemical Properties and Biological Activities." Superfood and Functional Food.

[2] Hano, C., & Tungmunnithum, D. (2020). "Plant Polyphenols, Antioxidant Capacity and Evidence of Health Benefits." Antioxidants.

[3] Ambriz-Pérez, D., et al. (2016). "Phenolic compounds: From plants to foods and health." Food & Function.

[4] Lin, D., et al. (2016). "Activities of Phenolic Compounds from Plant Sources." Molecules.

[5] Sandhu, A. K., & Guwanayake, M. (2023). "Bioavailability and Mechanisms of Action of Phenolic Compounds." Journal of Agricultural and Food Chemistry.

[6] Tungmunnithum, D., et al. (2018). "Flavonoids and Other Phenolic Compounds: Role in Health and Applications." Medicines.

[7] Apak, R., et al. (2016). "Antioxidant Capacity and Activity Measurement: Theory and Applications." Wiley Series on Methods and Applications in Analytical Chemistry.

[8] Halliwell, B., & Gutteridge, J. M. (1999). Free Radicals in Biology and Medicine. Oxford University Press, 3rd Edition.

[9] Brewer, M. S. (2011). "Natural Antioxidants: Sources, Compounds, Mechanisms of Action, and Applications." Comprehensive Reviews in Food Science and Food Safety.

[10] Halliwell , B., & Gutteridge , J. M. C. (2015). Free Radicals in Biology and Medicine (5th ed .). Oxford University Press.

[11] Phaniendra , A., Jestadi , D. B., & Periyasamy , L. (2015). Free radicals: Properties, sources, targets, and their implication in various diseases. Indian Journal of Clinical Biochemistry, 30(1), 11–26.

[12] Pacher , P., Beckman, J. S., & Liaudet , L. (2007). Nitric oxide and peroxynitrite in health and disease. Physiological Reviews, 87(1), 315–424.

[13] Sharma, P., Jha , A. B., Dubey , R. S., & Pessarakli , M. (2012). Reactive oxygen species, oxidative damage, and antioxidative defense mechanism in plants under stressful conditions. Journal of Botany, 2012, 217037.

[14] Brand-Williams, W., Cuvelier , M. E., & Berset , C. (1995). Use of a free radical method to evaluate antioxidant activity. LWT – Food Science and Technology, 28(1), 25–30.

[15] Liguori , I., Russo, G., Curcio , F., Bulli , G., Aran , L., Della- Morte , D., ... & Abete , P. (2018). Oxidative stress, aging , and diseases . Clinical Interventions in Aging , 13, 757–772.

[16] Medzhitov, R. (2008). Origin and physiological roles of inflammation. Nature, 454(7203), 428-435.

[17] Furman, D., et al. (2019). Chronic inflammation in the etiology of disease across the life span. Nature Medicine, 25(12), 1822-1832.

[18] Rock, K. L., & Kono, H. (2008). The inflammatory response to cell death. Annual Review of Pathology, 3, 99-126.

[19] Gunathilake, K., et al. (2018). In Vitro Anti-Inflammatory Properties of Selected Edible Leaves. Biomedicines, 6(4), 107.

[20] Mizushima, Y., & Kobayashi, M. (1968). Interaction of anti-inflammatory drugs with serum proteins. Journal of Pharmacy and Pharmacology, 20(3), 169-173.

[21] Madigan, M. T., et al. (2020). Brock Biology of Microorganisms. 16th Edition. Pearson Education.

[22] Tortora, G. J., Funke, B. R., & Case, C. L. (2019). Microbiology: An Introduction. 13th Edition. Global Edition.

[23] Willey, J., Sandman, K., & Wood, D. (2019). Prescott's Microbiology. 11th Edition. McGraw-Hill Education.

[24] Nikaido, H. (2003). Molecular basis of bacterial outer membrane permeability revisited. Microbiology and Molecular Biology Reviews, 67(4), 593-656.

[25] Bakkali, F., et al. (2008). Biological effects of essential oils – A review. Food and Chemical Toxicology, 46(2), 446-475.

[26] Chouhan, S., et al. (2017). Antimicrobial Activity of Essential Oils: Mechanisms of Action and Possible Synergy. Frontiers in Microbiology, 8, 424.

[27] Walsh, C., & Wencewicz, T. (2016). Antibiotics: Challenges, Mechanisms, Opportunities. ASM Press.

[28] Blair, J. M., et al. (2015). Molecular mechanisms of antibiotic resistance. Nature Reviens Microbiologie, 13(1), 42-51.

[29] Indrayanto, G., et al. (2021). Validation of In-Vitro Cytotoxicity Assay of Herbal Extracts. Profiles of Drug Substances, Excipients and Related Methodology, 46, 273-307.

[30] Evans, B. C., et al. (2013). Ex vivo red blood cell hemolysis assay for monitoring toxicity of synthetic compounds. Journal of Visualized Experiments, (73), e50166.

[31] ASTM F756-17. Standard Practice for Assessment of Hemolytic Properties of Materials. ASTM International.

[32] Koch, A., et al. (2005). Evaluation of plants used for antimalarial treatment by the Maasai of Kenya. Journal of Ethnopharmacology, 101(1-3), 95-99.

[33] American Diabetes Association (ADA). (2023). Classification and Diagnosis of Diabetes: Standards of Care in Diabetes. Diabetes Care Journal.

[34] Holt, R. I., et al. (2017). Textbook of Diabetes. 5th Edition. Wiley-Blackwell.

[35] Tundis, R., et al. (2010). Natural Products as α-Amylase and α-Glucosidase Inhibitors and their Hypoglycaemic Activity in the Treatment of Diabetes. Mini Reviews in Medicinal Chemistry.

[36] Sales, P. M., et al. (2012). α-Amylase Inhibitors: A Review of Raw Material and Isolated Compounds from Plant Source. Journal of Pharmacy & Pharmaceutical Sciences.

CHAPTER THREE

IN SILICO STUDIES

Introduction:

Computer simulation is one of the most prominent modern scientific tools that has revolutionized the field of pharmaceutical chemistry and drug design. Drug discovery and development have undergone a radical transformation in recent decades thanks to the tremendous advancements in computing power and artificial intelligence. Researchers can now study molecular interactions between potential drug compounds and target proteins within the computer system, eliminating the need for costly laboratory experiments at every stage of the research process [1].

1. Definition of Computer Simulation:

Computer simulation (in Silico) is defined as a set of mathematical and computational methods used to simulate the physical and chemical behavior of molecules at the atomic level. These methods include molecular dynamics, quantum mechanics, molecular mechanics, and molecular docking [2].

Molecular docking is one of the most widely used computer simulation techniques in pharmaceutical chemistry. It allows for the prediction of the binding position of a small molecule (ligand) within a target protein binding site and the estimation of the energy of this binding. Some of the most prominent programs used in this context are: Auto Dock, Glide, VINA, and Gold [3].

2. The Concept of Molecular Docking:

2-1. Definition and Basic Principles:

Molecular docking is a computational technique that aims to predict the preferred orientation of a small molecule (ligand) when it binds to a larger receptor molecule (protein) to form a stable complex. This concept is based on Emil Fischer's lock-and-key hypothesis (1894), as well as the induced fit model, which takes into account the structural flexibility of the protein. The forces that control molecular binding include hydrogen bonds, van der Waals forces, electrostatic interactions, desolvation effects, and hydrophobic interactions [4].

2-2. Steps of Molecular Docking:

a) **Receptor Preparation:** Removal of water molecules, addition of hydrogen, and calculation of molecular charges.

b) **Ligand Preparation:** Determining the rotational degrees of freedom and calculating the charges using a method Gasteiger-Marsili.

c) **Grid Box Definition:** Determining the location and size of potential links.

d) Docking Operations: Applying the algorithm to find the optimal position.

e) Results Analysis and Position Evaluation: Using cluster analysis to classify positions [5].

3. AutoDock 4.2:

3-1. Software Overview:

AutoDock is a free and open-source software package developed by the Olson Lab at the Scripps Research Institute in the USA. The software consists of two main components:

- AutoGrid: Pre-calculates energy maps of the target protein, speeding up evaluation calculations during docking.
- AutoDock: Performs the actual docking using different search algorithms.
- AutoDock uses an empirical scoring function based on a modified AMBER field force model, with entropy correction for rotational degrees of freedom [3,5].

3-2. Algorithms Used:

AutoDock 4.2 supports three main search algorithms:

Table(III-1) Comparison of search algorithms in molecular docking programs

Algorithm	Advantages	Recommended Usage
Simulated Annealing (SA)	Simple Fast	Small molecules with limited degrees of freedom
Genetic Algorithm (GA)	Effective For the spaces wide	Global/Comprehensive search
Lamarckian GA (LGA)	The best performance In a way general	Optimum and most common usage

The LGA algorithm is based on combining the genetic algorithm with the Solis & Wets local search algorithm, enabling local optimization of promising positions while maintaining global exploration of the matching space [6].

3-3. Energy Evaluation Function in AutoDock:

The scoring function in AutoDock is based on an empirical energy model that estimates the free bond energy (ΔG) according to the following equation:

$$\Delta G = W_{vdw} + W_{\text{hbond}} + W_{\text{elec}} + W_{\text{tor}} + W_{\text{sol}}$$ [3].

Where these components represent: van der Waals energy (W_{vdw}), hydrogen bond energy (W_{hbond}), electrostatic energy (W_{elec}), tensile energy (W_{tor}), and decomposition energy (W_{sol}) [6].

4. Detailed Work Procedures:

4-1. File Preparation:

AutoDock works with PDBQT files, an extension of the classic PDB format with the addition of two columns: Partial Charge and AutoDock Atom Type [5].

These files can be prepared using:

- ❖ AutoDockTools (ADT): A graphical interface integrated with AutoDock that simplifies all preparation steps.
- ❖ MGLTools: A comprehensive software package that includes ADT and advanced molecular visualization tools.
- ❖ Open Babel: An open-source program for converting molecular file formats [7].
- ❖ AutoDockTools via Python Scripts: For batch processing of large numbers of molecules.

4-2. Basic setup files:

table(III-2) File types and their functions in the Docking process

The file	Extension	Function / Description
Grid Parameter File	.gpf	He specifies settings account maps The network
Docking Parameter File	.dpf	It defines the parameters of the docking process.
Grid Map Files	.map	maps energy Calculated pre per type atom
Grid Data File	.fld	e specifiesH Dimensions The network And its location
Docking Log File	.dlg	It contains on results docking The complete

4-3. Key Parameters in LGA :

Several key parameters determine the quality of docking results:

table (III-3) Parameters and settings used for the Genetic Algorithm (GA)

Parameters	Value	Description
GA- Population Size	150	number Individuals in the society Genetic
GA- Number of Evaluations	2,500,000	Maximum Number of Energy Evaluations
GA- Number Generations	27,000	Maximum Number of Generations
GA- Mutation Rate	0.02	Crossover Rate
GA- Crossover Rate	0.8	an average intersection Genetic
Local Search Frequency	0.06	Local Search Frequency
Rmstol	2.0 Å	RMSD Cluster Tolerance (Rmstol)
GA-Run	10–100	Number of Docking Runs (GA-Run)

5. Free Binding Energy and Inhibition Constant:

The estimated free binding energy (ΔG) is the primary parameter for assessing the binding strength between a ligand and a protein. It is related to the inhibition constant (Ki) by the equation:

$$\Delta G = RT \ln(Ki)$$

where R is the universal gas constant (1.987 cal/mol·K) and T is the absolute temperature (typically 298.15 K). The more negative (lower) the binding energy, the stronger the binding and the lower the Ki value, indicating potentially higher pharmacological activity [8].

table (III-4) Classification of ligand binding affinity based on ΔG and Ki values

Range ΔG (mol/kcal)	Range K_i	Binding Affinity Classification
less From-10	less From1 nM	Very high affinity / Excellent
-8 to-10	1–100 nM	Excellent
-6 to-8	100 nM –10 µM	High affinity / Good
-4 to-6	10–1000 µM	Moderate affinity
greater From-4	greater From1 mM	Weak affinity

6. Cluster Analysis:

AutoDock performs cluster analysis using the root mean squared (RMSD) criterion to classify structurally similar positions into groups [9].

Cluster results indicate:

- One large cluster encompassing most positions: This suggests good convergence and stability in docking results, a positive indicator of reliability.
- Multiple clusters with similar numbers of individuals: This may indicate multiple docking sites or high matching flexibility.
- Many clusters with few individuals: This warrants increasing the number of runs or reconsidering the docking parameters.

AutoDock ranks the clusters in ascending order of lowest docking energy. Note that the highest-energy cluster is not necessarily the largest, and a larger cluster may have deeper statistical significance.

7. In Silico ADMET and Toxicity Profiling:

This computational phase aims to predict the in vivo pharmacokinetic behavior and safety profiles of natural compounds prior to experimental testing. This approach significantly optimizes time and resource management while mitigating the attrition rates of potential drug candidates in advanced development stages.

7-1. The SwissADME Platform:

SwissADME is a web-based computational tool developed by the Swiss Institute of Bioinformatics (SIB) to estimate key physicochemical, pharmacokinetic, and drug-likeness properties [10]. Its primary evaluation metrics include:

- Lipinski's Rule of Five: Assesses the drug-likeness of a compound to determine its oral bioavailability and gastrointestinal absorption capacity [11].

- Gastrointestinal (GI) Absorption and Blood-Brain Barrier (BBB) Permeability: Evaluated and visually represented using the brain Or intestinal EstimateD permeation predictive model (BOILED-Egg) [12].

- Cytochrome P450 (CYP) Inhibition: Predicts the interaction of molecules with major CYP450 isoforms to evaluate potential drug-drug interactions and metabolic stability [11].

7-2. The ProTox-II Server:

ProTox-II is a machine learning-based in Silico tool designed for the comprehensive prediction of chemical toxicity profiles [13]. The platform classifies compounds into six

toxicity hazard classes based on their predicted median lethal dose (LD_{50}), alongside estimating specific organ toxicities and toxicological endpoints, including:

- Mutagenicity (Genetic toxicity).
- Carcinogenicity (Oncogenic potential).
- Hepatotoxicity (Liver toxicity profiling) [13,14].

8. Detailed Energy Components:

AutoDock provides a detailed breakdown of energy components that helps in understanding the nature of the reaction:

- **Intermolecular Energy**: The sum of van der Waals energy, hydrogen bond energy, dehydrogenation energy, and electrostatic energy. It reflects the strength of the interaction between the ligand and the protein.
- **Internal Energy**: Reflects the internal conformation stress of the molecule when it is bound.
- **Torsional Free Energy**: The entropy penalty resulting from the restriction of rotational degrees of freedom during binding (0.2983 kcal/mol per degree) [3,6].

Bibliography:

[1] Sliwoski, G., et al. (2014). Computational methods in drug discovery. Pharmacological Reviews, 66(1), 334-395.

[2] Karplus, M., & McCammon, J. A. (2002). Molecular dynamics simulations of biomolecules. Nature Structural Biology, 9(9), 646-652.

[3] Morris, G. M., et al. (2009). AutoDock4 and AutoDockTools4: Automated docking with selective receptor flexibility. Journal of Computational Chemistry, 30(16), 2785-2791.

[4] Ferreira, L. G., et al. (2015). Molecular docking and structure-based drug design strategies. Molecules, 20(7), 13384-13421.

[5] Forli, S., et al. (2016). Computational protein–ligand docking and virtual screening with the AutoDock suite. Nature Protocols, 11(5), 905-919.

[6] Morris, G. M., et al. (1998). Automated docking using a Lamarckian genetic algorithm and an empirical binding free energy function. Journal of Computational Chemistry, 19(14), 1639-1662.

[7] O'Boyle, N. M., et al. (2011). Open Babel: An open chemical toolbox. Journal of Cheminformatics.

[8] Huey, R., et al. (2007). A semiempirical free energy force field with charge-based desolvation. Journal of Computational Chemistry.

[10] Bitencourt-Ferreira, G., & de Azevedo, W. F. (2019). Molegro Virtual Docking: A Powerful Tool for Drug Discovery. Methods in Molecular Biology.

[10] Daina, A., Michielin, O., & Zoete, V. (2017). SwissADME: a free web tool to evaluate pharmacokinetics, drug-likeness and medicinal chemistry friendliness of small molecules. Scientific Reports, 7(1), 1-13.

[11] Lipinski, C. A., Lombardo, F., Dominy, B. W., & Feeney, P. J. (2001). Experimental and computational approaches to estimate solubility and permeability in drug discovery and development settings. Advanced Drug Delivery Reviews, 46(1-3), 3-26.

[12] Daina, A., & Zoete, V. (2016). A BOILED-Egg to predict gastrointestinal absorption and brain penetration of small molecules. ChemMedChem, 11(11), 1117-1121.

[13] Banerjee, P., Eckert, A. O., Schrey, A. K., & Preissner, R. (2018). ProTox-II: a webserver for the prediction of toxicity of chemicals. Nucleic Acids Research, 46(W1), W257-W263.

[14] Drwal, M. N., Banerjee, P., Dunkel, M., Wettig, M. R., & Preissner, R. (2014). ProTox: a web server for the in Silico prediction of rodent oral toxicity. Nucleic Acids Research, 42(W1), W53-W58.

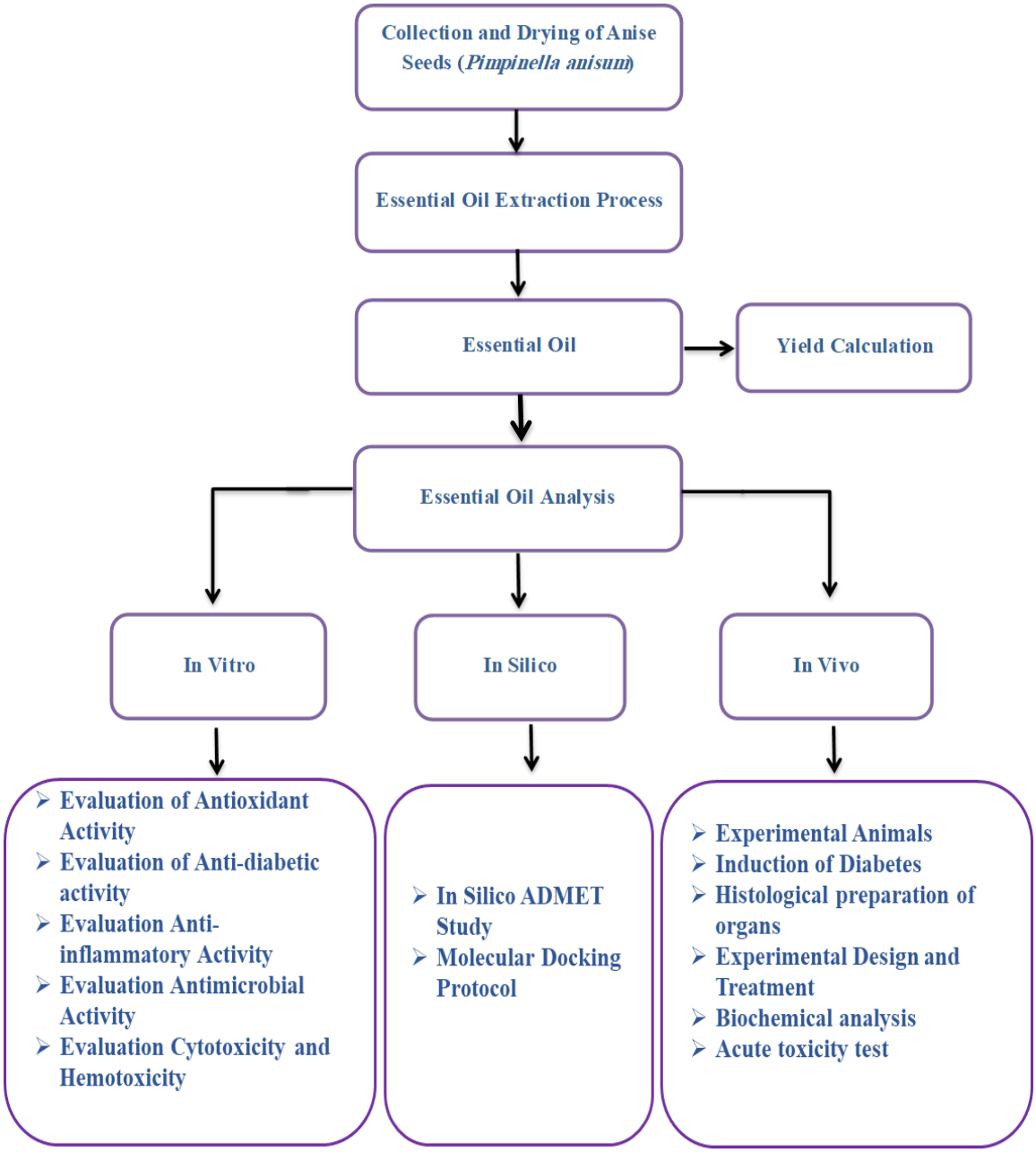
PRACTICAL PART

CHAPTER FOUR

METHODS AND MATERIALS

Introduction:

This study was conducted in the laboratory of the Faculty of Exact Sciences and the Laboratory of Applied Chemistry and Environment at the University of El Oued. This study aimed to extract the essential oil from the seeds of the anise plant (*Pimpinella anisum L*), which were collected from the El Oued region (Algeria) during the 2024–2025 season. The seeds were then dried under natural atmospheric conditions away from direct sunlight, and stored in paper bags in a cool, dry place until use.



figure(IV-1) Diagram illustrating the work plan of this study

1. Materials and Methods:

1-1. Used equipment:

- Clevenger type water distillation apparatus
- UV-visible spectrometer
- sensitive electronic scale

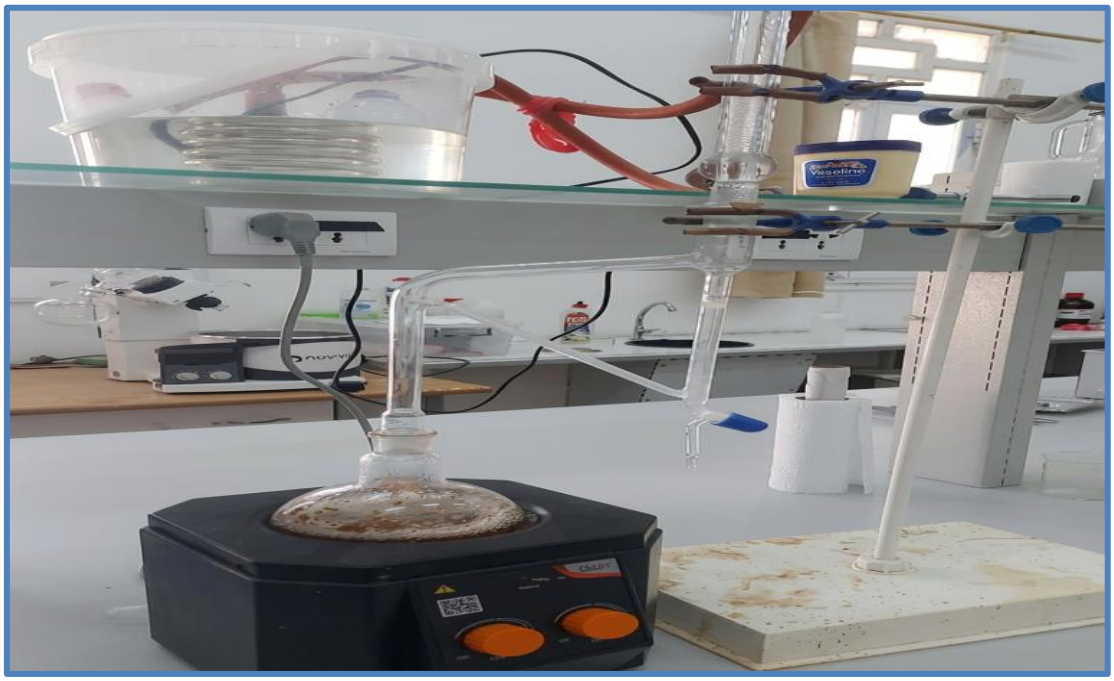


figure (IV-2) Clevenger device



figure(IV-4) UV-Visible device



figure (IV-3) sensitive electronic scale

1-2. Used materials:

- 2,2-diphényl-1- picryl hydrazyl DPPH
- methanol
- α-Amylase enzyme
- Saline phosphate

- hydrochloric acid HCl
- Lugol's solution
- starch solution

2. Essential oil extraction:

2-1. Hydrodistillation Method:

The essential oil of *Pimpinella anisum L* was extracted using the Hydrodistillation technique via a **Clevenger-type apparatus**. This method relies on the ability of water vapor to carry the volatile essential oils from the plant seeds. In this procedure, 50 g of dried seeds were placed in a 1-liter round-bottom flask containing 250 ml of distilled water. The mixture was heated for 3 hours at boiling temperature; the extraction time was recorded from the moment the first drop of distillate appeared in the Clevenger apparatus. The condensed essential oil was then collected and stored in a cool, dark environment to maintain its stability [1].

2-2. Calculation of Extraction Yield:

The extraction yield (R%) is defined as the ratio between the mass of the recovered essential oil and the initial mass of the plant material used. It was calculated according to the following equation:

$$R\% = \frac{m_f}{m_i} \times 100$$

Where:

R%: Extraction yield percentage.

$\mathbf{m_f}$: Final mass of the extracted essential oil (g).

$\mathbf{m_i}$: Initial mass of the plant seeds (g).

3. Gas Chromatography-Mass Spectrometry (GC-MS) Analysis:

The essential oil of *Pimpinella anisum L* was analyzed using Gas Chromatography coupled with Mass Spectrometry (GC-MS). This versatile technique enables the precise separation, as well as the qualitative and quantitative determination, of complex chemical compounds within a sample. By combining the high separation efficiency of gas chromatography with the high precision of mass spectrometry for molecular weight determination, this hyphenated technique serves as a fundamental tool in various research fields and industrial applications.

The GC-MS analysis of the anise essential oil was conducted according to the following analytical conditions:

table (IV-1)GC-MS operating parameters and conditions

Parameter	Value
Chromatographic Column	HP-5MS (30 m × 0.25 mm, film thickness 0.25 µm)
Carrier Gas	Helium at a flow rate of 1 mL/min
Injector Temperature	250 °C
Temperature Program	60 °C to 250 °C at a heating rate of 3 °C/min
Ionization Energy	70 eV
Mass Scan Range	*m/z* 35 – 450

Identification of Compounds:

The chemical constituents were identified by comparing their mass spectra with established scientific databases, specifically the NIST and Wiley libraries. Additionally, identification was confirmed by calculating the Kovats Retention Indices (RI) and comparing them with published reference values in the literature.

Note: This dual-identification approach, combining mass spectral matching with Retention Index (RI) validation, was employed to ensure the highest degree of accuracy and to eliminate any structural ambiguity between isomeric compounds.

Note: Compounds were identified based on a dual-matching system: (1) Mass spectral comparison with NIST and Wiley libraries, and (2) Comparison of calculated Kovats Retention Indices (RI) with reference values according to (Adams 2007) [2].

I.In Vitro Study :

1. Evaluation of Antioxidant Activity:

1-1. DPPH Radical Scavenging Assay:

The DPPH (2,2-diphenyl-1-picrylhydrazyl) assay is a widely used method to evaluate free radical scavenging capacity. This spectrophotometric test is based on the reduction of the purple-colored DPPH radical into a yellow-colored non-radical form (DPPH-H) by donating a hydrogen atom from the antioxidant compounds (essential oil). This reduction is monitored by measuring the decrease in absorbance using a UV-Vis spectrophotometer, which reflects the scavenging efficiency of the tested oil.

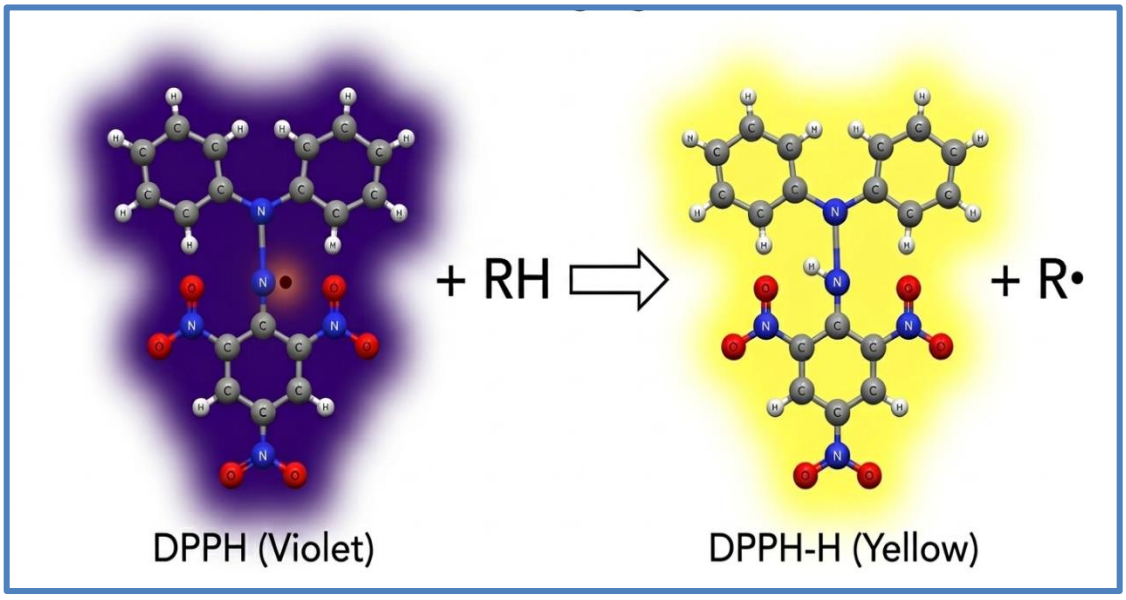


figure (IV-5) DPPH free radical reacts with an antioxidant compound

1-2. Experimental Procedure:

A 0.1 mM DPPH solution was prepared by dissolving 2 mg of DPPH in 50 ml of methanol, resulting in a deep purple solution.

A series of essential oil concentrations ranging from 0.4 to 10 mg/ml was prepared. For the assay, 0.1 ml of each concentration was mixed with 0.9 ml of the DPPH methanol solution. The mixtures were shaken and incubated in the dark for 30 minutes at room temperature [3].

1-3. Calculation of Antioxidant Capacity:

The antioxidant capacity is expressed by the IC_{50} value, defined as the concentration of the essential oil required to scavenge 50% of the DPPH radicals. This value is determined graphically from the plot of the inhibition percentage (I%) against the oil concentrations. The scavenging activity (I%) is calculated using the following formula:

$$I(\%) = \left[\frac{(A_0 - A_1)}{A_0}\right] \times 100$$

Where:

$\mathbf{A_0}$: Absorbance of the DPPH solution in the absence of the sample (control).

$\mathbf{A_1}$: Absorbance of the DPPH solution in the presence of the sample.

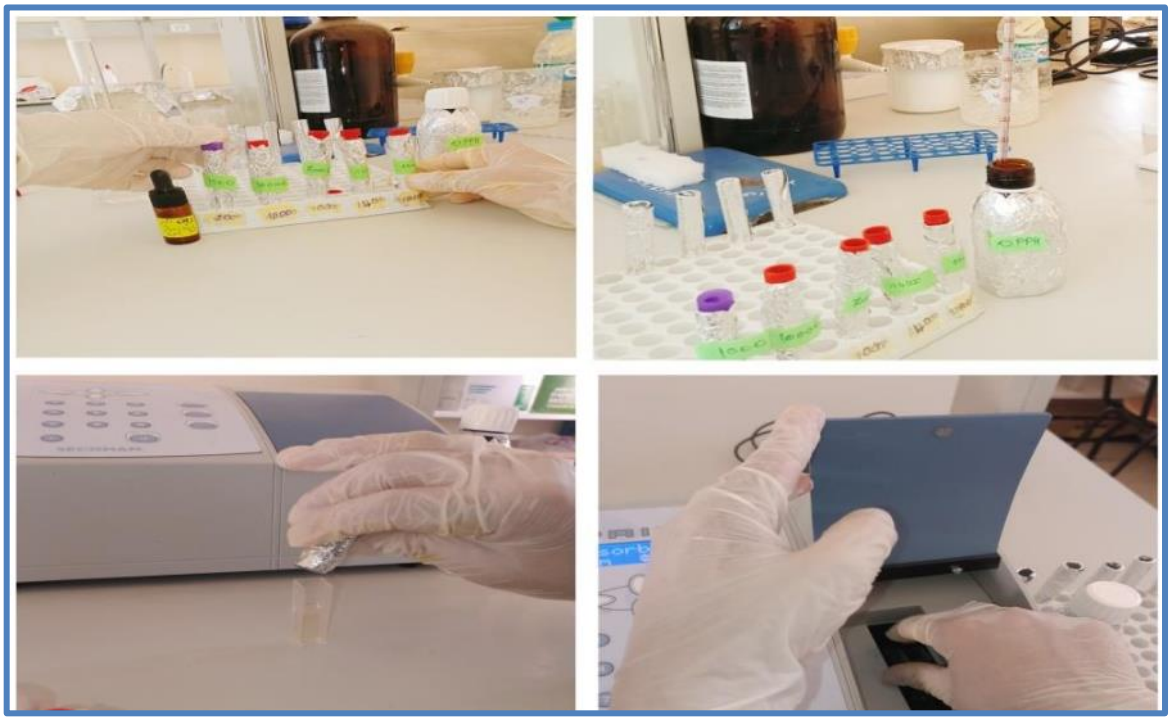


figure (IV-6) An illustration of how the DPPH test works.

2. Evaluation of Anti-diabetic activity :

This protocol aims to know the extent of the effectiveness of the substance (essential oil) in preventing the enzyme from breaking down starch. It is a very common test in diabetes research, where we used the starch-iodine method to evaluate the ability of the essential oil to inhibit the α-Amylase enzyme.

Different concentrations of the essential oil were prepared in test tubes, then to each of them was added:

- 100 µl of Saline phosphate buffer.
- 100 µl of the essential oil solution.
- 100 µl of α-Amylase enzyme.

The tubes were incubated at human body temperature (37 °C) for 10 minutes. The goal here is to allow the oil to react with the enzyme before adding the starch. Then, 100 µl of starch solution is added to each tube, and the tubes are left for 30 minutes at (37 °C). During this time, the enzyme tries to break down the starch, while the essential oil tries to inhibit the enzyme from doing its job. The reaction was stopped by adding 50 µl of HCl (1 M) and 100 µl of Lugol's solution, which is a reagent containing iodine that reacts with the remaining starch to give a dark (blue/purple) color. Dilution is done by adding 1 ml of distilled water to each tube. Absorbance was measured at a wavelength of 580 nm.

The inhibition percentage I(%) is calculated using the equation:

$$I(\%) = \left(\frac{Abs\ Extract - Abs\ Control}{Abs\ Extract}\right) \times 100$$

And the IC_{50} value was derived from the drawn curves.

(**Note**: This study follows the methodology of Righi, N. A et al. 2024) [4].

3. Evaluation Anti-inflammatory Activity:

To evaluate the anti-inflammatory activity of aniseed oil, we followed a protocol based on measuring the oil's ability to inhibit heat-induced mutagenesis of bovine serum albumin (BSA). We began by dissolving the oil in hexane to ensure homogeneity, then prepared a series of six concentrations via binary dilutions ranging from 50% to 1.56% (v/v). One milliliter of 0.3% BSA solution was mixed in buffer (TBS, pH 6.4) with the diluted oil volumes, with the final reaction volume adjusted to 2.5 milliliters using distilled water.

The experiment included a negative control consisting of BSA and water only to represent maximum protein mutagenesis, and a positive control consisting of solvent (hexane) and aspirin. The mixture was first incubated at 37°C for 15 minutes to enhance the reaction between the oil and protein components, then heated at 70°C for 10 minutes to induce mutagenesis, followed by a 20-minute cooling period. Finally, optical absorbance was measured at a wavelength of 660 nm. The decrease in absorbance compared to the negative control indicates the oil's success in inhibiting protein denaturation and protecting its structural integrity under heat stress. The inhibition ratio was calculated according to the standard equation:

$$inhibition(\%) = \left(\frac{A_0 - A}{A_0}\right) \times 100$$

where A_0 represents the absorbance of the negative control sample, while A represents the absorbance measured in the presence of the oil. All measurements were performed in triplicate to ensure reproducibility and analytical reliability.

(**Note** :This study follows the methodology of Bailey-Shaw et al., 2017) [5].



figure(IV-7) Steps for performing a protein mutagenesis (BSA) inhibition test.

4. Evaluation Antimicrobial Activity:

To evaluate the antibacterial activity of vegetable oil, the agar well diffusion method was used against two reference strains: *Escherichia coli ATCC 25922 and Staphylococcus aureus ATCC 25923.* The process began by dissolving the oil in hexane to obtain a homogeneous mother solution, followed by the preparation of a series of dilutions at concentrations of 50%, 25%, 10%, and 5%. The bacterial culture density was adjusted to match the McFarland 0.5 standard (10^6 CFU/mL), and the cultures were then uniformly spread onto the surfaces of Mueller-Hinton agar plates. Subsequently, 6-mm diameter wells were drilled in the agar, and 50 µL of each concentration was added to the corresponding wells, with pure hexane used as a negative control. The plates were incubated at 37°C for 24 hours, after which the diameters of the inhibition zones surrounding each hole were measured, with diameters exceeding 6 mm indicating antibacterial activity.

(**Note** :This study follows the methodology of Bonev et al., 2008 [6]; Kiehlbauch et al., 2000 [7])

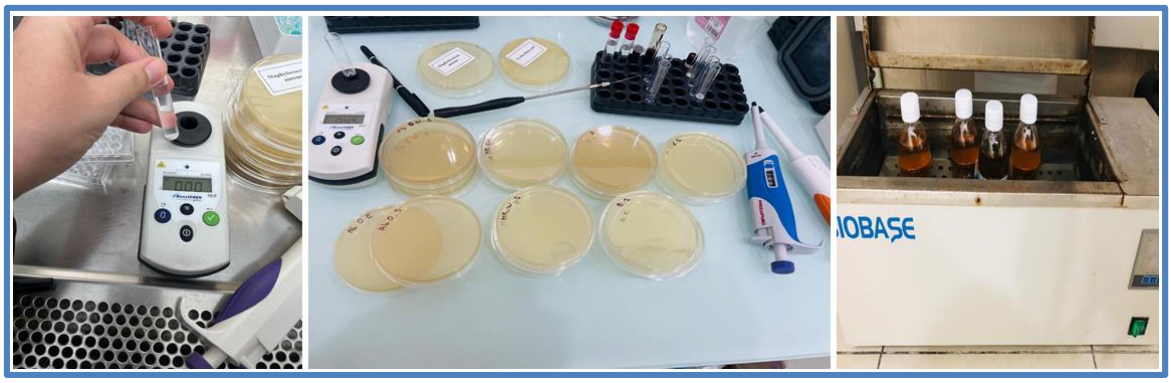


figure (IV-8) practical steps for the burrowing diffusion method

5. Evaluation Cytotoxicity and Hemotoxicity as Biosafety Standards:

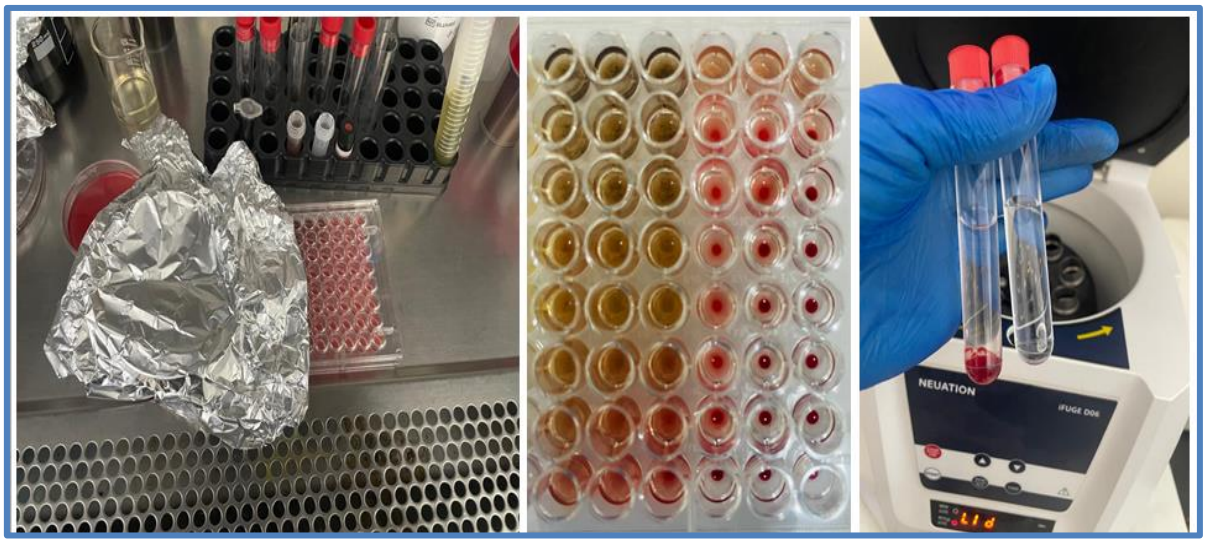
To assess the cytotoxic effect of vegetable oil on cell membrane integrity, a hemolytic activity assay was performed using 96-well micro platelets. The process began with the collection of fresh human blood in heparin-laced tubes. Red blood cells were then isolated and washed three times with 1X buffer (PBS) at 1000 g centrifugation for 5 minutes. The cells were then resuspended in the buffer to obtain a 2% cell suspension. Six oil concentrations were prepared via binary dilutions ranging from 50% to 1.56% (v/v), with 100 µL of the red blood cell suspension added to each well, followed by 100 µL of the corresponding oil concentration. Hydrogen peroxide (H_2O_2) was used as a positive control to induce complete hemolysis, and PBS as a negative control. The plates are incubated at

37°C for one hour with gentle stirring, then separated by centrifugation to allow the healthy cells to settle. 100 µL of the supernatant is then withdrawn, and the absorbance is measured at 540 nm to estimate the amount of hemoglobin released. Finally, the hemolysis ratio is calculated to assess the biosafety of the oil according to the following equation:

$$Hemolysis(\%) = \left(\frac{A_s - A_n}{A_p - A_n}\right) \times 100$$

where A_s represents the absorbance of the sample, A_n represents the absorbance of the negative control, and A_p represents the absorbance of the positive control. All experimental conditions were performed in triplicate to ensure reproducibility and reliability of the obtained results.

(**Note** :This study follows the methodology of Kim et al., 2015) [8].



Figure(IV-9) Hemolysis test using (96-well microplate) technology and a centrifuge.

II.In Silico Study:

1. In Silico ADMET Study:

To evaluate the biosafety and pharmacokinetic properties of the key compounds identified in the essential oil of *Pimpinella anisum L*, a computational evaluation was conducted across three main axes:

1-1. Physicochemical Properties:

The molecules were examined according to (Lipinski's Rule of Five-Ro5) using the **SwissADME** platform[9]. This involved assessing conformity to criteria such as molecular weight, lipid profile (MLogP), and hydrogen bonding to confirm their membrane permeability and intestinal absorption.

1-2. Pharmacokinetic Profile (ADME):

Compounds' ability to cross the blood-brain barrier (BBB) and their absorption in the gastrointestinal (GI) tract were analyzed using the **BOILED-Egg** model. Additionally, their interaction with cytochrome P450 (CYP) enzymes and P-glycoprotein (P-gp) was investigated to determine their metabolic stability and potential drug interactions using the **SwissADME** platform[9].

1-3. Toxicological Assessment:

A thorough toxicity profiling was performed via the **ProTox-II** server[10]. The lethal dose (LD_{50}) was estimated, organ toxicity (e.g., hepatotoxicity) was determined, genetic and immunological toxicological pathways were examined, and the effect of the compounds on cellular signaling pathways was assessed to support their safe use in future therapeutic applications.

2. Molecular Docking Protocol:

2.1. Preparation Phase:

A. Receptor Preparation (Protein):

- **Structure Acquisition:** The three-dimensional structure of the target protein (e.g., PDB ID: 6N2W) is retrieved from the **RCSB Protein Data Bank** in .**pdb** format.
- **Pre-processing (Cleaning):** All crystallographic water molecules, heteroatoms (HETATM), non-essential ions, and co-crystallized native ligands are removed to obtain a clean protein structure.
- **Optimization:** Polar hydrogen atoms are added to satisfy valence, and Kollman charges are assigned to the amino acid residues to model the electrostatic potential accurately.
- **File Conversion:** The refined protein structure is exported and saved in **PDBQT** format using **AutoDockTools (ADT).**

B. Ligand Preparation:

- **Ligand Sketching:** The 3D chemical structures of the phytochemical compounds (e.g., Anethole, Estragole) are constructed using molecular modeling software.
- **Energy Minimization:** Geometric optimization and energy minimization are performed to reach the global minimum energy state (most stable conformation).
- **Torsion Tree Definition:** Rotatable bonds are identified and defined to allow for ligand flexibility during the docking simulation.

- **File Conversion:** The optimized ligands are saved in **PDBQT** format, incorporating Gasteiger partial charges.

2.2. Method Validation (Re-docking):

To validate the accuracy and reliability of the molecular docking protocol and the scoring function, a self-docking (Re-docking) procedure is performed prior to screening the phytochemical compounds:

- Ligand Extraction: The co-crystallized native ligand is chemically isolated from the active site of the prepared target protein structure.

- Re-docking Simulation: The extracted native ligand is redocked into the designated catalytic pocket utilizing the identical grid box parameters and search algorithm configured for the study.

- RMSD Calculation: The top-ranked docking conformation of the redocked ligand is structurally superimposed onto its original crystallographic binding posture. The Root-Mean-Square Deviation (RMSD) is calculated to quantify the structural variance.

- Validation Criterion: An RMSD value of less than 2.0 Å is utilized as the threshold for a successful validation, confirming that the docking parameters are highly capable of reproducing the experimentally observed binding modes.

2.3. Grid Box Configuration:

The search space for the docking simulation is defined by establishing a Grid Box:

- The grid is centered on the **Active Site** (catalytic pocket) of the enzyme.
- Specific coordinates (X, Y, Z center) and dimensions (Size) are set with a defined Spacing (typically 0.375 Å) to encompass all key residues involved in ligand-protein interactions.

2.4. Docking Simulation:

- The molecular docking is executed using a search algorithm, such as the Lamarckian Genetic Algorithm (LGA) [11], to explore the conformational space of the ligand within the binding site.
- For each docking run, numerous binding poses are generated. The software evaluates these poses using a Scoring Function, which estimates the Free Binding Energy (ΔG_{bind}).

2.5. Post-Docking Analysis:

The resulting docking complexes are analyzed based on the following criteria:

- **Binding Affinity:** The top-ranked poses are selected based on the lowest (most negative) binding energy (kcal/mol), indicating the highest thermodynamic stability.
- **Molecular Interactions:** Visual analysis is performed (using tools like **Discovery Studio Visualizer**) to characterize the non-covalent interactions, including:
  - **Hydrogen Bonding:** Identifying specific amino acid residues acting as donors or acceptors.
  - **Hydrophobic Interactions:** Mapping alkyl and pi-alkyl contacts.
  - **$\pi-\pi$ Stacking:** Observing aromatic ring alignments between the ligand and the receptor.

III. In vivo Study:

1. Experimental Animals:

Adult male Wistar rats (180–200 g) were obtained from the institutional animal facility and acclimatized for one week before experimentation. Animals were maintained under standard laboratory conditions (22 ± 2 °C, relative humidity 50–60%, and a 12 h light/dark cycle) with free access to a standard pellet diet and water ad libitum. All experimental procedures were conducted in accordance with institutional ethical guidelines for the care and use of laboratory animals and complied with internationally accepted principles for animal research. (National Research Council, 2011) [12].

2. Induction of Diabetes:

Diabetes was induced in the experiment through a single intraperitoneal injection of alloxan monohydrate (150 mg/kg body weight), freshly dissolved in cold sterile 0.9% saline. Alloxan causes diabetes by selectively destroying pancreatic β-cells via reactive oxygen species, resulting in insulin deficiency and high blood sugar [13]. To avoid initial hypoglycemic shock, animals had free access to a 10% glucose solution for 24 hours after injection. Fasting blood glucose levels were measured after 72 hours with a portable glucometer (Accu-Chek®, Roche, Germany). Rats with fasting blood glucose levels of 250 mg/dL or higher (about 13.9 mmol/L) were deemed diabetic and included in the study.

3. Acute toxicity test:

Pimpinella anisum L essential oil was administered to rats orally at varying doses (25, 50, 75, and 100 mg/kg body weight). Then, the animals were monitored for 72 hours for any signs of abnormal behavior or mild allergic reactions, and subsequently observed daily for 21 days to assess delayed toxicological effects. No mortality or behavioral

abnormalities were detected at any tested dose, including the highest dose tested, 100 mg/kg body weight.

4. Experimental Design and Treatment:

After induction and confirmation of diabetes, rats were randomly assigned to four groups (n = 5 per group):

A. **Normal control (N):** non-diabetic rats receiving vehicle (distilled water) orally (gavage) once daily for 28 days.

B. **Diabetic control / Negative control (NC):** diabetic rats receiving vehicle (distilled water) orally (gavage) once daily for 28 days.

C. **Positive control (PC):** diabetic rats treated with metformin (125 mg/kg/day, p.o.) once daily for 28 days.

D. **Treatment (T):** diabetic rats treated with solution of *Pimpinella anisum L* essential oil (100 mg/kg/day, p.o.) once daily for 28 consecutive days.

The selection of **METFORMIN** as the reference drug was based on the protocol described by X et al. (2023), and the doses of the essential oil of *(Pimpinella anisum L)* were determined by the results of the acute toxicity test, which confirmed the safety of the selected concentrations.

Treatments were prepared fresh and given consistently at the same time each day. Throughout the study, body weight, food intake, and water consumption were recorded weekly to monitor metabolic health and potential treatment-related toxicity.

5. Biochemical analysis:

At the end of the treatment period, animals were fasted overnight, and blood samples were collected via tail vein puncture under light anesthesia. Fasting blood glucose (**FBG**) was measured immediately with a calibrated glucometer. Glycated hemoglobin (**HbA1c**) was determined using a commercial diagnostic kit according to the manufacturer's instructions. Liver function biomarkers, including alanine aminotransferase (**ALAT**) and aspartate aminotransferase (**ASAT**), were quantified using standard enzymatic assay kits to assess hepatic safety and the treatment's metabolic impact.

6. Histological preparation of liver, pancreas, and kidney:

At the end of the treatment period, rats were euthanized under deep anesthesia in accordance with institutional animal care guidelines. The liver, pancreas, and kidneys were immediately excised, gently rinsed in cold normal saline to remove residual blood, and

trimmed into representative tissue pieces (~3–5 mm thick). Specimens were fixed in 10% neutral buffered formalin for 24–48 h at room temperature.

After fixation, tissues were processed by routine paraffin histology: dehydration through graded ethanol, clearing in xylene, and embedding in paraffin wax. Paraffin blocks were sectioned at 4–5 µm on a rotary microtome. Sections were mounted on glass slides, dried, deparaffinized in xylene, and rehydrated through descending ethanol concentrations to water. Slides were stained with hematoxylin and eosin (H&E), then dehydrated, cleared, and cover-slipped with a permanent mounting medium [14]. Stained sections were examined by light microscopy for histoarchitecture and pathological alterations, and representative photomicrographs were obtained.

Bibliography

[1] Council of Europe. (2020). European Pharmacopoeia (10th ed.). European Directorate for the Quality of Medicines & HealthCare. Strasbourg.

[2] Adams, R. P. (2007). Identification of Essential Oil Components by Gas Chromatography/Mass Spectrometry (4th ed.). Allured Publishing Corporation. Carol Stream, Illinois.

[3] Brand-Williams, W., Cuvelier, M. E., & Berset, C. (1995). Use of a free radical method to evaluate antioxidant activity. LWT - Food Science and Technology, 28(1), 25-30.

[4] McCue, P., & Shetty, K. (2004). Inhibitors of α-amylase and α-glucosidase from natural sources of diabetes management. Frontiers in Biology, 19(1), 41-47.

[5] Bailey-Shaw, Y. A., Williams, L. A., Junor, G. A., Green, C. E., Hibbert, S. L., Salmon, C. N., & Smith, A. M. (2017). In vitro evaluation of the anti-inflammatory potential of selected Jamaican medicinal plants using the bovine serum albumin (BSA) denaturation assay. International Journal of Pharmacy and Pharmaceutical Sciences, 9(4), 114-121.

[6] Bonev, B., Hooper, J., & Parisot, J. (2008). Principles of assessing bacterial susceptibility to antibiotics using the agar diffusion method. Journal of Antimicrobial Chemotherapy, 61(6), 1295-1301.

[7] Kiehlbauch, J. A., Hannett, G. E., Salfinger, M., Archinal, W., Monserrat, C., & Carlyle, C. (2000). Use of the National Committee for Clinical Laboratory Standards guidelines for antimicrobial susceptibility testing. Journal of Clinical Microbiology, 38(9), 3341-3348.

[8] Kim, S. J., De Castro, M. C., & Kim, J. H. (2015). In vitro hemolytic activity and cytotoxicity screening of essential oils from aromatic plants. Journal of Applied Biological Chemistry, 58(3), 211-217.

[9] Daina, A., Michielin, O., & Zoete, V. (2017). SwissADME: a free web tool to evaluate pharmacokinetics, drug-likeness and medicinal chemistry friendliness of small molecules. Scientific Reports, 7(1), 1-13.

[10] Banerjee, P., Eckert, A. O., Schrey, A. K., & Preissner, R. (2018). ProTox-II: a webserver for the prediction of toxicity of chemical compounds. Nucleic Acids Research, 46(W1), W257-W263.

[11] Morris, G. M., Huey, R., Lindstrom, W., Sanner, M. F., Belew, R. K., Goodsell, D. S., & Olson, A. J. (2009). AutoDock4 and AutoDockTools4: Automated docking with selective receptor flexibility. Journal of Computational Chemistry, 30(16), 2785-2791.

[12] National Research Council. (2011). Guide for the Care and Use of Laboratory Animals (8th ed.). National Academies Press. Washington, DC.

[13] Szkudelski, T. (2001). The mechanism of alloxan and streptozotocin action in B cells of the rat pancreas. Physiological Research, 50(6), 537-546.

[14] Suvarna, S. K., Layton, C., & Bancroft, J. D. (2018). Bancroft's Theory and Practice of Histological Techniques (8th ed.). Elsevier. London.

CHAPTER FIVE

RESULTS AND DISCUSSION

1. Results of Essential Oil Extraction:

A study was conducted on the Anise plant *(Pimpinella anisum L)* due to its significant essential oil content.

1.1. Physical Properties of the Essential Oil:

After extracting the essential oil from the seeds of *Pimpinella anisum L*, the following physical characteristics were observed:

- Physical State: Liquid at room temperature.
- Color: Pale yellow.
- Odor: Distinctive aromatic odor characteristic of the plant.

1.2. Essential Oil Yield:

The essential oil was extracted using the hydro-distillation method. The yield was calculated based on the relationship defined in the experimental section (Materials and Methods), using the following parameters:

table (V-1) Results of oil extraction yield

Initial mass of seeds (mi)	Mass of extracted oil (mf)	Yield (R%)
50g	0.480g	0.96%

1.3. Discussion of Extraction Yield:

The obtained result indicates that for every 100 g of dry matter of *Pimpinella anisum L*, 0.96g of essential oil was recovered. In previous literature, the essential oil yield for anise seeds typically ranges between 1% and 4%. Therefore, a yield of 0.96% is considered a scientifically logical and acceptable value.

Yields approaching 1% in Algerian aromatic plants are often associated with a high concentration of active compounds. This can be attributed to the arid climatic conditions of the El Oued region, which directly influence the plant's oil-secreting glands and secondary metabolism.

2. Gas Chromatography-Mass Spectrometry (GC-MS) Analysis:

The results of the gas chromatography-mass spectrometry (GC-MS) analysis of anise oil *(Pimpinella anisum L)* showed a rich chemical diversity, with **31 chemical compounds** identified as shown in the following table:

table (V-2) Results of GC MS analysis of the essential oil of the (Pimpinella anisum L)

No.	Component	Chemical Formula	Molar Mass (g/mol)	Percentage (%)
1	**Anethole**	$C_{10}H_{12}O$	148.20	**74.4**
2	**Estragole**	$C_{10}H_{12}O$	148.20	**6.3**
3	**Caryophyllene oxide**	$C_{15}H_{24}O$	220.35	**4.3**
4	**Linalool**	$C_{10}H_{18}O$	154.25	**2.8**
5	**p-Anisaldehyde**	$C_8H_8O_2$	136.15	**2.2**
6	**alpha-Curcumene**	$C_{15}H_{22}$	202.34	**1.1**
7	**cis-Anethole**	$C_{10}H_{12}O$	148.20	**0.9**
8	**alpha-Himachalene**	$C_{15}H_{24}$	204.35	**0.8**
9	**beta-Bisabolene**	$C_{15}H_{24}$	204.35	**0.8**
10	**Geranyl acetate**	$C_{12}H_{20}O_2$	196.29	**0.7**
11	**beta-Vetivenene**	$C_{15}H_{22}$	202.34	**0.6**
12	**Nerol acetate**	$C_{12}H_{20}O_2$	196.29	**0.5**
13	**alpha-Bisabolol**	$C_{15}H_{26}O$	222.37	**0.5**
14	**Linalyl acetate**	$C_{12}H_{20}O_2$	196.29	**0.4**
15	**beta-Caryophyllene**	$C_{15}H_{24}$	204.35	**0.4**
16	**trans-Pseudoisoeugenyl 2-methylbutyrate**	$C_{15}H_{20}O_2$	232.32	**0.4**
17	**Hotrienol**	$C_{10}H_{16}O$	152.23	**0.3**
18	**Camphor**	$C_{10}H_{16}O$	152.23	**0.3**
19	**beta-Elemene**	$C_{15}H_{24}$	204.35	**0.3**
20	**beta-Myrcene**	$C_{10}H_{16}$	136.23	**0.2**
21	**Butyric acid, hexyl ester**	$C_{10}H_{20}O_2$	172.26	**0.2**
22	**delta-Elemene**	$C_{15}H_{24}$	204.35	**0.2**
23	**Ylangene**	$C_{15}H_{24}$	204.35	**0.2**
24	**trans-beta-Farnesene**	$C_{15}H_{24}$	204.35	**0.2**
25	**gamma-Eudesmol**	$C_{15}H_{26}O$	222.37	**0.2**
26	**Limonene**	$C_{10}H_{16}$	136.23	**0.1**
27	**1,8-Cineole**	$C_{10}H_{18}O$	154.25	**0.1**
28	**trans-beta-Ocimene**	$C_{10}H_{16}$	136.23	**0.1**
29	**D-Menthone**	$C_{10}H_{18}O$	154.25	**0.1**
30	**alpha-Longipinene**	$C_{15}H_{24}$	204.35	**0.1**
31	**beta-Himachalene oxide**	$C_{15}H_{24}O$	220.35	**0.1**

The results in the table above show a clear dominance of Phenylpropanoids, with **anethole** registering the highest percentage at **74.4%**, followed by **Estragole** at **6.3%**. These results are consistent with international standards and previous research classifying anethole as the chemo stereotype of this plant, primarily responsible for the therapeutic properties observed in this study. The high anethole content enhances the oil's ability to stabilize proteins and prevent their denaturation. Furthermore, the presence of secondary compounds at significant concentrations, such as **Caryophyllene oxide (4.3%)** and

linalool (2.8%), plays a pivotal role in producing a synergistic effect. This chemical synergy enhances the oil's efficacy, as these components contribute to increased cell membrane permeability and facilitate the binding of anethole to the active sites of the target enzymes.

The chemical fingerprint of this sample reflects the quality of the plant material in the arid regions of Algeria, which opens up prospects for using this oil as a natural and effective resource.

3. Antioxidant Activity:

3-1. Assessment of Antioxidant Activity:

The antioxidant activity of the *Pimpinella anisum L* essential oil was evaluated using the DPPH free radical scavenging assay, as described in Chapter Four. The absorbance of the radical was measured at 517 nm. The test was performed across a range of different concentrations to monitor the scavenging capacity. The results are summarized in the following table and figure:

table (V-3) Percentage (I%) at different concentrations using the DPPH test.

C (mg/ml)	**0.40**	**0.90**	**2**	**3**	**5**	**6**	**10**
I_C(%)	9.57	16.17	25.57	35.14	54.45	62.54	**79.53**

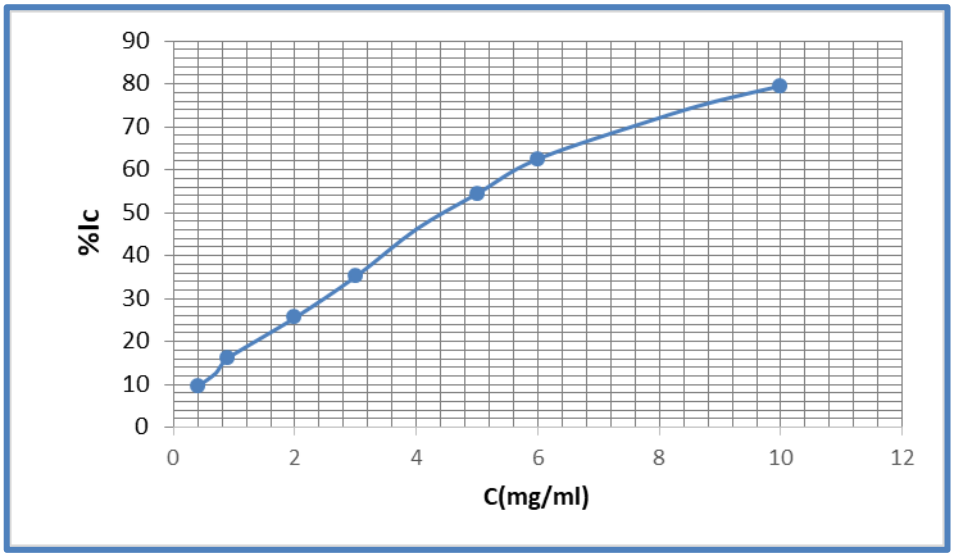


figure (V-1) The curve of change in free radical inhibition (DPPH) as a function of oil concentrations

3-2. Results and Discussion:

The evaluation of the free radical inhibition ability of *Pimpinella anisum L* essential oil demonstrates a distinct (concentration-dependent) antioxidant activity. Based on the data presented in *table (V3)* and *figure (V1)*, a strong positive correlation exists between the essential oil concentrations and the **inhibition percentage (*IC%*)**. The scavenging activity initiated at a modest **9.57%** at the lowest concentration (**0.40 mg/mL**) and increased progressively to reach a maximum efficacy of **79.53%** at **10 mg/mL**.

These results reflect the ability of the oil's phytochemical constituents to react with **DPPH radicals** by converting them into the stable form (**DPPH-H**). This chemical transformation explains the decrease in absorbance measured at **517 nm** as concentrations increase. Quantitatively, the half-maximal inhibitory concentration **(IC_{50})** was estimated at approximately **4.38 mg/mL**, a value that signifies the oil's efficiency in radical scavenging.

Chemically, this antioxidant potency is attributed to the richness of Anise essential oil in phenolic and terpenoid compounds, particularly **Anethole**, the primary constituent. Anethole is characterized by its ability to donate hydrogen atoms to free radicals, thereby terminating the oxidation chain reaction. Furthermore, the arid climatic conditions of the "**El Oued**" region play a pivotal role in stimulating the plant's secondary metabolism.

Such environmental stress often leads to a higher concentration of bioactive compounds within the oil's secretory glands. This explains the significant biological results obtained, despite the extraction yield (**0.96%**) being at the lower end of the ranges reported in previous literature.

4. Anti-diabetic activity:

4-1. Assessment of anti-diabetic activity:

We assessed the anti-diabetic activity of the essential oil based on an α-amylase inhibition assay, following the protocol described in the previous chapter. The results of the α-amylase inhibition as a function of the essential oil concentrations are shown in the following table and figure:

table (V-4) Percentage inhibition of α-amylase of oil as a function of concentrations

C (mg/ml)	3	4	5	7	8	9	10
I_C(%)	22.76	47.22	57.96	75.64	80.49	83.97	85.54

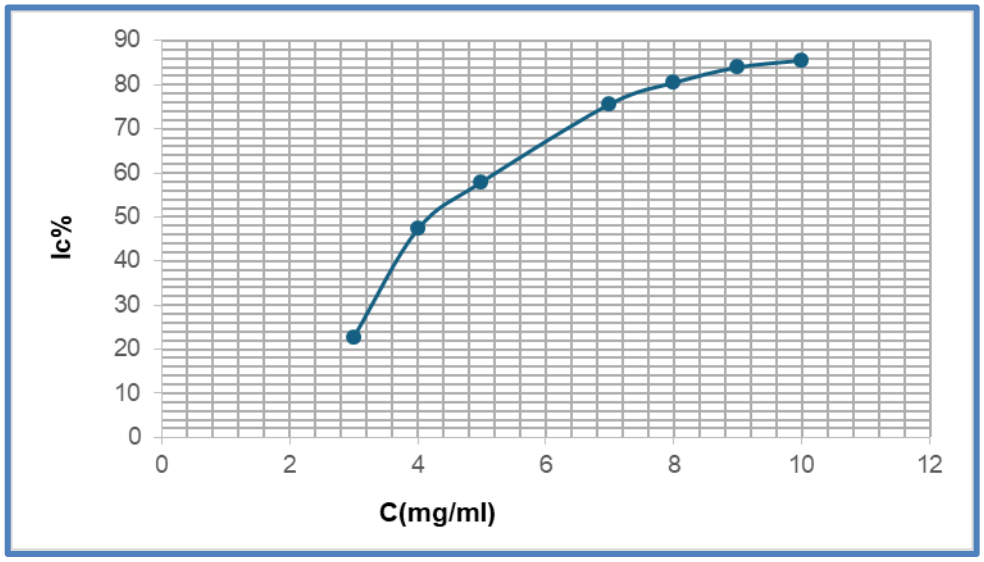


figure (V-2) Curve showing the change in the inhibition ratio of α-Amylase as a function of oil concentration.

4-2. Results and Discussion:

The experimental data and the corresponding graphical representation reveal a significant **dose-dependent relationship** between the essential oil concentration and the inhibition percentage. The inhibitory activity increased progressively from **22.76%** at a concentration of **3 mg/mL**, reaching a peak inhibition of **85.54%** at **10 mg/mL**.

This concentration-dependent behavior underscores the efficiency of the oil's phytochemical constituents in binding to the enzyme's active sites, thereby preventing its interaction with the starch substrate.

The **half-maximal inhibitory concentration (*IC_{50}*)** of the *Pimpinella anisum L* essential oil against **α-Amylase** was determined to be **4.26 mg/mL**. Biologically, this inhibitory potency is attributed to the ability of the oil's components to induce **conformational changes** in the enzyme structure or to engage in **competitive inhibition** with the substrate (starch). Such activity suggests a potential role for the oil in mitigating **postprandial hyperglycemia**.

A value of ***IC_{50}* = 4.26 mg/mL** is considered highly effective for a crude essential oil. In pharmacological evaluation, a lower ***IC_{50}*** value is a direct indicator of the extract's superior biological potency and inhibitory strength.

5. Anti-inflammatory Activity:

5-1. Assessment of Anti-inflammatory Activity :

We assessed the anti-inflammatory activity of the vegetable oil using the bovine serum albumin (BSA) protein denaturation test according to the protocol we studied in the Methods and Means chapter. The study yielded the results shown in the following table and figure:

table (V-5) Anti-inflammatory activity of essential oil using protein denaturation inhibition assay.

Concentration (% v/v)	% Inhibition
1.5625	1.90%
6.25	7.30%
12.5	10.00%
25	12.80%
50	14.00%
Negative control	0%
Positive control (Aspirin)	67.70%

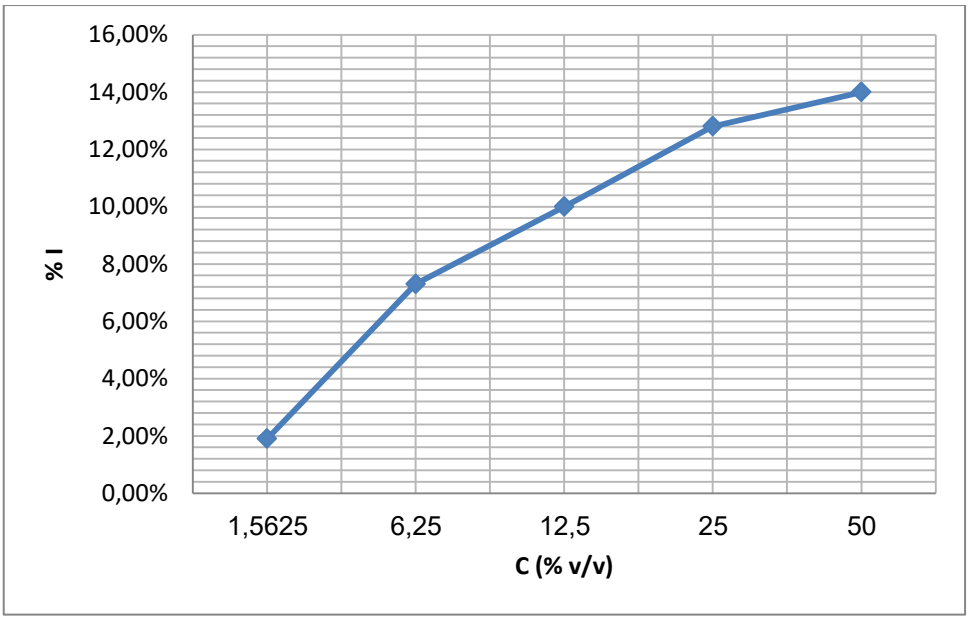


figure (V-3) A curve showing the percentage of protein denaturation inhibition as a function of anise oil concentrations.

5-2. Results and Discussion:

Experimental results presented in the table and figure above demonstrate a clear concentration-dependent inhibitory effect. The highest inhibition rate of **14%** was recorded at a concentration of **50% (v/v)**, while this activity progressively decreased with dilution, reaching **1.9%** at the **1.56% (v/v)** concentration.

This efficacy is attributed to the capacity of the oil's bioactive compounds to bind to the protein's functional sites, thereby enhancing its structural stability. This binding prevents the exposure of self-antigenic determinants that typically trigger inflammatory responses due to thermal stress. Although the inhibitory potential of the essential oil remained below that of the positive control (Aspirin), which achieved a high inhibition rate of **67.7%** under the same experimental conditions, the results confirm that the oil possesses protein-protective properties that contribute to mitigating biochemical processes associated with inflammation. These statistical data, measured at a wavelength of **660 nm**, support the role of the oil's hydrophobic constituents in maintaining protein structural integrity.

6. Antimicrobial Activity:

6-1. Assessment of Antimicrobial Activity:

The antibacterial activity of the essential oil was evaluated using the agar well diffusion method, following the protocol described in the previous chapter, the results of the inhibition test, based on the concentrations of the essential oil, are shown in the following table:

table (V-6) Antimicrobial activity of the essential oil against tested bacterial strains

	Microbial inhibition (mm) OIL				Co . Neg.
Strains used	**50%**	**25%**	**10%**	**5%**	
Escherichia coli ATCC 25922	**16**	**12**	**NI**	**NI**	**NI**
***Staphylococcus aureus* ATCC 25932**	**15**	**11**	**NI**	**NI**	**NI**

NI = No Inhibition

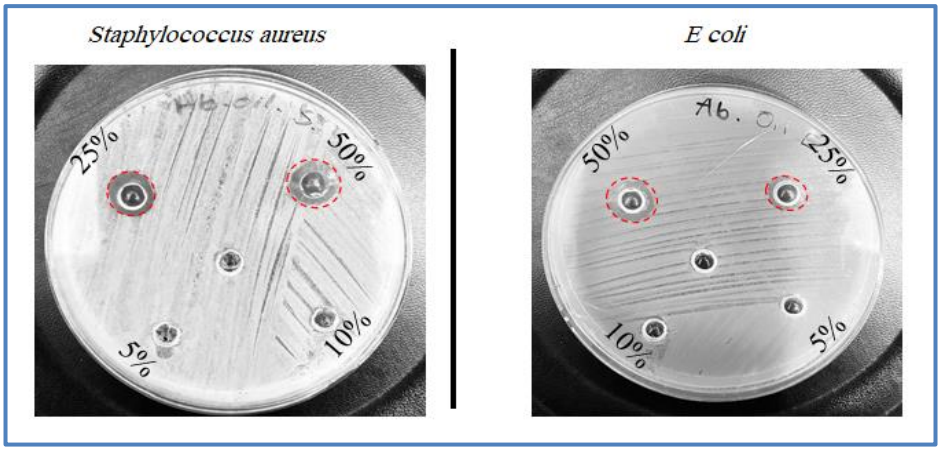


figure (V 4) Antibacterial activity of the essential oil on Mueller-Hinton agar plates

6-2. Results and Discussion:

Experimental results indicated that the oil possesses distinct inhibitory efficacy against the tested bacterial strains:

Escherichia coli (as a model for **Gram-negative bacteria**) and Staphylococcus aureus (as a model for **Gram-positive bacteria**).

Analysis of the data reveals that the antimicrobial activity is primarily concentration-dependent. At a concentration of **50%**, the oil recorded inhibition zones of **16 mm** against E. coli and **15 mm** against S. aureus. As the concentration decreased to **25%**, the potency declined, yielding inhibition diameters of **12 mm** and **11 mm**, respectively. Notably, the inhibition zones disappeared completely (NI: No Inhibition) at lower concentrations **(10% and 5%).**

This biological effect is attributed to the ability of the oil's bioactive constituents to penetrate bacterial cell walls. Despite the structural complexity of the Gram-negative cell envelope in **E.coli,** which features an outer lipopolysaccharide (LPS) membrane, the oil demonstrated significant penetrative efficiency, explaining the slightly larger inhibition zone compared to the Gram-positive strain. The mechanism of inhibition is likely linked to the hydrophobic nature of the oil's compounds, which disrupt cytoplasmic membrane permeability, leading to the leakage of vital cellular components.

The absence of activity at concentrations below **25%** suggests that the Minimum Inhibitory Concentration (MIC) falls within the range of **10% to 25%.** This implies the necessity of maintaining a specific concentration threshold to overcome bacterial resistance mechanisms and ensure the effective diffusion of active substances through the agar medium.

7. Cytotoxicity and Hemotoxicity as Biosafety Standards:

7-1. Assessment of Antimicrobial Activity:

After conducting a hemolysis test according to the protocol described in Chapter 4, the following experimental results were obtained:

table (V-7) Hemolysis percentage of Pimpinella anisum L essential oil (Mean ± SD).

Concentration (mg/mL)	Hemolysis (%)
40	**85.9 ± 2.9**
20	**75.8 ± 4.5**
10	**81.1 ± 4.7**
5	**9.8 ± 3.1**
2.5	**9.9 ± 4.1**
1.25	**8.4 ± 4.8**
Positive control	**100.0 ± 0.0**
Negative control	**0.0 ± 0.0**

7-2. Results and Discussion:

The results showed that the effect of the essential oil on human red blood cells is highly dose-dependent. At high concentrations (above 10 mg/ml), the oil exhibited strong hemolytic activity, with a hemolysis rate exceeding 75%. This high level of hemolysis is attributed to the direct interaction between the hydrophobic components of the oil and the cytoplasmic membrane of red blood cells, leading to membrane rupture. In contrast, a significant decrease in toxicity was observed at concentrations of 5 mg/ml and below, where the hemolysis rate did not exceed 9.9%. This marked difference indicates a clear margin of biosafety at low concentrations. These results confirm the potential use of this essential oil in topical or systemic pharmaceutical formulations, provided that non-hemolytic concentrations are maintained to ensure the integrity of cell membranes.

8. In Silico ADMET Study:

This predictive study was conducted using the SwissADME and ProTox-II platforms, and the results were as follows:

8-1. Results In Silico ADMET and Toxicity Profiling:

The in Silico evaluation of the major chemical constituents of *Pimpinella anisum L* essential oil provided critical insights into their pharmacokinetic (ADME) profiles and safety margins.

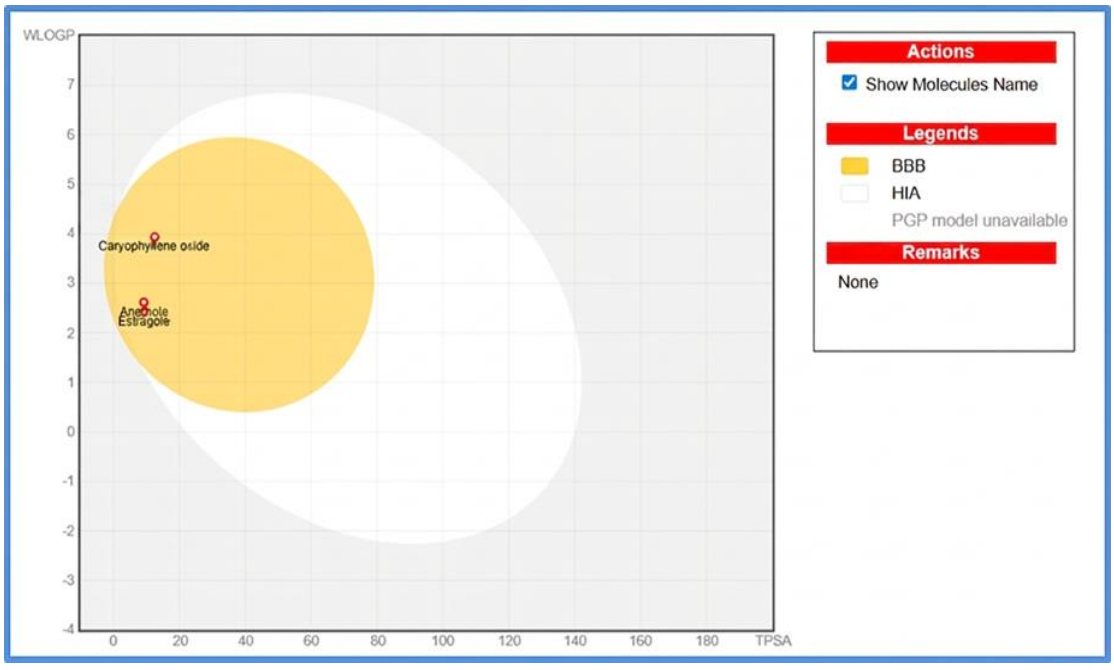


figure (V-5) BOILED-Egg model for predicting gastrointestinal absorption (HIA) and brain penetration (BBB) of the studied compounds

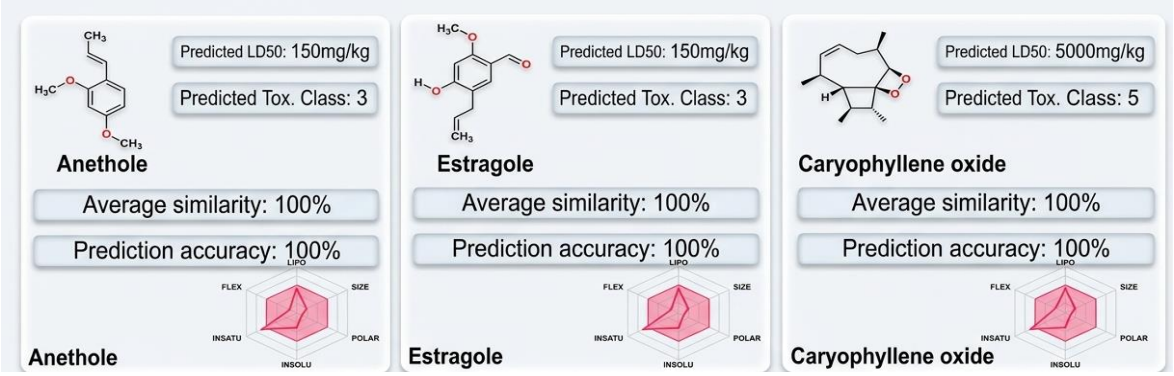


figure (V-6) Predicted acute toxicity (LD50) and toxicity classes and Bioavailability radars illustrating the physicochemical properties and drug-likeness of the major compounds in Pimpinella anisum L essential oil, obtained via the SwissADME platform and using the ProTox-II server.

table (V-8) Prediction of physicochemical properties, pharmacokinetics (ADME), and acute toxicity of the major compounds of Pimpinella anisum L essential oil.

Compound (Ligand)	M. W (g/mol)	Lipinski Violation	GI Absorption	BBB Permeant	Brenk Alerts	Toxicity Class	LD50 (mg/kg)
Anethole	148.20	0	High	Yes	1 (isolated alkene)	3	150
Estragole	148.20	0	High	Yes	1 (isolated alkene)	3	150
Caryophyllene oxide	220.35	0	High	Yes	2 (isolated alkene)	5	5000

8-2. Discussion In Silico ADMET and Toxicity Profiling:

8.2.1. Physicochemical Properties and Lipinski's Rule of Five:

The physicochemical attributes of the three investigated compounds demonstrate high drug-likeness. According to Lipinski's Rule of Five (Ro5), all evaluated compounds (Anethole, Estragole, and Caryophyllene oxide) exhibited zero violations. This indicates optimal membrane permeability, suitable molecular weight, and favorable structural stability, which are essential criteria for high oral bioavailability.

8.2.2. Pharmacokinetic Profile (BOILED-Egg Model):

Reflecting the visual data from the BOILED-Egg lipid-affinity plot, the pharmacokinetic behavior of the compounds showed high efficiency:

Gastrointestinal Absorption & Brain Penetration: All three studied compounds (Anethole, Estragole, and Caryophyllene oxide) are positioned within the yolk (yellow zone) of the model. This position reflects a simultaneous capacity for High GI Absorption and BBB Permeation, suggesting substantial potential for systemic bioavailability and central nervous system (CNS) bioactivity.

8.2.3. Toxicological Assessment and Safety Margins:

The ProTox-II platform revealed a clear variation in the degree of acute toxicity among the selected compounds, classifying them into distinct safety profiles:

High-Risk Compounds (Class 3): Anethole and Estragole exhibited the highest acute toxicity with a predicted **LD_{50}** of 150 mg/kg (Toxicity Class 3). This pronounced toxicity necessitates strict dosage regulation and careful narrow therapeutic window management in future in vivo studies.

Low-Risk/Safe Compounds (Class 5): Caryophyllene oxide demonstrated an excellent safety boundary with a predicted **LD_{50}** of 5000 mg/kg (Toxicity Class 5), showing a wide safety margin and designating it as a highly tolerable scaffold.

8.2.4. Structural Alerts (Brenk Alerts):

The Brenk structural alerts identified specific reactive moieties in the three compounds, notably isolated alkenes (1 alert for both Anethole and Estragole, and 2 alerts for Caryophyllene oxide). While these chemical alerts often flag potential metabolic instability or promiscuous protein binding in synthetic drugs, in natural essential oils, these reactive centers are frequently the core driving force behind their therapeutic interactions with target proteins.

9. Molecular Docking:

9-1. Results of Validation (Re-docking):

Before analyzing the *Pimpinella anisum L* essential oil components, the docking protocol was validated via self-docking (re-docking). The native co-crystallized ligands, Myricetin and Acarbose, were extracted and re-docked into the active sites of their respective proteins, α-Amylase (PDB ID: 4GQR) and α-Glucosidase (PDB ID: 3W37). The accuracy of the docking was assessed using the Root Mean Square Deviation (RMSD) between the predicted position and the original experimental crystal position, As presented in Table (V-9).

table (V-9) Molecular Redocking Validation Results

Target protein (PDB ID)	Native Ligand	Binding Energy (kcal/mol)	Ref RMSD (Å)
α –Amylase 4GQR	Myricetin (MYC)	-6.72	1.97
α-Glucosidase 3W37	Acarbose	-8.97	1.50

9-2. Discussion And Analysis Results Of Validation (Re-docking):

The results of the re-docking validation demonstrate that the docking protocol used is highly accurate and reliable. A docking simulation is considered successful and biologically relevant if the RMSD value between the re-doped configuration and the experimentally crystallized ligand position is less than the universally accepted lower limit of 2.0 angstroms. As shown in Table (V9), both target proteins successfully met this criterion. For α-glucosidase (3W37), the native inhibitor Acarbose showed excellent structural alignment with a low RMSD value of 1.50 angstroms and a high binding energy of -8.97 kcal/mol. For α-amylase (4GQR), Myricetin re-docking resulted in a binding energy of -6.72 kcal/mol and a mean radical standard deviation of 1.97 angstroms. Although this value is close to the upper limit, it remains within the acceptable range (<2.0 angstroms). Therefore, these results confirm the validity of the criteria, grid-square dimensions, and evaluation functions used in this study. The current computational setup is highly reproducible in terms of experimental correlation patterns, ensuring that subsequent hypothetical screening of *Pimpinella anisum L* essential oil components against these antidiabetic targets will be robust and reliable.

9-3. Molecular Docking Simulation Results:

To evaluate the inhibition efficiency, quantify binding affinities (ΔG), and elucidate the precise intermolecular interactions within the catalytic pockets of the target enzymes, an in silico molecular docking study was conducted using **AutoDockTools** and **Discovery Studio** software.

The investigation focused on two key therapeutic targets regulating carbohydrate metabolism: α-Amylase (PDB ID: 4GQR) and α-Glucosidase (PDB ID: 3W37).

The table below summarizes the dynamic binding energies and predicted biological targets of the compounds studied, along with the reference drug:

table (V-10) Molecular docking results of selected ligands with target proteins

Ligand	Target protein	PDB ID	Binding Energy (kcal/mol)	Biological Activity
Anethole	α -Amylase	4GQR	-4.34	Antidiabetic
	α-Glucosidase	3W37	-5.43	Antidiabetic
Caryophyllene oxide	α -Amylase	4GQR	-5.88	Antidiabetic
Estragole	α-Glucosidase	3W37	-5.25	Antidiabetic
Metformin	α -Amylase	4W93	-5.83	Antidiabetic

9-4. Discussion and analysis of Docking results :

The in silico molecular docking simulations revealed distinct variations in the binding capabilities of the investigated compounds within the enzymatic architectures of the biological targets, providing a molecular-level understanding of their inhibitory mechanisms. The negative values obtained for the free binding energy (ΔG) theoretically validate the thermodynamic spontaneity and stability of the ligand-receptor complexes, where a lower (more negative) energy score indicates a superior binding affinity.

9-4.1.Inhibitory Efficacy Against α-Amylase (PDB ID: 4GQR):

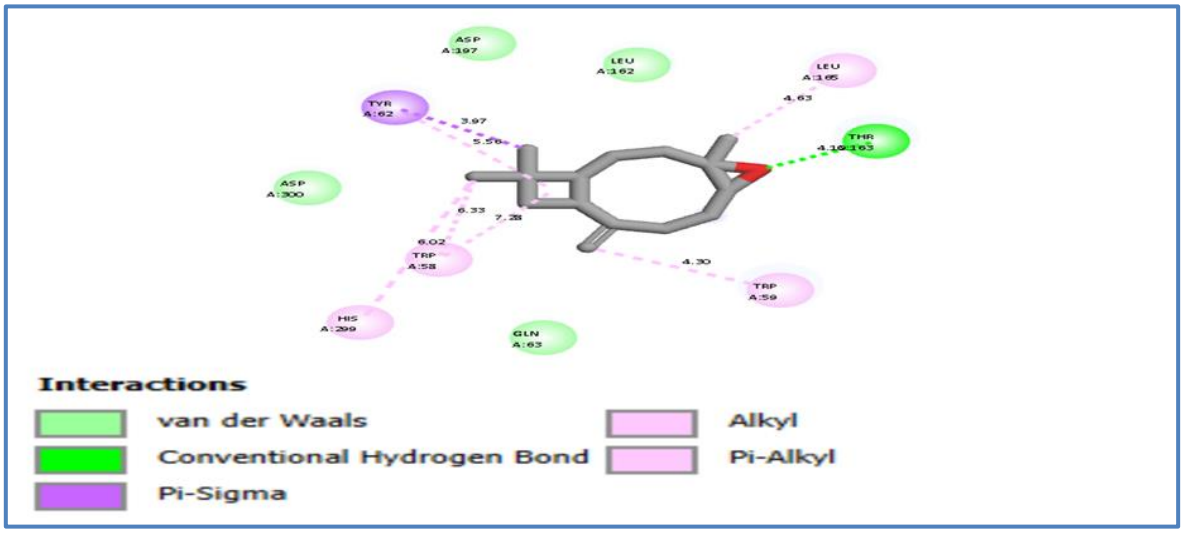


figure (V- 7)2D interaction map of Caryophyllene oxide in 4GQR

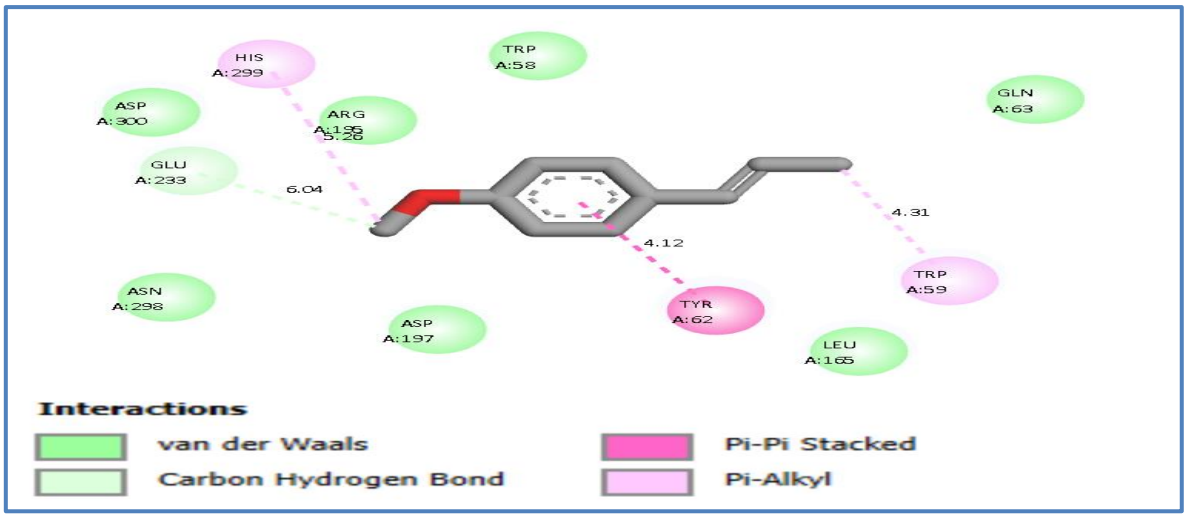


figure (V-8) 2D interaction map of Anethole in 4GQR

The computational screening unveiled a highly promising antidiabetic profile for the ***Caryophyllene oxide***. This compound demonstrated a remarkable binding affinity with a free energy score of -5.88 kcal/mol, outperforming the commercial standard antidiabetic

drug ***Metformin*** (-5.83 kcal/mol).The superior thermodynamic stability of the Caryophyllene oxide-4GQR complex is driven by a well-anchored interaction network combining polar and hydrophobic forces (*figure (V 07)*). Specifically, the oxygen atom of the epoxide ring forms a highly directed, conventional hydrogen bond with the **THR 163** residue at a short distance of 4.10Å. This anchor is reinforced by two crucial π–Sigma interactions with the aromatic ring of **TYR 62** at distances of 3.97Å and 5.56 Å. Furthermore, owing to its bulky hydrocarbon skeleton, Caryophyllene oxide maximizes hydrophobic interactions within the non-polar pocket, establishing an Alkyl bond with **LEU 165** (4.63 Å) and multiple, robust π–Alkyl interactions with **TRP 58** (6.33 Å, 6.02 Å, and 7.21 Å, **TRP 59** (4.30 Å), and **HIS 299**. The complex is further stabilized by a complementary van der Waals envelope involving **ASP 197**, **LEU 162**, **GLN 63**, and **ASP 300**.

Conversely, ***Anethole*** exhibited a lower binding affinity within the same enzyme pocket (4GQR), scoring a binding energy of -4.34 kcal/mol. Its binding mode is predominantly governed by aromatic interactions (*figure (V 08)*), highlighted by a strong π–π stacked interaction between its benzene nucleus and the **TYR 62** residue (4.12 Å). Additionally, its methoxy group (-OCH_3) and lateral double bond form π–Alkyl links with **HIS 299** (5.26 Å) and **TRP 59** (4.31 Å), respectively. A weak carbon-hydrogen bond with **GLU 233** (6.04 Å) and a peripheral van der Waals cloud with **ASP 300**, **ARG 195**, **TRP 58**, **GLN 63**, **LEU 165**, **ASP 197**, and **ASN 298** complete its structural positioning.

9-4.2.Inhibitory Efficacy Against α-Glucosidase (PDB ID:3W37):

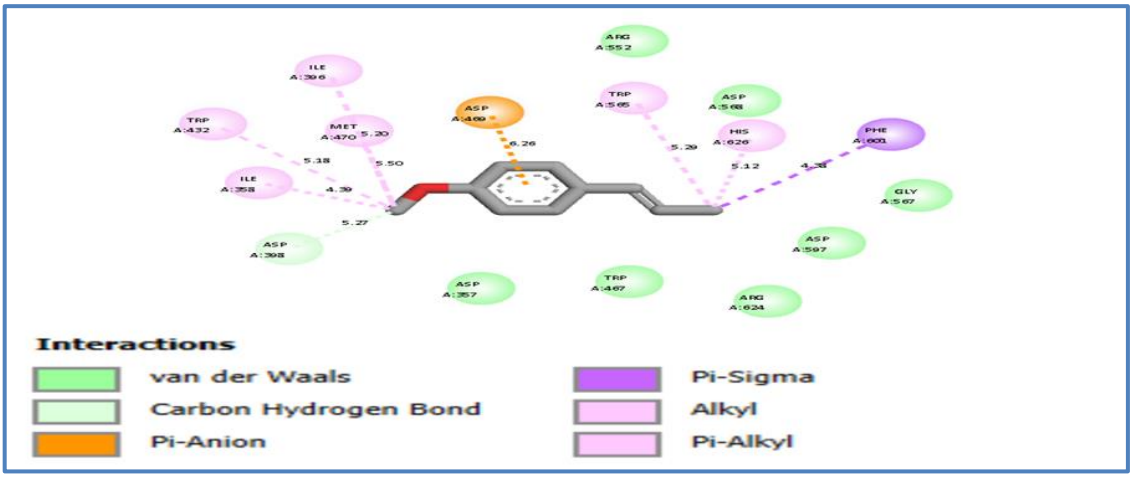


figure (V-9) 2D interaction map of Anethole in 3W37

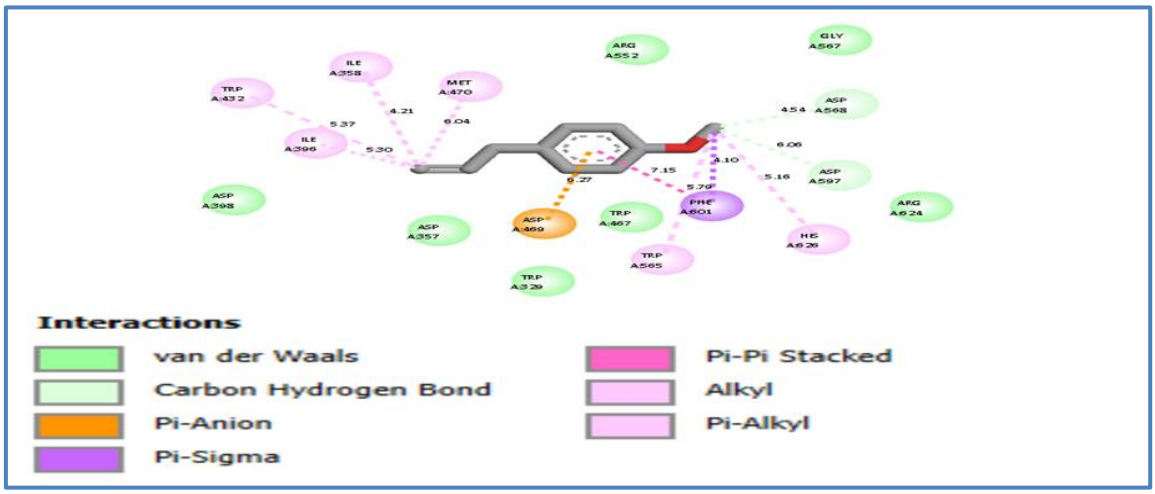


figure (V-10) 2D interaction map of Estragole in 3W37

Regarding the α-Glucosidase receptor, the simulation demonstrated comparable binding energies between the two competing isomers, with a marginal preference for ***Anethole*** (-5.43 kcal/mol) over ***Estragole*** (-5.25 kcal/mol).Anethole successfully fits into the catalytic site of 3W37 through a highly specific electrostatic π−Anion interaction between its aromatic ring and the carboxylate group of the catalytic residue **ASP 409** (6.26 Å). This is supported by dual Alkyl and π–Alkyl interactions at the methoxy moiety with **MET 470** (5.20 Å and 5.50 Å). The structural stability is expanded via an extensive π–Alkyl network involving **ILE 396**, **TRP 432** (5.18 Å), **ILE 358** (4.39 Å), **TRP 516** (5.29 Å), and **HIS 626** (5.12 Å), alongside a short, highly-directed π–Sigma bond with **PHE 601** (4.78 Å). A spatial carbon-hydrogen bond with **ASP 398** (5.27 Å) assists in stereo chemical orientation, while a surrounding van der Waals network (**ARG 552**, **ASP 568**, **GLY 567**, **ASP 597**, **ARG 624**, **TRP 467**, and **ASP 357**) maintains the ligand's positional integrity *figure (V-9)*.

On the other hand, ***Estragole*** displays a geometrically analogous binding topology within the 3W37 receptor pocket. Its central aromatic nucleus is similarly anchored via a π–Anion interaction with the pivotal **ASP 409** residue (6.27 Å). A directed π–Sigma interaction locks its methoxy oxygen onto the aromatic framework of **PHE 601** at a distance of 4.10 Å. Its aliphatic alkyl tail and aromatic core participate in an intricate Alkyl and π–Alkyl web with **TRP 432** (5.37 Å), **ILE 358** (4.21 Å), **ILE 396** (5.30 Å), **MET 470** (6.04 Å), **PHE 601** (7.15 Å and 5.76 Å), **TRP 516**, and **HIS 626** (5.16 Å). The spatial arrangement of the ligand is structurally confined by two carbon-hydrogen bonds at the oxygen terminal with **ASP 568** (4.54 Å) and **ASP 597** (6.09 Å), heavily

supplemented by a continuous van der Waals shell consisting of **ARG 552**, **GLY 567**, **ARG 624**, **TRP 467**, **ASP 357**, **TRP 519**, and **ASP 398** (*figure (V 10)*).

9-4.3.Structural Interpretation of Complex Stability:

the notable molecular stability exhibited by these naturally derived ligands within the target antidiabetic proteins is heavily attributed to their ability to precisely mimic natural substrate binding patterns. The synergistic combination of hydrogen bonding (providing high spatial specificity) and hydrophobic/aromatic interactions (π–bonds, Alkyl, and π–Anion forces which drive thermodynamic stabilization) minimizes the free energy of the system. These in silico findings strongly corroborate the in vitro and in vivo hypotheses, validating these phytochemicals as potent, natural scaffolds for the development of effective postprandial hyperglycemia inhibitors.

10.In vivo antidiabetic activities:

10-1. Antihyperglycemic effect and glycemic control:

The present study demonstrates clear Antihyperglycemic and Antiglycation effects of *Pimpinella anisum L* essential oil (100 mg/kg) in alloxan-induced diabetic rats, as evidenced by significant improvements in fasting blood glucose (FBG) and HbA1c *table (V-11)*. Diabetic rats exhibited severe hyperglycemia (**1.12 ± 0.09g/L**) and elevated **HbA1c** (**14.10 ± 1.24 mmol/mol**), confirming persistent β-cell dysfunction and chronic metabolic disturbance induced by alloxan. Treatment with of *Pimpinella anisum L* essential oil markedly reduced fasting blood glucose to (**0.45 ±0.17 g/L**), close to the normal control value (**0.71 ± 0.12 g/L**) and comparable to **METFORMIN** (**0.68 ± 0.46 g/L**). This indicates a strong improvement in glucose homeostasis, likely through enhanced peripheral glucose uptake, improved insulin sensitivity, and partial protection of pancreatic function.

Similarly, HbA1c was significantly reduced to (**6.91 ± 1.14 mmol/mol**), indicating effective long-term blood glucose control and reduced protein glycation. This confirms that the effect is sustained over time and not limited to a transient reduction in glucose levels.

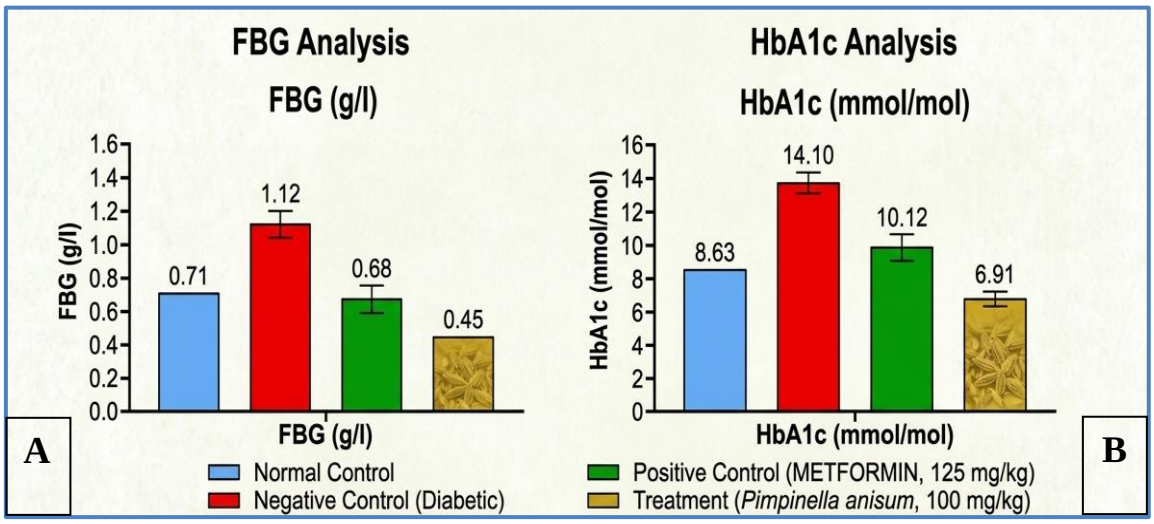
This potent activity may be related to the chemical composition of anise essential oil, which is rich in bioactive compounds that enhance insulin sensitivity, increase glucose uptake in peripheral tissues, and reduce glucose production in the liver, as well as its role in protecting beta cells from oxidative stress caused by alloxan; thus strongly supporting the possibility of using this essential oil as a natural and effective therapeutic agent for

managing diabetes with efficacy comparable to standard treatments such as **METFORMIN**.

table (V-11) Effect of Pimpinella anisum L essential oil (100 mg/kg) on fasting blood glucose and HbA1c in diabetic rats

Parameter	Normal Control	Negative Control (Diabetic)	Positive Control (METFORMIN, 125 mg/kg)	Treatment (*Pimpinella anisum L*, 100 mg/kg)
FBG (g/l)	0.71 ± 0.12**	1.12 ± 0.09	0.68 ± 0.46**	0.45 ± 0.17**
HbA1c (%)	2.94 ± 0.29**	3.44 ± 0.11	3.08 ± 0.41**	2.78 ± 0.10**
HbA1c (mmol/mol)	8.63 ± 2.7*	14.10 ± 1.24	10.12 ± 4.43^{ns}	6.91 ± 1.14*

Values are presented as mean ± standard deviation (n = 5). Statistical significance compared to the negative control group: (ns) non-significant, *P< 0.05, **P < 0.01. (One-way ANOVA followed by Tukey's multiple comparisons test).



figure(V-11) Effect of Pimpinella anisum L essential oil (100 mg/kg) on fasting blood glucose (A) and HbA1c levels (B) in alloxan-induced diabetic rats.

10-2. Hepatoprotective activity:

The present results demonstrate a clear hepatoprotective effect of *Pimpinella anisum L* essential oil (100 mg/kg) in alloxan-induced diabetic rats, as evidenced by markedly elevated serum **ALT** and **AST** in diabetic animals and their significant reduction following treatment *table (V 12)*. The diabetic control group showed severe hepatic injury, reflected by pronounced increases in ALT (**131.96 ± 51.97 IU/L**) and AST (**218.66 ± 22.06 IU/L**), indicating hepatocellular membrane disruption and leakage of

intracellular enzymes into the circulation. These alterations are commonly associated with alloxan-induced oxidative stress and secondary hepatic dysfunction.

Treatment with *Pimpinella anisum L* essential oil significantly attenuated these alterations, reducing ALT to **51.40 ± 6.72 IU/L** and AST to **159.10 ± 11.64 IU/L**, indicating substantial restoration of hepatocellular integrity. The effect was comparable to that of METFORMIN (ALT: **35.12 ± 3.72 IU/L**; AST: **131.89 ± 9.99 IU/L**), suggesting a protective effect against diabetes-induced liver injury. The normalization trend in these enzymes indicates stabilization of hepatocyte membranes and reduced enzyme leakage, reflecting improved liver function.

The hepatoprotective activity of *Pimpinella anisum L* essential oil may stem from its rich content, which are well documented for their antioxidant and membrane-stabilizing properties. These bioactive constituents likely reduce lipid peroxidation, scavenge reactive oxygen species, and enhance endogenous antioxidant defenses, thereby limiting alloxan-induced oxidative damage in hepatic tissue. In addition, improved glycemic control may indirectly protect the liver by reducing glucose-mediated oxidative stress and metabolic overload. Overall, *Pimpinella anisum L* essential oil exhibits significant hepatoprotective effects in diabetic conditions, supporting its role in mitigating diabetes-associated liver dysfunction. These findings further strengthen its potential as a multifunctional antidiabetic agent with both metabolic and organ-protective properties .

table (V-12) Effect of Pimpinella anisum L essential oil (100 mg/kg) on serum liver enzymes in diabetic rats

Parameter	**Normal Control**	**Negative Control (Diabetic)**	**Positive Control (METFORMIN, 125 mg/kg)**	**Treatment (*Pimpinella anisum L*, 100 mg/kg)**
ALT (IU/L)	35.77 ± 7.43	131.96 ± 51.97	40.85 ± 2.90	51.40 ± 6.72*
AST (IU/L)	68.25 ± 8.72	218.66 ± 22.06	115.00 ± 15.21	159.10 ± 11.64*

Values are expressed as mean ± SD (n = 5). Statistical significance versus negative control: **P< 0.01 (ANOVA, Tukey's post hoc test).*

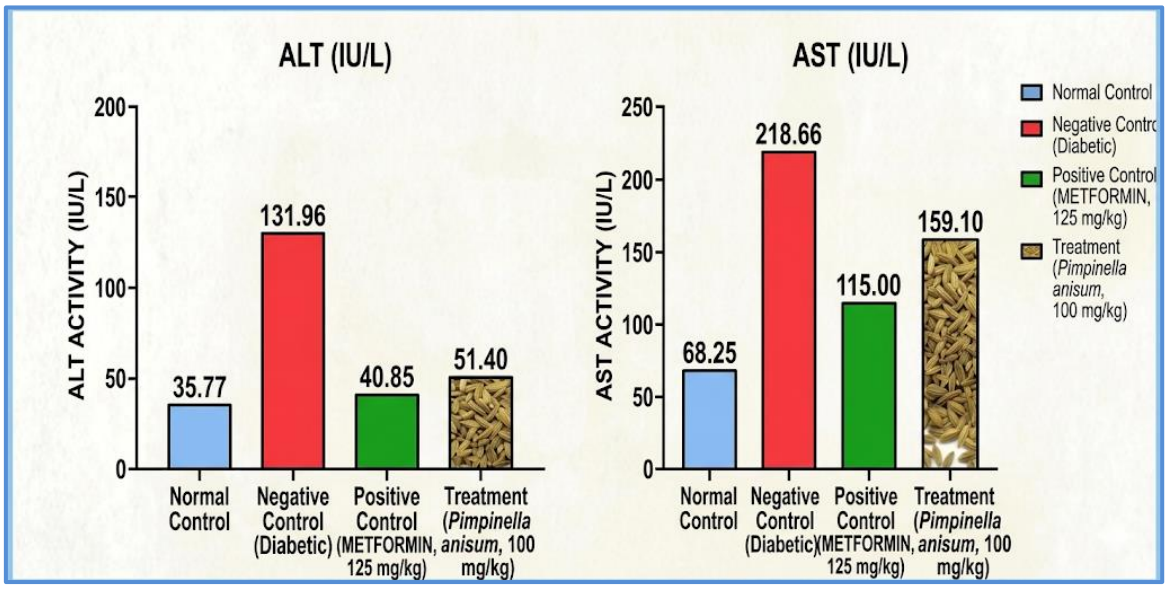


figure (V-12) Effect of Pimpinella anisum L essential oil on serum liver enzymes (ALT and AST) in diabetic rats compared with control and metformin groups.

10-3. Mechanistic basis:

The antihyperglycemic and hepatoprotective effects of *Pimpinella anisum L* essential oil observed in alloxan-induced diabetic rats are most plausibly explained by a multi-target mode of action, supported by its phytochemical complexity. Alloxan-induced diabetes is primarily driven by β-cell oxidative injury; therefore, the significant reductions in FBG and HbA1c are consistent with attenuation of oxidative stress and preservation of residual β-cell function, resulting in improved endogenous insulin availability and glycemic control. In parallel, the essential oil's volatile bioactive compounds, predominantly phenylpropanoids (such as anethole) and monoterpenesmay enhance insulin sensitivity and peripheral glucose utilization and may also suppress hepatic glucose output by modulating antioxidant and anti-inflammatory signaling. The in vitro α-amylase inhibition further suggests an additional contribution through reduced carbohydrate digestion and a dampened postprandial glycemic load. The marked normalization of ALT and AST indicates protection against diabetes-associated hepatic injury, likely mediated by reduced lipid peroxidation, stabilization of hepatocyte membranes, and reinforcement of endogenous antioxidant defenses, together with an indirect benefit from improved glucose homeostasis.

These integrated pathways are summarized schematically in **figure (V13)** and provide a coherent mechanistic basis for the dual antidiabetic and hepatoprotective

activities of *Pimpinella anisum L* essential oil, although targeted assessment of insulin status, oxidative stress biomarkers, inflammatory mediators, and histopathology would strengthen mechanistic confirmation.

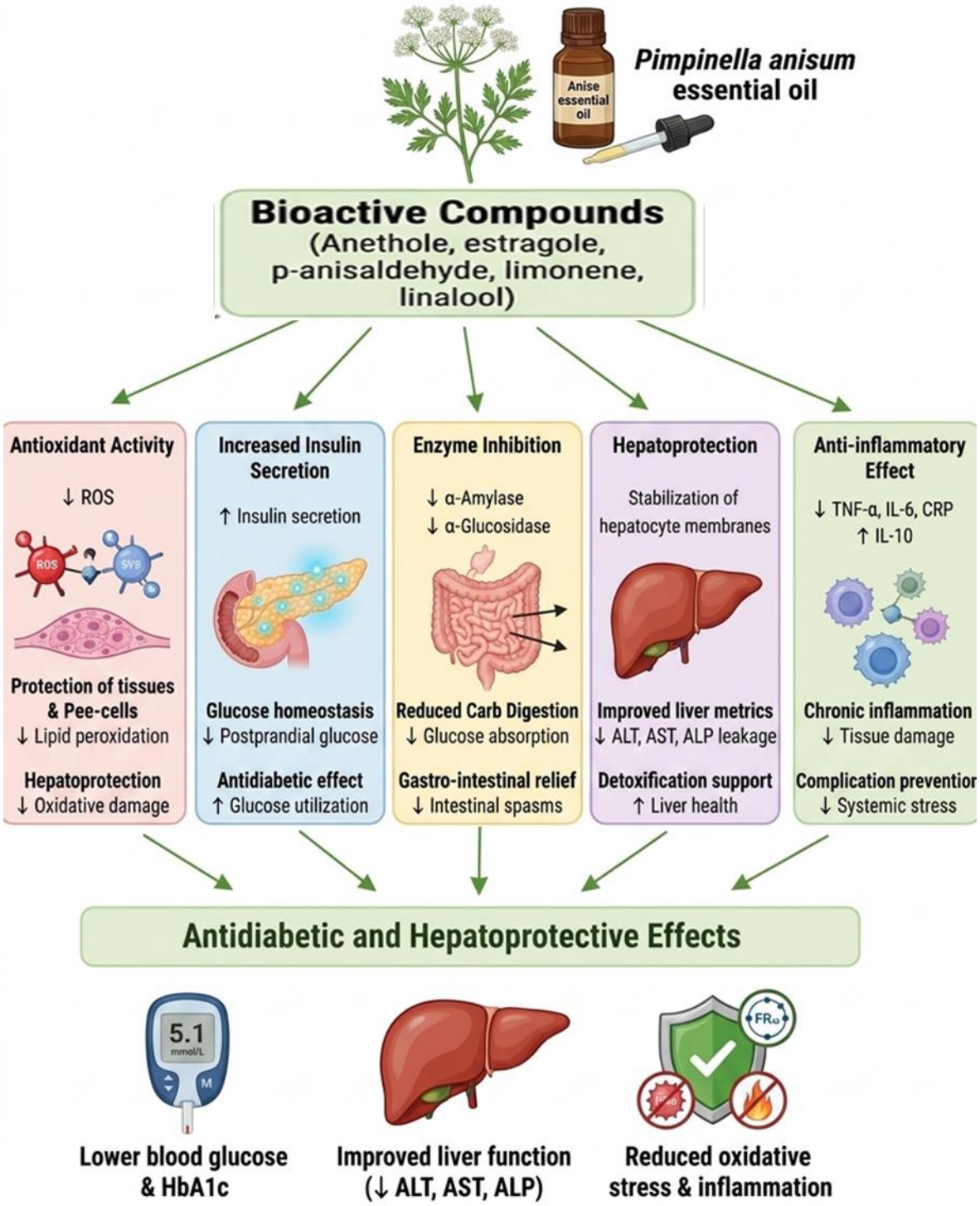


figure (V-13) Graphical abstract of the multi-target antidiabetic and hepatoprotective mechanisms of Pimpinella anisum L essential oil.

10-4. Histopathological Analysis:

10.4.1.Liver Histology:

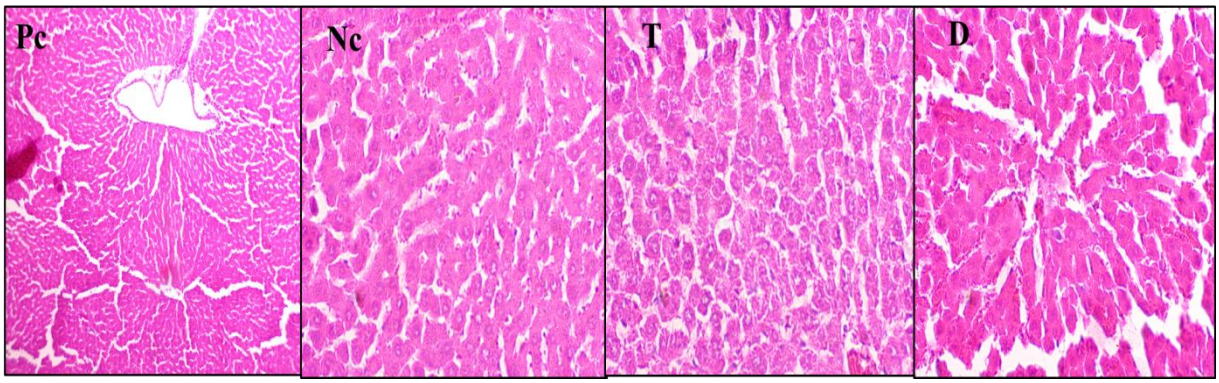


figure (V 14) Comparative histological analysis of liver sections from Normal Control (Nc), Diabetic Control (D), Treatment (Pimpinella anisum L, T), and Positive Control (Metformin, Pc) groups, X400.

A). Histological Interpretation of Liver Sections:

Based on the provided histological sections of the liver, prominent microarchitectural variations were observed among the different experimental groups:

1. Normal Control Group (Nc):

The hepatic tissue in this group exhibits a completely intact and healthy histological architecture. The hepatocytes are well-organized in regular cords or plates radiating symmetrically around the central axis, with distinct, non-dilated hepatic sinusoids in between. The hepatocytes feature well-defined, centrally located spherical nuclei and a homogenous cytoplasm, showing no signs of vacuolar degeneration, steatosis (fatty changes), or inflammatory cell infiltration.

2. Diabetic / Negative Control Group (D):

This group demonstrates severe and conspicuous histopathological alterations in liver architecture, resulting from untreated induced diabetes. There is a noticeable disruption and loss of the typical radiating cord-like arrangement of hepatocytes. Marked vacuolar degeneration and cytoplasmic lysis are clearly evident, accompanied by severe congestion and prominent dilation of the hepatic sinusoids-consequences of cellular death and damage driven by diabetes-associated oxidative stress. Additionally, several hepatocytes display nuclear pyknosis (shrinkage) or karyolysis (dissolution).

3. Treatment Group (T) / *Pimpinella anisum L* (100 mg/kg):

A remarkably profound improvement in the hepatic microarchitecture is observed compared to the diabetic group (D). Treatment with *Pimpinella anisum L* essential oil at a

dose of 100 mg/kg exerts a robust cytoprotective effect; the hepatocytes have largely restored their organized cord-like arrangement, and intracellular vacuolar degeneration is significantly minimized. These findings highlight the potent hepatoprotective efficacy of *Pimpinella anisum L* in mitigating cellular damage and counteracting diabetes-induced oxidative stress.

4. Positive Control Group (Pc) / METFORMIN (125 mg/kg):

This reference group demonstrates a near-complete restoration of the normal hepatic architecture, serving as the benchmark for therapeutic efficacy. The parenchyma appears highly organized around the central vein, preserving the structural integrity of both hepatic cords and sinusoids, with an absolute absence of degenerative changes. Notably, the histological recovery observed in the *Pimpinella anisum L* group (T) closely parallels and matches the therapeutic efficiency of this standard reference drug (Metformin).

B). Histological Conclusion:

In conclusion, the histopathological evaluation successfully confirms that diabetes induction (Group D) causes severe structural devastation in liver tissue. Conversely, administration of *Pimpinella anisum L* essential oil at 100 mg/kg (Group T) significantly aids in tissue repair, cellular regeneration, and hepatoprotection, demonstrating a therapeutic efficiency that closely approaches that of the standard reference drug, Metformin.

10.4.2.Kidney Histology:

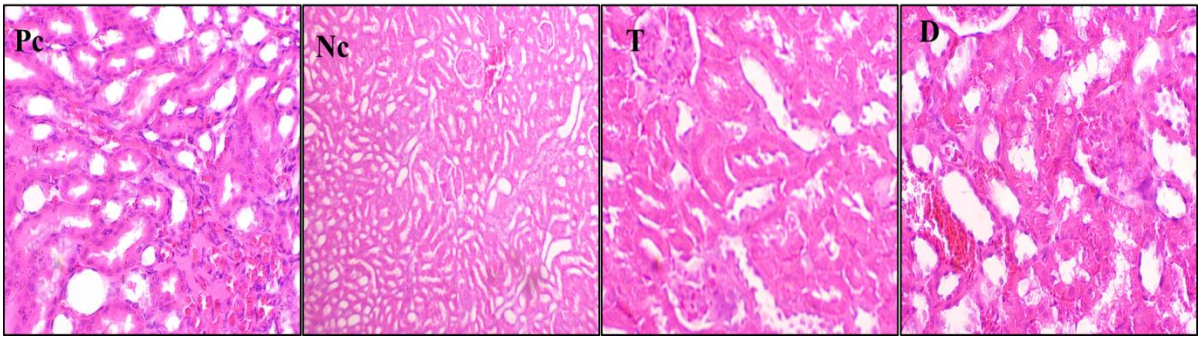


figure (V 15) Comparative histological analysis of Kidney sections from Normal Control (Nc), Diabetic Control (D), Treatment (Pimpinella anisum L, T), and Positive Control (Metformin, Pc) groups, X400.

A). Histological Interpretation of Kidney Sections:

Based on the provided histological sections of the renal tissue, prominent histopathological variations and microarchitectural changes were observed among the different experimental groups:

1. Normal Control Group (Nc):

The renal tissue in this group exhibits a completely intact, healthy, and typical histological architecture. The renal glomeruli and Bowman's capsules are well-preserved, maintaining their normal capsular spaces. Both proximal and distal renal tubules appear intact, lined with structured simple cuboidal epithelium featuring distinct cellular borders and a homogenous cytoplasm. Furthermore, the tubular lumens are completely clear, showing no signs of casts, debris, or cellular autolysis.

2. Diabetic / Negative Control Group (D):

This group demonstrates severe and conspicuous histopathological damage within the renal parenchyma, characteristic of untreated diabetic nephropathy. Pronounced hypertrophy or structural distortion is observed in the glomeruli, accompanied by abnormal expansion or constriction of Bowman's space. The most prominent alterations are detected within the renal tubules, which manifest severe vacuolar degeneration and focal necrosis of the lining epithelial cells. Additionally, marked interstitial blood vessel congestion and a loss of distinct tubular outlines are clearly evident-consequences of cellular injury driven by accumulated free radicals and diabetes-induced oxidative stress.

3. Treatment Group (T) /*Pimpinella anisum L* (100 mg/kg):

A remarkably profound improvement in the renal microarchitecture and a distinct protective effect are observed compared to the diabetic group (D). Administration of *Pimpinella anisum L* essential oil at a dose of 100 mg/kg demonstrates a high therapeutic capacity to restore and repair both glomerular and tubular structures. The glomeruli have largely regained their near-normal morphology, while the rates of tubular vacuolar degeneration and lysis are significantly minimized. Moreover, the interstitial tissue shows a marked reduction in congestion, highlighting the potent antioxidant, anti-inflammatory, and nephroprotective efficacy of this essential oil.

4. Positive Control Group (Pc) / METFORMIN (125 mg/kg):

This reference group demonstrates a near-complete restoration of the normal renal histoarchitecture, serving as the benchmark for therapeutic comparison. The renal tubules and glomeruli appear highly organized and neatly arranged, closely resembling the normal control group (Nc). The lining epithelial cells of the tubules remain structurally intact and uniform, with an absolute absence of necrotic changes. Notably, the nephroprotective efficiency observed in the *Pimpinella anisum L* group (T) closely parallels and matches the therapeutic performance of this standard reference drug (Metformin).

B). Histological Conclusion:

In conclusion, the histopathological evaluation successfully confirms that diabetes induction (Group D) inflicts severe structural devastation upon the renal glomeruli and tubules. Conversely, treatment with *Pimpinella anisum L* essential oil at a dose of 100 mg/kg (Group T) provides robust nephroprotection, effectively facilitating tissue repair and cellular regeneration with a therapeutic efficiency that closely approaches that of the standard reference drug, Metformin.

10.4.3.Pancreas Histology:

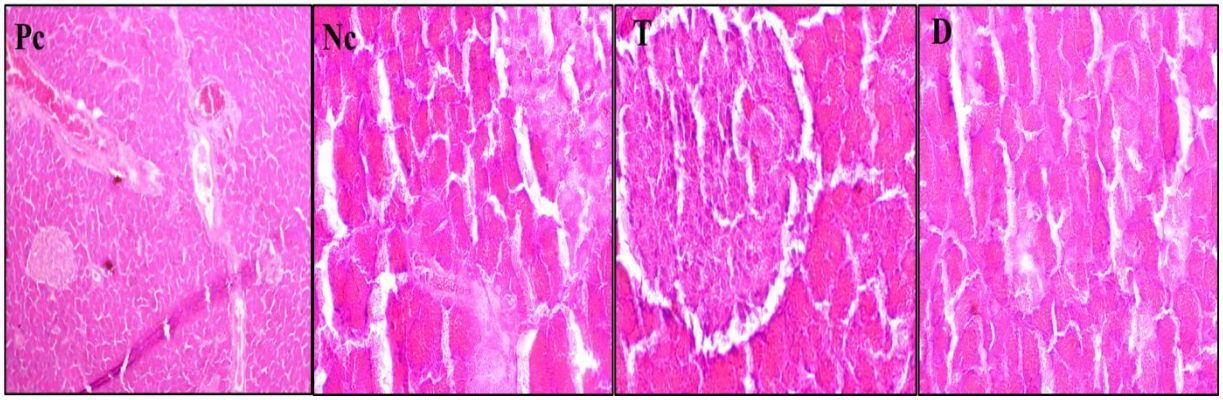


figure (V 16) Comparative histological analysis of Pancreas sections from Normal Control (Nc), Diabetic Control (D), Treatment (Pimpinella anisum L, T), and Positive Control (Metformin, Pc) groups, X400.

A). Histological Interpretation of Pancreas Sections:

Based on the provided histological sections of the pancreatic tissue, prominent microarchitectural changes and histopathological variations were observed among the different experimental groups:

1. Normal Control Group (Nc):

The pancreatic tissue in this group exhibits a completely intact, healthy, and typical histological architecture. The Islets of Langerhans are well-defined and clearly demarcated, surrounded by the outer, deeply stained exocrine acinar cells. The endocrine cells within the islets (primarily beta and alpha cells) appear densely packed, well-organized, and structurally sound, supported by a normal capillary network with an absolute absence of any atrophic or degenerative changes.

2. Diabetic / Negative Control Group (D):

This group demonstrates severe and conspicuous destruction and atrophy within the Islets of Langerhans resulting from untreated induced diabetes. Marked shrinkage and a profound reduction in the overall size and surface area of the islets (severe islet atrophy)

are clearly evident. This is accompanied by a sharp decline in cellular density within the islets-particularly the insulin-secreting beta cells-along with a disruption of their architectural framework. The tissue exhibits cellular lytic changes, vacuolation, and focal infiltration of inflammatory cells, which directly accounts for the impaired insulin secretion associated with the disease.

3. Treatment Group (T) / *Pimpinella anisum L* (100 mg/kg):

A remarkably profound improvement in the pancreatic microarchitecture and robust cytoprotection are observed compared to the diabetic group (D). Treatment with *Pimpinella anisum L* essential oil at a dose of 100 mg/kg demonstrates high therapeutic efficacy in pancreatic tissue remodeling. The Islets of Langerhans have largely restored their typical size and regular circular boundaries. Notably, there is a prominent increase in cellular density within the islets compared to the diabetic group, with a complete absence of severe lytic changes. These findings clearly indicate the potent beta-cell protective and regenerative capacity of this essential oil, driven by its exceptional antioxidant properties against oxidative stress.

4. Positive Control Group (Pc) / METFORMIN (125 mg/kg):

This reference group demonstrates a near-complete restoration of the normal, highly organized pancreatic histoarchitecture. Both the exocrine acini and endocrine Islets of Langerhans are precisely organized and neatly defined, closely resembling the normal control group (Nc). The islets show an expanded cellular mass and a complete disappearance of histopathological damage. Crucially, the therapeutic and protective efficiency observed in the *Pimpinella anisum L* group (T) closely parallels and matches the positive outcomes of this standard reference drug (Metformin).

B). Histological Conclusion:

In conclusion, the histopathological evaluation successfully confirms that diabetes induction (Group D) causes severe atrophic devastation and destruction of the pancreatic Islets of Langerhans. Conversely, the administration of *Pimpinella anisum L* essential oil at a dose of 100 mg/kg (Group T) significantly protects these islets from cellular death and effectively stimulates the regeneration of their microarchitectural structure. This therapeutic performance closely approaches that of the standard reference drug, Metformin (Group Pc), thereby validating its potent role in enhancing insulin secretion and maintaining glycemic control.

GENERAL SUMMARY

GENERAL SUMMARY:

The Algerian environment abounds with medicinal plant resources. This study represents an important scientific milestone in valuing this wealth, focusing on the extraction and characterization of the essential oil from anise seeds *(Pimpinella anisum L)* , and evaluating its biological efficacy and biosafety through an integrated approach that included in vitro, in vivo, and in Silico testing. This work culminated in a set of core findings that can be summarized as follows:

1. **Chemical Yield and Characterization:** The extraction process recorded a reasonable and acceptable yield of essential oil approaching 0.96%. Gas chromatography-mass spectrometry (GC-MS) analysis revealed the dominance of anethole as the major and characteristic chemo type component of this plant at a rate of 74.4%, supported by important secondary compounds such as Estragole, Caryophyllene oxide, and Linalool.
2. **In Vitro Biological Activity:** The essential oil demonstrated an excellent capacity to scavenge free radicals (DPPH) with a half-maximal inhibitory concentration **(IC_{50})** of 4.38 mg/mL. Additionally, it showed efficiency in inhibiting protein denaturation (anti-inflammatory effect) and inhibiting the α-amylase enzyme, as well as exhibiting antibacterial activity against the tested strains (E. coli and S. aureus), while displaying total biosafety against human hemolysis.
3. **In Vivo Study:** Results on diabetic mice confirmed the ability of the essential oil (at a dose of 100 mg/kg) to reduce fasting blood glucose and glycated hemoglobin (HbA1c) levels, while protecting and regenerating pancreatic β-cells. It also demonstrated outstanding hepatoprotection, manifested by a decrease in liver enzymes (*ALT* and *AST*) associated with oxidative stress.
4. **In Silico Simulation:** Computerized molecular docking simulations provided in-depth structural insights into the antidiabetic potential of the selected compounds. Caryophyllene oxide demonstrated a binding affinity to the α-amylase enzyme with a free energy value of (-5.88 kcal/mol), surpassing the commercial antidiabetic drug metformin (-5.83 kcal/mol). Furthermore, the computational ADMET study confirmed excellent pharmacokinetic properties, underscoring its suitability as a drug.

Future Perspectives:

Based on these promising results, we recommend pursuing the following research avenues:

The compelling results of this study provide a solid foundation for developing natural anti-diabetic agents from Algerian anise *(Pimpinella anisum L)* . Future research should prioritize the isolation and evaluation of key active ingredients, such as Caryophyllene oxide and anethole, to verify their superiority over conventional drugs.

Industrial and functional food applications: Explore the potential for incorporating this bioactive oil into functional foods or food formulations, leveraging its dual efficacy as a natural anti-diabetic agent and a safe food preservative thanks to its antimicrobial properties.

Green antioxidant alternatives in pharmaceuticals: Utilize the exceptional free radical scavenging capacity of Algerian anise *(Pimpinella anisum L)* oil as a natural and safe alternative to synthetic antioxidants (such as BHA and BHT) in various pharmaceutical and therapeutic preparations.

Targeted antimicrobial interventions: Exploiting the potent antibacterial activity of anise oil as a promising bio similar to combat localized bacterial infections by improving the minimum inhibitory concentration (MIC) at specific sites.

APPENDICES



Figure 1 Oral Gavage in Laboratory Mice



Figure 2 the sequential arrangement of the dye baths and chemical solutions (xylene, alcohol in decreasing and increasing concentrations, hematoxylin, and eosin) used in the preparation of tissue slides of sections (liver, kidney, and pancreas).



Figure 3 the rotating microtome (Microm HM 325) during the preparation of thin tissue sections; the paraffin mold is shown fixed in the specimen holder and the paraffin strip formed on the blade.



Figure 4 the tissue embedding device (SLEE MPS/P1) is used to cast samples of the studied organs inside metal molds and cover them with liquid paraffin wax to obtain cohesive molds suitable for cutting.



Figure 5 the automated tissue processing device (SLEE MTP) is used to sequentially immerse studied organ samples within fixation, drying, clarification, and paraffin permeation stations.

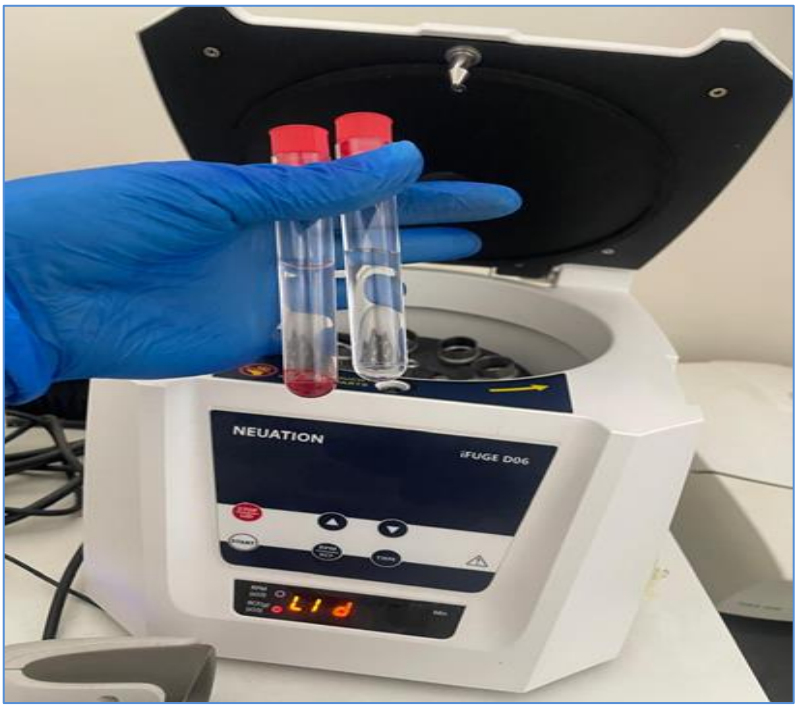


Figure 6 the laboratory centrifuge (Neuation iFuge D06) used for separating and settling samples, and the test tubes prepared for the centrifugation and balancing process are shown.



Figure 7 the optical density meter (bioMérieux DensiCHEK Plus) is used to prepare the bacterial suspension to a concentration that matches the McFarland scale (e.g., 0.5 McF) before using it in the antimicrobial activity test.